CHALMERS
UNIVERSITY OF TECHNOLOGY

Unconventional support assessment for mines in sedimentary bedrock

Applicability of rock classification systems in horizontally bedded sandstone

Master's thesis in Infrastructure and Environmental Engineering

John Boberg
Julius Detlofsson

DEPARTMENT OF ARCHITECTURE AND CIVIL ENGINEERING
CHALMERS UNIVERSITY OF TECHNOLOGY
Gothenburg, Sweden 2022
www.chalmers.se

Master's thesis 2022

Unconventional support assessment of mines in sedimentary bedrock

Applicability of rock classification systems in horizontally stored sandstone

JOHN BOBERG
JULIUS DETLOFSSON

CHALMERS
UNIVERSITY OF TECHNOLOGY

Department of Architecture and Civil Engineering
Division of Geology and Geotechnics
Chalmers University of Technology
Gothenburg, Sweden 2022

Unconventional support assessment of mines in sedimentary bedrock
Applicability of rock classification systems in horizontally stored sandstone

John Boberg
Julius Detlofsson

Supervisor at Chalmers: Eleni Gerolymatou, Architecture & Civil Engineering, Chalmers
Supervisor at Sweco: Christian Andersson Höök, Sweco AB
Examiner: Minna Karstunen, Architecture & Civil Engineering, Chalmers

Master's Thesis 2022
Department of Architecture and Civil Engineering
Division of Geology and Geotechnics
Chalmers University of Technology
SE-412 96 Gothenburg
Telephone +46 31 772 1000

Cover: Picture taken in Kvarntorp Mine Typeset in LaTeX

Printed by Chalmers Reproservice
Gothenburg, Sweden 2022

Unconventional support assessment of mines in sedimentary bedrock
Applicability of rock classification systems in horizontally stored bedrock
JOHN BOBERG
JULIUS DETLOFSSON
Department of Architecture and Civil Engineering
Chalmers University of Technology

Abstract

Coal mining has been a huge industry ever since the industrial revolution but has in more recent years started to be phased out as renewable energy sources have been further prioritised by our society. In order to not let the vast knowledge and experience of the coal mining industry fade, this study seeks to evaluate the applicability of *Coal Mine Roof Rating*, CMRR, in other settings. The assessment of the classification system is performed through a comparison to *Rock Mass Rating*, RMR. Both systems are evaluated through a case study of the *Kvarntorp mine*, a *sedimentary sandstone* mine in Sweden. The mine has been excavated through *room and pillar mining*, resulting in horizontal rooms with pillars of rock between them. The geological properties of the bedrock were partly gathered from older investigations from the mine and partly through extrapolations and estimations based on properties of rock in similar conditions. The *Geological strength index*, GSI, along with the *Generalized Hoek-Brown failure criterion* was utilised to characterize the rock quality.

Two-dimensional *finite element analysis* was utilised to assess the system numerically. Two models with differing approaches to evaluate joint sets and weakness zones were created in the software *RS2*. The models were used to assess the stability of 13 different scenarios, covering both the different classification systems and the prospect of heightening the roof of the mine.

The behaviour of the two model types was very similar, showing no major discrepancies. Their output indicates that the *support recommendations* from the classification systems don't affect the vertical displacement of the roof or the general behaviour of the model. However, the roof suffers from yielded elements and *bolting* is necessary to control these loose blocks. The CMRR support recommendation is deemed to be the most efficient alternative in the Kvarntorp mine but it requires thorough assessment of any weakness zones in the mine. If the weakness zones are hard to assess, the RMR support recommendation is deemed the safer alternative even though it is potentially too conservative. As the study was only conducted for the one case of Kvarntorp, these findings are not directly applicable in other settings but may instead be considered as indicators for the potential to utilise CMRR in sedimentary bedrock.

Keywords: *coal mine roof rating, rock mass rating, Kvarntorp mine, sedimentary sandstone, room and pillar mining, geological strength index, generalized Hoek-Brown failure criterion, finite element analysis, RS2, support recommendation, bolting*

Acknowledgements

Firstly, we would like to express special gratitude to Eleni Gerolymatou, our supervisor at Chalmers. Eleni has given us splendid guidance and support during the whole study and has put a large effort into assisting us thoroughly. Furthermore, her humour has been very refreshing, relieving our sanity when the work was arduous.

Secondly, our genuine thanks go out to Christian Andersson-Höök whom has supervised us from Sweco. Christian established the idea for the study and provided us with a clear scope and objective. His clear guidance throughout the stages of the project and his vast experience has been very valuable to us.

Furthermore, Nikola Ristov at Sweco allowed us to accompany him to the Kvarntorp mine for a site visit. He gave us a detailed tour of the mine providing us with great information on-site. His experience from investigating the mine for several years allowed us to get a thorough perspective of the risks and obstacles associated with the mine which was of great assistance during the study. A second thanks goes out to Nikola who also provided us with specific information regarding the existing support in the mine.

A special thanks also goes out to Andreas Langenbach at Sweco for providing us with the archived material from the initial investigations of the mine and helping us understand certain complications at the site. He was also great lunch company at many occasions.

We would also like to thank Jesper Knutsson of the Water Environment Technology division and Anders Karlsson of the Geology and Geotechnics division at Chalmers for their assistance during our laboratory tests.

Additionally, a special thanks goes out to the student Eric Nilsson at Chalmers for assisting us with supplementary material for the laboratory tests.

Lastly, our warmest appreciations are extended to Jonas Eriksson and Elin Thulin for their splendid support, company and friendship.

JOHN BOBERG & JULIUS DETLOFSSON, Gothenburg, June 2022

List of Acronyms

Below is the list of acronyms that have been used throughout this thesis listed in alphabetical order:

ASTM	American Society for Testing and Materials
CMRR	Coal Mine Roof Rating
Comp. Str.	Compressive Strength
ESR	Excavation Support Ratio
FEM	Finite Element Method
GPa	Gigapascal
GSI	Geological Strength Index
JSM	Jättestor Maskin
kPa	Kilopascal
kN	Kilonewton
NGI	Norwegian Geotechnical Institute
MN	Meganewton
MPa	Megapascal
RMR	Rock Mass Rating
RPM	Rotations per minute
RRW	Thickness Weighted Average
RQD	Rock Quality Designation
PFAFF	Preliminary Force Assessment for Failure
PRSUP	Preliminary Support
SDI	Slake Durability Index
SGU	Sveriges Geologiska Undersökning *(Swedish Geological Investigation)*
SL1	Sandstone Layer 1
SL2	Sandstone Layer 2
SL3	Sandstone Layer 3
SL4	Sandstone Layer 4
SL5	Sandstone Layer 5
SRF	Stress Reduction Factor
Tens. Str.	Tensile Strength
UCS	Uniaxial Compressive Strength
UTS	Uniaxial Tensile Strength
UR	Unit Rating
2D	Two-dimensional
3D	Three-dimensional

Nomenclature

Below is the nomenclature of parameters that have been used throughout this thesis.

Parameters

A	Mass of slake durability drum and samples at natural moisture content
a	Hoek-Brown parameter
A_s	Cross section area of bolt *[m^2]*
$A_{Largestblock}$	Area of the face of the largest block
B	Mass of slake durability drum plus oven-dried samples before first slake durability cycle
C	Mass of slake durability drum
C_c	Capacity *[kN]*
D	Disturbance factor
E	Young's modulus
E_{joint}	Stiffness of joint
E_{normal}	Normal stiffness of joint
E_{shear}	Shear stiffness of joint
e	Euler's number
$F_{Largestblock}$	Force of largest possible block *[kN]*
F_{mt}	Maximum tensile capacity of bolt *[kN]*
f_{yd}	Tensile capacity of bolt *[MPa]*
f_{yk}	Characteristic tensile capacity of steel *[MPa]*
g	Gravity coefficient
h	Height of weak rock *[m]*
L_{bolt}	Length of bolt *[m]*
$L_{Largestblock}$	Length of the largest block
m_i	Material dependant Hoek-Brown parameter

N_b	Number of bolts per row
S_b	Spacing between rows of bolts *[m]*
SDI	Slake durability index
S_1	Distance between the bolts in the tunnels lengthwise direction *[m]*
S_1	Distance of the bolt in the tunnels cross-section width *[m]*
$V_{Largestblock}$	Volume of largest possible block *[m^3]*
w	Percentage of water content
W_d	Design load *[kN]*
W_e	Entry width of tunnel *[m]*
W_f	Mass of slake durability drum and oven-dried samples retained after the second slake durability cycle
W_k	Characteristic load *[kN]*
$\overline{x}$	Average distance between discontinuities *[m]*
γ_{ss}	Unit weight of sandstone
γ_{cs}	Unit weight of clay shale
γ_d	Safety coefficient
$\gamma_{G:dst}$	Safety coefficient
γ_{ob}	Unit weight of overburden
γ_s	Unit weight of shale
γ_y	Partial coefficient for different materials and purposes
ϵ	Strain
ν	Poision's ratio
ρ	Density *[kg/m^3]*
σ	Stress *[kPa]*
σ'_1	Effective major principal stress *[MPa]*
σ'_1	Effective minor principal stress *[MPa]*
σ'_{ci}	Effective unconfined compression strength *[MPa]*

Contents

List of Figures

List of Tables

1
Introduction

This chapter serves as an introduction to the study and the topic it investigates. It presents the origin and general structure of the work as well as necessary information required to follow the report.

1.1 Background

Mining has been a large part of our society for generations. As an industry, it has played a major role in shaping the world we live in today, but the world has also shaped the industry itself. Technological advances and an ever-changing demand of different types of ore have forced the industry to continuously evolve since it's appearance. The changing nature of the business coupled with the inevitability of mines becoming depleted has led to over a million abandoned mines in the world [1]. Oftentimes, an abandoned mine can prevent the land where it is located from being put to other use [2]. As a result, several different ways of repurposing mines have been introduced through the years in order to make use of the land domain. A common approach spearheaded by mushroom grower Herman Knaust which came in the 1950s was to turn the space into secure storage facilities [3]. In Kvarntorp, Sweden, an old sedimentary sandstone mine was partly repurposed into a test site in 1992 by Atlas Copco (currently known as Epiroc) along with sandstone mining in a smaller scale. Just 8 years later, the sandstone mining operations in the mine were discontinued all-together which opened up the possibility of also using it as a secure storage facility [4]. As of 2022, the mine is still being used for both of these purposes and there are even plans to expand the operations. The safety and stability of the mine is therefore still of high importance. As a result, Sweco has been contracted to carry out continuous inspections of the mine in order to assess the integrity of it.

Another very common mining operation performed in sedimentary bedrock is coal mining. Coal mining has been a major industry with thousands of workers for a long time and it has in general been a very profitable enterprise. The large amounts of resources have allowed the coal industry to develop effective methods and a more streamlined process of assessing the integrity of a mine, thus simplifying the work and reducing the amount of resources required. This is commonly done through a classification system called Coal Mine Roof Rating, CMRR [5]. The system is similar to other more well established systems such as Rock Mass Rating, RMR and the NGI´s Q-system, which are more common practice in Sweden [6][7].

However, ever since the beginning of the industrial revolution, the climate and the global temperatures have been changing drastically. This is attributed to an increasing amount of carbon dioxide in the atmosphere, which the use of fossil fuels such as coal contribute significantly to [8]. This has led to new legislature and the public's opinion in general turning against such forms of fuel. As a result, coal mining is being phased out in many parts of the world. Though, even if the industry itself is fading, the long history and the accumulated knowledge that exist may still be valuable. As sedimentary mines are repurposed and some form of operations are continued, the need to easily be able to assess the stability of them remain. The ability to utilise the already available classification system for coal mines, but in another geological setting, would simplify the process immensely.

1.2 Purpose and Vision

The purpose of this study is to investigate if the CMRR classification system is applicable outside of the coal mining industry and if it is able to streamline the inspection and ongoing classification work that is is done by Sweco in Kvarntorp, Sweden. This study aims to assess the following:

- Investigate how CMRR has historically been used for coal mines and how it can be applicable to other situations
- Establish if CMRR can conveniently be utilised for the continuous assessment of the Kvarntorp mine in Sweden
- Investigate shortcomings and strengths of CMRR compared to other classification systems, existing structures and other support alternatives using finite element analysis.
- Assess how finite element analysis can be utilised to compare rock classification systems

1.3 System Boundaries

This study's is made with stability as its main focus. The purpose is to examine and evaluate different classification systems and their suitability in a sandstone mine in Kvarntorp. Consequently, social and economical aspects will not be investigated and evaluated thoroughly. Furthermore, mining strategies and performance will not be taken into account to any large extent.

Several input parameters for the assessment have to be estimated or extrapolated from already available test results or data. The scope and resources of this study do not allow for extensive testing of the Kvarntorp site and consequently the study will have to rely on what is already known. The effects of this are further discussed in Section 5.1.

The assessment and comparison of the different classification systems will solely be carried out using finite element analysis through the software RS2. The study will not utilise traditional analytical methods in order to limit the scope of the study.

Furthermore, the finite element analysis will be carried out in 2D and not 3D, even if the mine is a 3D problem in reality. The effects of this are further discussed in Section 5.5.

The models used for the finite element analysis will be limited in size to only include three adjacent mine rooms, as the full mine is too large to model for the scope of the study. Consequently, the study is to be considered as a case work that seeks to represent the most common conditions present in the mine.

2
Theoretical Frame of Reference

The following chapter will present the theoretical framework this thesis will base its investigations on.

2.1 The Mining Process

Coal mining is done in one of two ways. Surface mining is done on shallow coal deposits where the coal bed simply can be reached by removing the top soil. Miners remove the soil in steps until the deposits are reached, which creates an open pit mine where the coal can be excavated [9].

The other way of doing it is what is called underground mining or deep mining. This is done in deposits that are far from the surface, usually several hundreds of meters below the surface, which would make it impractical to dig down to such depths. This way of mining is similar to how iron ore deposits are reached in the Swedish LKAB iron mines in northern Sweden. Coal mines are generally reached by vertical shafts or ramps to the depths where the deposits are located and then excavated horizontally in a forward direction [9][10].

The alternative of deep mining is what is suitable to utilise CMRR for. Furthermore, the sandstone mine in Kvarntorp is also a deep mine which is further described in Section 2.5.1, hence why CMRR may be applicable.

2.1.1 Comparison to tunneling

Underground mining and civil constructions such as road tunnels do share a lot of similarities. When mining underground it is common to use a vertical mine shaft or a descending road to reach the ore or other desired natural resource. Well in place at the correct depth, the miners then proceed to drive the extraction in a forward direction in a similarly manner to how a tunnel face is driven forward. In other words, miners create tunnels underground in the direction of the paydirt [11] [12].

The main difference between civil and mining rock construction is that mine openings are temporary and are usually closed after the extraction has been completed, where as tunnels usually are expected to function for decades. This puts further focus on making civil tunnel supports to be more resilient to corrosion and mechanical damage than what is necessary for temporary mine openings [11] [13].

As a result, when old temporary mines are closed but are planned to be re-purposed, like in the case of Kvarntorp, the strength and the support over time needs to be re-evaluated to revise the first intention of making the supports temporary.

2.2 Present Methods and Guidelines

Trafikverket (*The Swedish Transport Administration*) has a general guidelines for rock structures called 'Projektering av Bergskonstruktioner' (*Design of Rock Structures*). [14]. These in combination with the methods described i Eurocode are what makes up the basis for any rock structure. Trafikverket has guidelines regarding design, construction and maintenance where they both state demands and general guidelines which are developed by themselves. Furthermore, national legislation is always binding if any conflict of the two would occur [14].

The process of anchoring a weak roof into an overlaying stronger layer is described in Trafikverkets guide [14], but there are no such guidelines in regards to using bolts where the layers are of the same strength and width as described in section 2.2, described by Bjurströms and Heimersson in their report [15].

However, in TRVK Tunnel 11 which is Trafikverket's specific guidelines for road and railway tunnels, pre-tensioned bolts are described. The demands specified in TRVK 11 are for untensioned bolts in general as well as pre-tensioned with a tensile strength less than 800 MPa. Other bolts can be used, but if they are not described in AMA (*Guidance for the preparation of particular conditions for Building and Civil Engineering Works and Building Services Contracts*) a specific set of regulations and specifications must be assessed [16].

Such requirement specifications are not limited to but must include [16]:

- Methods for reaching desired stability, durability, protection against water leakage, protection against freezing damages as well as over all safety in the tunnel
- Methods for verifying the fire-safety in the tunnel
- Material requirements
- Environmental impact and methods to minimize it
- Methods for the construction phase
- Methods used for inspections and verifications
- Description for how future use and maintenance will be performed.

A proposal with special regulations and specifications shall then be approved by the developer. The bolts described in TRVK 11 are required to have a minimum diameter of 20mm and the use of any type of bolts for permanent reinforcement requires verification that the bolts meet the requirements for stability and durability [16].

2.2.1 Roofs with a strong overlaying layer and untensioned bolts

When bolting in roofs where stronger layers are located above the tunnel roof the preferred method is to drill a hole in the roof and fasten the bolts in the stronger layer and letting the weaker roof rest on the bolts. This is illustrated in Figure 2.1. The bolts are usually not pretensioned and rely on the roof deformation in order to activate [15]. Furthermore, this method does not take the strength of the rock itself into consideration [14].

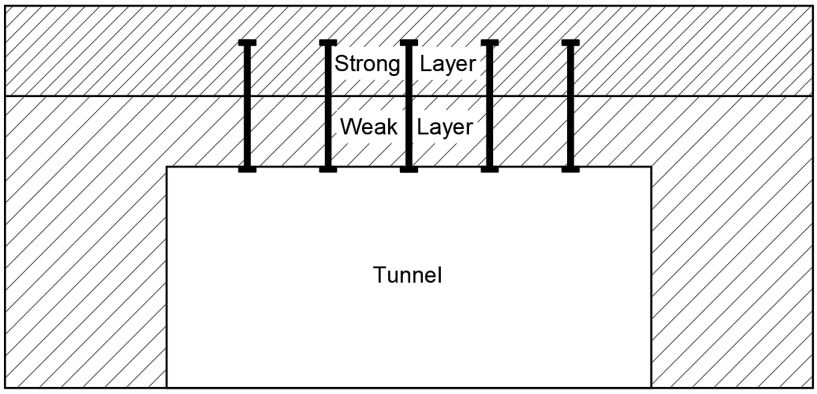

Figure 2.1: Bolting in strong layer

Trafikverket has guidelines for how calculations are to be performed. The method described here is derived from their guidelines 'Projektering av Bergskonstruktioner' [14]. The method only considers the actual weight of the weak rock and therefore the fundamental idea is to determine that the design load is smaller than the strength of the bolts.

$$W_{\mathrm{d}} < A_{\mathrm{s}} \cdot f_{yd} \tag{2.1}$$

Where A_s is the cross section area of the bolt and W_d is the design load and can be expressed by:

$$W_{\mathrm{d}} = W_{\mathrm{k}} \cdot \gamma_{\mathrm{d}} \cdot \gamma_{\mathrm{G:dst}} \tag{2.2}$$

$\gamma_{\mathrm{G:dst}}$ and γ_{d} are safety coefficents from Table 2.1. W_k is the characteristic load and calculated according to:

$$W_{\mathrm{k}} = S_1 \cdot S_2 \cdot h \cdot g \cdot \rho \tag{2.3}$$

where :

h = weight of the weak rock *[m]*

g = gravity coefficient

ρ = the density of the rock *[kg/m3]*

S_1 = distance between the bolts in the tunnels lengthwise direction*[m]*

S_2 = distance of the bolt in the tunnels cross-section width *[m]*

f_{yd} is determined by:

$$f_{yd} = \frac{f_{yk}}{\gamma_s} \tag{2.4}$$

where :

γ_s = partial coefficient for different materials purposes interpreted from the most fitting parameter in Table 2.1

f_{yk} = characteristic tensile capacity of steel *[MPa]*

Equations 2.1, 2.2, 2.3, 2.4 can then be used to create the following expression:

$$W_k = S_1 \cdot S_2 \cdot h \cdot g \cdot \rho \tag{2.5}$$

Table 2.1: Table of partial coefficients $\gamma_{G:dst}$ γ_d

	Partial coefficients
Intended design	$\gamma_{G:dst}$
Permanent, unfavorable load	1.1
Exceptional	-
Safety class	γ_d
2	0.91
3	1.0

2.2.2 Roofs with homogeneous layers above

It is not possible to anchor bolts in a stronger layer located above when all layers are of the same thickness and strength, since all layers are of equal bearing capacity. This is common in tunnels and mines constructed in sedimentary rocks such as coal mines. Instead pre-tensioned bolts that compress the layers located above are used in order to create a unified laminated beam that functions as the roof. The bolts needs to be protected against corrosion depending on how permanent of a structural element they become. [15]

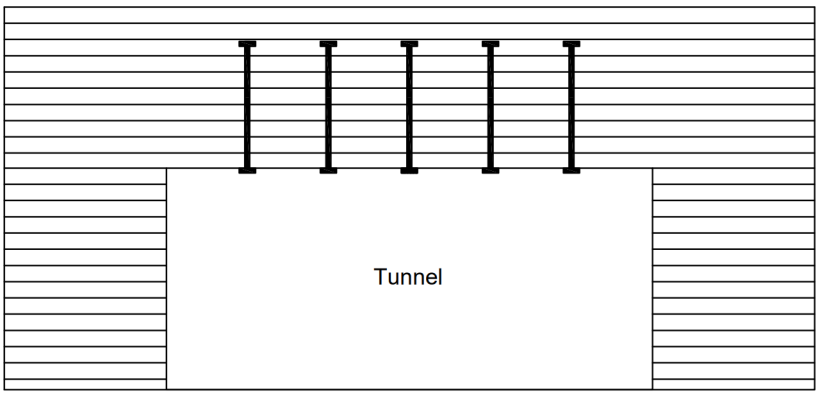

Figure 2.2: Bolting in weak and uniform layers

2.2.3 Bolts in Kvarntorp

Based on a site visit at the Kvarntorp mine it was determined that all bolts, new and old, were bolted in a pattern as shown in Figure 2.3. This systematic bolting continued throughout the mine except in some minor locations where extra bolts had been fitted. The old bolts that were originally fitted had served their lifespan and replacement bolts have been fitted in most of the active test facilities and storage rooms, in almost the same location and in the same pattern.

No bolts in the mine are tensioned [17]. Even though the mine does not have a strong uniform layer above the roof, as described in Section 2.2.1, to support passive bolts it is still the preferred method. The way that this bolts are fitted is by grouting the entire length of the bolt and creating a firm surface for the bolt to adhere to.
Since the bolts are fully grouted, the support they provide is based on adhering the layers together instead of compressing them together into a sort of beam as described in Section 2.2.2.

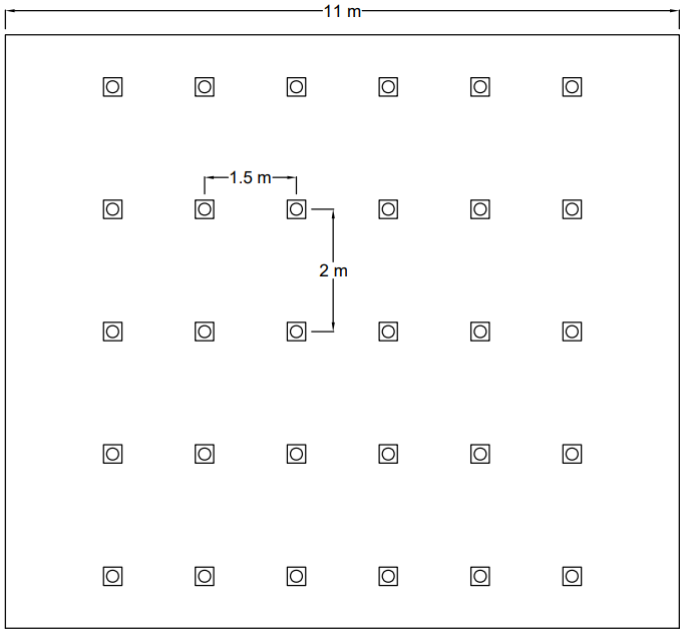

Figure 2.3: The existing bolt patterns in the Kvarntorp mine

2.3 Rock Classification Systems

Nowadays, highly sophistical methods that are used to classify rock strength through numerical analysis exist. In general, these methods are desirable when they are possible to use. However, tasks oftentimes become so complex that it is not feasible to model the problem through numerical analysis. Instead, there are different, more convenient methods available that are largely built on prior knowledge and experience. What has worked before and what will most likely work again? In order to compile and assess several years of accumulated experience, different classification schemes have been introduced. These systems look to attribute numerical values to

rock mass properties that are deemed to influence the behaviour of the rock. The values are combined into a total rating for the rock mass, which signify what design is necessary [11]. Design aspects that have been evaluated through such systems include:

- Stable spans of unsupported excavations
- Stand-up times of given unsupported spans
- Support requirements for various spans
- Cavability
- Stable pit slope angles
- Hanging wall caving angles
- Fragmentation

While these systems offer a conventional and simple approach to assessing the necessary support, there are also major shortcomings that need to be taken into account. In particular, trustworthy results are only received when the application of the system is in line with the rock masses and circumstances that it was initially developed for. If the circumstances are different, the systems may instead lead to faulty or even disastrous results [11]. Among these systems, the most prominent and commonly used are Bienawski's RMR-system and Bartin et. al's Q-system [6][7]. While they have very much in common, their intended uses vary slightly as they were developed using data from different circumstances. Furthermore, within coal mines the most prominent system is the Coal Mine Roof Rating, which will also be described in this section [5].

2.3.1 Rock Mass Rating, RMR

The Rock Mass Rating, RMR, was developed using data from excavations in sedimentary bedrock in South Africa [11]. The first widely used version of it was presented in 1976 by Bieniawski, who also later updated the system in 1989 [14] [6]. It consists of the following five parameters.

1. **Strength of intact rock material** is the uniaxial compressive strength of the intact rock [11]. It is defined as the strength measured on rock specimen with a diameter of 50mm and can be assessed through the following tests [14]:
   - Uniaxial test
   - Point-load tests
   - Results from prior tests in the same or similar rockbed
   - Index-testing through ISRM standard
2. **Rock Quality Designation, RQD,** is a quantification of the discontinuity spacing. It can either be determined through drill core mapping or calculated through Equation 2.6 and 2.7 [14].

$$RQD = 100e^{-0.1\lambda} \cdot (0.1\lambda + 1) \tag{2.6}$$

$$\lambda = 1/\overline{x} \tag{2.7}$$

where $\overline{x}$ is the average distance between discontinuities measured in meters. In the case of λ values between 6-16 per meter, RQD can be calculated through Equation 2.8 [14].

$$RQD = -3.68\lambda + 110.4 \tag{2.8}$$

3. **Spacing of Joints** indicates the perpendicular average distance between joint sets in the rockbed [14]. The term joints is used to describe all discontinuities in this context [11]. Furthermore, the rating acquired from this parameter is intended for a rockbed with three joint sets. The determination of the rating should be treated conservatively if the amount of joint sets is less than three and an increase of the rating by 30% is adviced in such cases [14].
4. **Condition of Joints** indicates the aperture or separation between discontinuities as well as their continuity or persistance, their surface roughness and the character of any in-filling material [14][11].
5. **Groundwater Conditions** represent the groundwater conditions in the bedrock. A forecast of the groundwater flow or pressure can be made through hydrological investigations or groundwater modeling. In this case, the groundwater condition can be described and rated by inflow per 10 meter tunnel length. If this is not feasible it can instead be determined through the ratio between joint water pressure to major principal stress or by a qualitative observation to determine general conditions [14][11].

The rating value for each of these parameters is obtained through Table A.1. The actual rock mass rating is obtained by adding these parameter values together as per Equation 2.9.

$$RMR = R_1 + R_2 + R_3 + R_4 + R_5 \tag{2.9}$$

This rating can be adjusted to take into account the influence of the rock discontinuities orientation through the corrections described in Part B of Table A.1. The expressions used in this part of the table are further explained in part F. The values from Part B are added to the rock mass rating but as they are negative they will reduce the rating. This table further shows how to make use of the total rating. The class assigned to rock mass from it's total rating is described in Part C on a scale from 'very poor rock' to 'very good rock'. Part D shows an interpretation of the rating through average stand-up time for underground excavations as well as the cohesion and friction angle of the rock mass [11]. Furthermore, assistive guidelines regarding the classification of discontinuity conditions are found in Part E.

The support recommendation acquired from RMR is dependant on the rating itself. Figure 2.2 shows the recommendations based on the rating.

Table 2.2: Recommended support based on the rock mass rating [6]

Rock mass class	Excavation	Support		
		Rock bolts (20 mm diam., fully bonded)	*Shotcrete*	*Steel sets*
1. Very good rock RMR: 81-100	Full face: 3 m advance	Generally no support required except for occasional spot bolting		
2. Good rock RMR: 61-80	Full face: 1.0-1.5 m advance; Complete support 20 m from face	Locally bolts in crown, 3 m long, spaced 2.5 m with occasional wire mesh	50 mm in crown where required	None
3. Fair rock RMR: 41-60	Top heading and bench: 1.5-3 m advance in top heading; Commence support after each blast; Commence support 10 m from face	Systematic bolts 4 m long, spaced 1.5-2 m in crown and walls with wire mesh in crown	50-100 mm in crown, and 30 mm in sides	None
4. Poor rock RMR: 21-40	Top heading and bench: 1.0-1.5 m advance in top heading; Install support concurrently with excavation - 10 m from face	Systematic bolts 4-5 m long, spaced 1-1.5 m in crown and walls with wire mesh	100-150 mm in crown and 100 mm in sides	Light ribs spaced 1.5 m where required
5. Very poor rock RMR < 21	Multiple drifts: 0.5-1.5 m advance in top heading; Install support concurrently with excavation; shotcrete as soon as possible after blasting	Systematic bolts 5-6 m long, spaced 1-1.5 m in crown and walls with wire mesh. Bolt invert	150-200 mm in crown, 150 mm in sides, and 50 mm on face	Medium to heavy ribs spaced 0.75 m with steel lagging and forepoling if required. Close invert

2.3.2 Q-System

The original version of the Q-system was presented in 1974 by Barton, Lien and Lunde [7]. It was developed with the aim of being able to estimate support requirements for tunnels in hard rock in Scandinavia [11]. The five original parameters have remained since then, with a new parameter called Stress Reduction Factor, SRF, added in 1993 [18]. While the parameters remained the same, the system was further updated by Barton in 2002 [14][19].
The six parameters used in the Q-system are presented below.

1. **Rock Quality Designation, RQD,** is assessed as presented in Section 2.3.1. It is advised to be assessed in three perpendicular orientations, with several measurements in each direction, using the average value of RQD in each direction for the final assessment of Q [11]. It is further described by the Norwegian Geotechnical Institute that for weakly consolidated or strongly weathered non-cohesive material, for example clay, RQD should be valued as 10. This is the case even if no discontinuities are found, as the whole material is to be considered as a weakness zone [20].
2. **Joint Set Number, J_n,** represents the amount of joint sets in the rock mass. It can vary between 0.5 for massive rock with few or no joints and 20 for disintegrated rock [11]. It is also influenced by the foliation, schistosity and

the layering of the rock. The value for J_n only take into account joints that define blocks in the rock mass [14].

3. **Joint Roughness Number, J_r**, represents the roughness of the joints. It can vary between 0.5 for sleek planar joints to 4 for discontinuous joints [14]. The roughness is to be determined in the direction where gliding is the most probable and shall be determined for the least favourable joint set in terms of stability with both orientation and shear resistance in consideration [19].
4. **Joint Alteration Number, J_a,** represents the condition or alteration degree of the structures in the rockbed. It can vary from 0.75 for tight, healed, rigorous, non-softening and impermeable filling materials up to 20 for thick, continuous zones or bands of clay [14] [11].
5. **Joint Water Reduction Factor, J_w**, represents the groundwater or inflow of water into the tunnel or rock structure. In some cases it can be determined in an early stage through geological interpretations and hydrogeological investigations. It is commonly determined as the tunnel is driven forward as it is more conventional. As a result, the pre-grouting affects the value of J_w and therefore also the final Q-value. Furthermore, the inflow into the tunnel may vary with time as cracked or broken material is washed away and if the tunnel or room is close to the surface it may vary with the season. The value of J_w can vary between 0.05 for exceptionally high continuous inflows without any noticeable decrease by time to 1.0 for dry or minor inflows such as moisture or occasional dripping [14][11].
6. **Stress Reduction Factor, SRF**, is a factor that corresponds to the effect of stresses acting on the rock mass. It varies between 0.5 for high stress but tight rock structure conditions without any noticeable decay and 400 for heavy rock burst conditions or heavy squeezing rock pressures and instantaneous dynamic deformations in the rock [11]. The factor is determined by establishing what the current rock mass condition is from four main conditions:
   - Weakness zones that cross, and are deemed to influence, the stress-conditions around the tunnel or rock structure
   - Capable rock with rockstress issues
   - Creeping rock that shows time-based deformation or behavior
   - Swelling rock caused by clay minerals in contact with moisture

   As a main condition has been established for the rock, there are further more detailed classification conditions that are used to find the final value of SRF for the rock [14].

The Q-value is calculated through Equation 2.10 using the values garnered for each parameter. In the equation the parameters are paired together two and two, forming three different parts that each represents a part of the rock quality. $\frac{RQD}{J_\mathrm{n}}$ represent the block size, $\frac{J_\mathrm{r}}{J_\mathrm{a}}$ represent the frictional shear strength between blocks and $\frac{J_\mathrm{w}}{SRF}$ represent the active stress. If a part is deemed irrelevant it can be taken out of the equation [14].

$$Q = \frac{RQD}{J_\mathrm{n}} \cdot \frac{J_\mathrm{r}}{J_\mathrm{a}} \cdot \frac{J_\mathrm{w}}{SRF} \tag{2.10}$$

The Q-value is then used to determine the required rock support through Table 2.3, with the Q-value represented on the x-axis. The y-axis is calculated through Equation 2.11, where ESR is a factor dependent on the safety requirements of the underground opening. A low ESR value indicates that a high level of safety is necessary while a low value indicates that a lower safety level is acceptable.

$$y = \frac{\text{Span or height in meters}}{\text{ESR}} \tag{2.11}$$

Table 2.3: Permanent support recommendations based on Q-value and span/ESR [20]

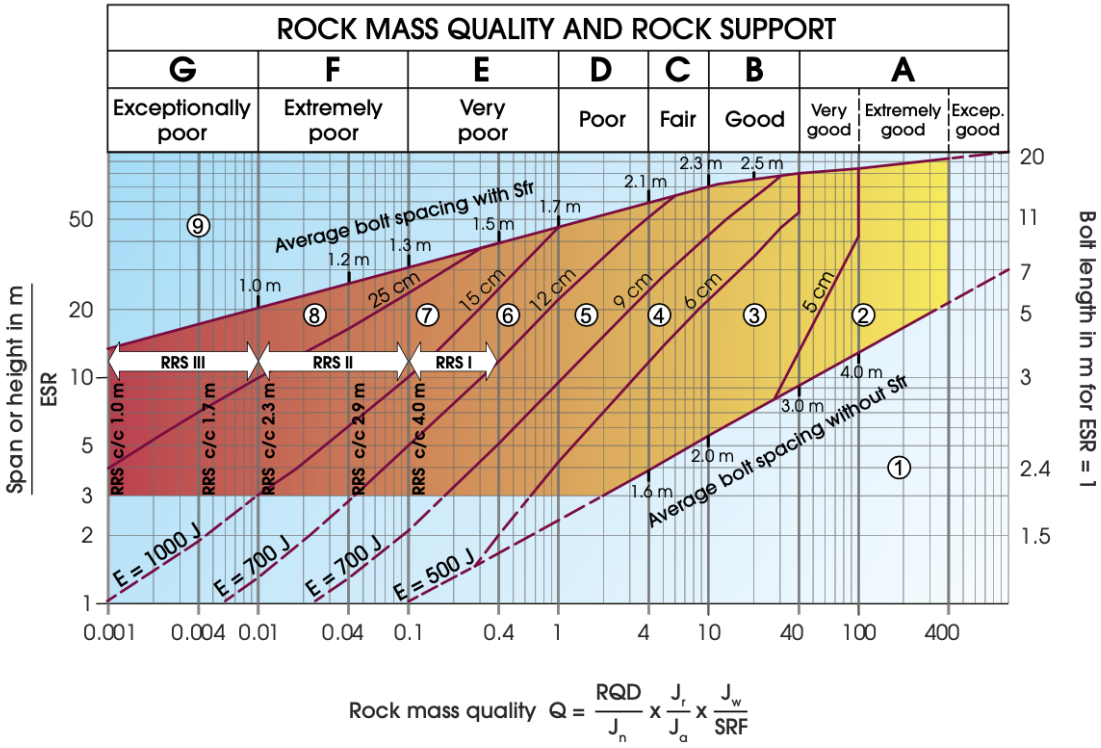

Support categories

① Unsupported or spot bolting
② Spot bolting, **SB**
③ Systematic bolting, fibre reinforced sprayed concrete, 5-6 cm, **B+Sfr**
④ Fibre reinforced sprayed concrete and bolting, 6-9 cm, **Sfr (E500)+B**
⑤ Fibre reinforced sprayed concrete and bolting, 9-12 cm, **Sfr (E700)+B**
⑥ Fibre reinforced sprayed concrete and bolting, 12-15 cm + reinforced ribs of sprayed concrete and bolting, **Sfr (E700)+RRS I +B**
⑦ Fibre reinforced sprayed concrete >15 cm + reinforced ribs of sprayed concrete and bolting, **Sfr (E1000)+RRS II+B**
⑧ Cast concrete lining, **CCA** or **Sfr (E1000)+RRS III+B**
⑨ Special evaluation

Bolts spacing is mainly based on Ø20 mm

E = Energy absorbtion in fibre reinforced sprayed concrete

ESR = Excavation Support Ratio

Areas with dashed lines have no empirical data

RRS - spacing related to Q-value

I **Si30/6 Ø16 - Ø20 (span 10m)**
D40/6+2 Ø16-20 (span 20m)

II Si35/6 Ø16-20 (span 5m)
D45/6+2 Ø16-20 (span 10m)
D55/6+4 Ø20 (span 20m)

III D40/6+4 Ø16-20 (span 5 m)
D55/6+4 Ø20 (span 10 m)
Special evaluation (span 20 m)

Si30/6 = Single layer of 6 rebars, 30 cm thickness of sprayed concrete
D = Double layer of rebars
Ø16 = Rebar diameter is 16 mm
c/c = RSS spacing, centre - centre

2.3.3 Coal Mine Roof Rating, CMRR

Coal Mine Roof Rating was developed in the mid nineties as a way to combine site characterization and engineering design. The driving forces behind it were similar to other classification systems like RMR and Q, in that it tries to make a complex problem more comprehensive. It utilizes the shared and accumulated experience and knowledge of what works and what does not in order to streamline any initial design plans for supports underground [5].

CMRR works in two parts, first it characterizes the different layers, which are called units in the rating system. The units assessed are all within the span of the bolt length. Each unit is then given a unit rating "UR". The unit rating consists of different parameters that are added together. The ratings are based on Table 2.4 - 2.7. The final UR is the sum of all the individual rating as per Equation 2.12. To manage and present the observations and test results for the CMRR classification the chart seen in A.1 can be used.

$$\begin{aligned} UR = &\text{ UCS Rating} \\ &+\text{Discontinuity Intensity Rating} \\ &+\text{Discontinuity Shear Strength Rating} \\ &+\text{Multiple Discontinuity Adjustment} \\ &+\text{Moisture Sensitivity Deduction} \end{aligned} \tag{2.12}$$

Table 2.4 shows which CMRR-rating that corresponds different compression strengths. Either from conventional laboratory compression tests or by assessing it from the indentation a ball peen hammer makes in the rock when hit. See Figure A.1 for visualization of the indentations.

Table 2.4: Uniaxial compression strength ratings and ball peen hammer approximations recreated from [5]

Ball Peen Hammer Classification	**Williamson UCS Range [MPa]**	**CMRR UCS Range [MPa]**	**CMRR Rating**
Molds	<7	14	5
Craters	7-21	14-35	10
Dents	21-56	35-70	15
Pits	56-105	70-120	22
Rebounds	105	120	30

Table 2.5 gives the user a CMRR-rating based on the observation of the joints and the cohesion within them. To test the cohesion, one can use a hammer and a chisel and based on how much force in necessary, one can then assess how strong the cohesion would be and receive a CMRR-rating from the table. If the bedding is without joints or discontinuities it is possible to apply the test to the intact rock mass.[5]

Table 2.5: CMRR-rating for Bedding/Discontinuity recreated from [5]

Roughness	**Cohesion**			
	Strong	**Moderate**	**Weak**	**Slickensided**
Jagged	35	29	24	10
Wavy	35	27	20	10
Planar	35	25	16	10

Table 2.6 is linked to the moisture sensitivity and presents a corresponding CMRR-rating to both and immersion test as well as a slake durability test. Note that this CMRR-rating is negative and is thus used as a reduction.

Table 2.6: Moisture Sensitivity Classes and ratings from both immersion and slake durability tests recreated from [5]

Moisture Sensitivity Class	**Rating Adjustment**	**Immersion Index**	**Slake Durability Index**
Not sensitive	0	0-1	98-100
Slightly sensitive	-3	2-4	92-98
Moderately sensitive	-7	5-9	80-92
Severely sensitive	-15	9	80

Table 2.7 creates a rating based on the persistence and spacing of the discontinuity of the rock mass. As an example: If a joint set is longer than 3m (has a persistance of >3m) and the individual joints within the set are spaced by one meter, then the rating would be 25.

Table 2.7: Bedding/discontinuity intensity rating for underground data recreated from [5]

	Spacing				
Persistence	>1.8 [m]	0.6-1.8 [m]	0.2-0.6 [m]	60-200 [mm]	<60 [mm]
0-1 [m]	35	30	24	17	9
1-3 [m]	32	27	21	15	9
>3 [m]	30	25	20	13	9

The second part is to calculate the roof rating. These units are weighted together in order to create the thickness weighted average called RRW, calculated through Equation 2.13 [5].

$$RRW = \frac{UR_1 \cdot L_1 + UR_2 \cdot L_2 + UR_3 \cdot L_3}{L_1 + L_2 + L_3} \tag{2.13}$$

Where:

$$L_{bolt} = L_1 + L_2 + L_3 \tag{2.14}$$

L_1, L_3, L_3 are the actual thickness of the layers unless any layer thickness exceeds the bolt length. In that case the last L will be the remaining length of the bolt as illustrated in Figure 2.4

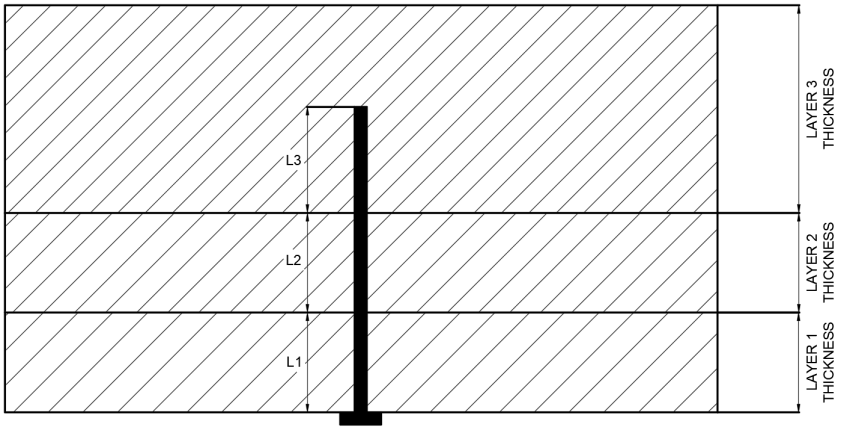

Figure 2.4: Illustration of how the layer thickness is included in CMRR

To get the final CMMR-rating, different reduction indexes are added to the RRW. An example of this is the moisture reduction seen in Figure 2.6.
To then utilize the CMRR in practical support applications in determining the preliminary support (PRSUP) Equation 2.15 is used [21].

$$PRSUP = \frac{L_{bolt} \cdot N_b \cdot C_c}{14.5 \cdot S_B \cdot W_e} \tag{2.15}$$

where :

L_{bolt} = length of the bolt *[m]*
N_b = number of bolts per row
C_c = capacity *[kN]*
S_b = spacing between rows of bolts *[m]*
W_e = entry width *[m]*

An empirical study found that the value for PRSUP in order to solve for the desired parameter was: [21]

- $PRSUP = 15.5 - 0.23 \cdot CMRR$ (Low cover)
- $PRSUP = 17.8 - 0.23 \cdot CMRR$ (High and moderate cover)

2.3.4 Geological Strength Index, GSI

The original Geological strength index was first introduced in 1994 and 1995 by Dr. Ewert Hoek and Hoek et. al respectively [22]. It is a rock characterization and classification system, which was originally intended to make it possible for educated observations to be represented as a numerical value [23]. The system uses a chart to determine the GSI-value. The original chart has seen some changes over the years but has in general stayed the same. The one published by Hoek and Marinos in 2000 can be seen in Figure A.2. The GSI-value received is a numerical value between 0 and 100, where 100 represents completely intact and structurally sound rock. This value is then utilized in the generalized Hoek Brown failure criterion to calculate the principal stresses and plotting the failure plane. Unlike the Mohr-Columb failure criterion, the Hoek-Brown criterion is nonlinear.

Unlike the other rock mass classification systems such as the Q-system and the Rock Mass Rating system (RMR), the Geological strength index does not suggest anchoring and supports directly. As mentioned earlier, GSI is merely a method to visually observe the surroundings and make it applicable to the the Hoek-Brown failure criterion in order to calculate the failure plane.
What makes the GSI system quite hard for inexperienced engineers is that the descriptive axis of the chart may seem arbitrary which can lead to a misuse of the system if its outputs are used directly in numerical models [24].

2.3.5 Generalized Hoek-Brown

The Generalized Hoek-Brown failure criterion is expressed by the following Equations 2.16 through 2.19 [22].

$$\sigma_1' = \sigma_3' + \sigma_{ci} \cdot (m_b \frac{\sigma_3'}{\sigma_{ci}} + s)^a \tag{2.16}$$

$$m_b = m_i \cdot e^{(\frac{GSI-100}{28-14D})} \tag{2.17}$$

$$s = e^{(\frac{GSI-100}{9-3D})} \tag{2.18}$$

$$a = \frac{1}{2} + \frac{1}{6}(e^{-GSI/15} - e^{-20/3}) \tag{2.19}$$

where :

σ_1' = the major effective principal stress at failure MPa
σ_3' = the minor effective principal stress at failure MPa
m_i = material dependent Hoek-Brown parameter
σ_{ci} = unconfined compression strength MPa
D = disturbance factor

The disturbance factor D is linked to how well or rather how much the excavation itself affects the surrounding of the tunnels. D spans from 0 to 1 depending on the quality of the excavation where D=0 represents perfectly executed blasting with

minimal influence of the surrounding rock or excavated with a road-header tunnel boring machine in good quality rock. Values closer to 1 is used for worse performed blasting in lesser quality rock. Where damage from the blasting extends around 2-3m into the existing rock structure [22]. The variable is sometimes simplified to simply 0.5 [22].

m_i is a material dependent constant and can be derived from the ratio between the compressive and the tensile strength of the rock [22].

Figure 2.5 shows how the the failure surface looks like after utilizing the GSI-value in the Hoek-Brown failure criterion. It also shows the relation between tension and compression and failure would occur.

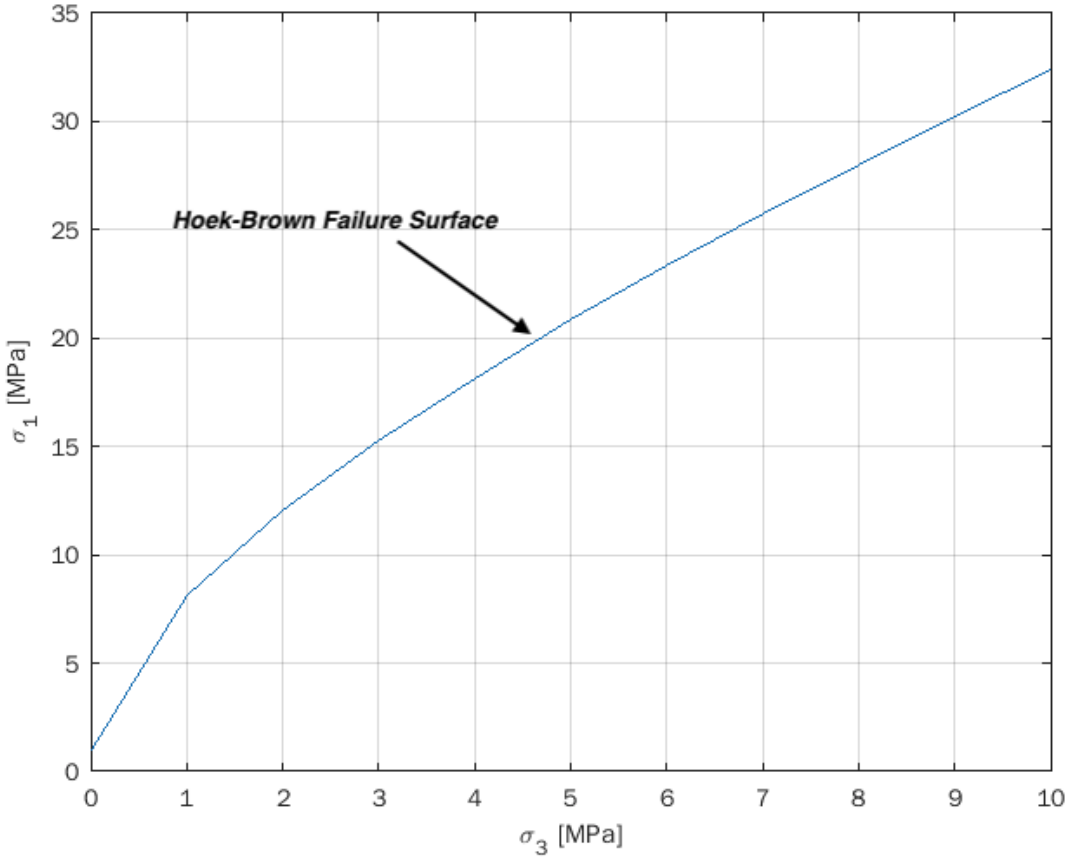

Figure 2.5: Schematic illustration of how the Failure Surface looks in the non-linear failure criterion.

In figure 2.5, σ_1 is plotted as a function of σ_3 using equation 2.16. This assumes that σ_1 always will be greater than σ_3. Stresses above the line are not possible and failure will occur along the line. Every stress value that occurs underneath the graph will not result in failure.

2.3.6 Area of use for RMR and Q-system

In a study conducted to find differences and similarities between the most common classification systems for rock, the Q-system was found to be the most sensitive to variations in parameters. Though, it was also found to be the simplest and most convenient to use [25]. However, the Q-system was created for use in hard rock in Scandinavia, while the RMR system was created for sedimentary rock similarily to CMRR [6][7]. Furthermore, RMR is more commonly used in mining studies compared to the Q-system [26].

2.4 Numerical Analysis

The numerical analysis utilises the Finite Element Method (FEM) through the software RS2, created by Rocscience. The software is suitable for both mining and civil applications [27].

2.5 Existing Conditions in Kvarntorp

This section presents the geological foundation of the Kvarntorp area and the mine itself. The data used in this chapter has been compiled of archived material from Sweco, publicly available data from the Swedish Geological Research, SGU as well as observations from a study visit to the mine by the authors. Furthermore, several tests where performed on rock from the site in order to garner the necessary input data. The theoretical context of the tests is presented in Section 2.6, while the detailed execution of the tests is outlined in Section 3.1.

2.5.1 Geological foundation

The area around the Kvarntorp mine consist of shale clay and sandstone as described in Section 1.1 [28] [29]. Eight boreholes were created for the initial geological investigations performed in 1980 for the mining operations and their location is mapped in Figure 2.6. These boreholes and the data collected from them were used to evaluate the thickness of the different layers as well as their geological characterization [29]. A cross section of the geological foundation in the Kvarntorp area is illustrated in Figure 2.7. The sandstone that is mined is a type called lingulid sandstone which is located upon a layer of mickwitzia sandstone, which is a common geological structure around the area of Kvarntorp [30]. The mickwitzia sandstone is reported to be sensitive to water as it may significantly reduce it's strength. However, it is also reported that there is a relatively low inflow of water from overlaying layers due to the impermeable nature of the clay shale. Furthermore, above the layer of lingulid sandstone there is a layer of phosphorite sandstone, with a thickness varying between 1.20 and 2.50 meters [29]. As the lingulid sandstone layer is of highest relevance in this study, it will from here on simply be referred to as the sandstone while the other two will be referred to with their respective full name.

Figure 2.6: Satellite image of the Kvarntorp area with boreholes 1-11 mapped

Within the sandstone layer, slightly different properties were found at different depths. This affected the mining operation as it was only economically viable to mine the sandstone of the highest quality. As a result of this, the geological investigations carried out for the mining operations had the sandstone layer divided into five different sublayers, which are illustrated in Figure 2.7. In the material it is described that sandstone layer 4 and 5 were deemed profitable to mine. Furthermore, these two layers are separated from the above sandstone by a segment of gray striped sandstone. This segment is apparent in all eight boreholes and the thickness of it varies between 0.03 and 0.17 meters. Therefore, it is also an indicator as to at what depth the mine tunnels have been excavated [29].
The geological properties of the different sublayers are presented below.

Sandstone Layer 1 (SL1) consists of fairly light to light fine-grained sandstone with slightly gray features. It has local additions of phosphorite in the top parts of the layer as well as occasional bands of shale clay. The thickness of the layer varies from 0.7 to 1.2 meters.
Sandstone Layer 2 (SL2) consists of varied layers of sandstone and shale clay in different proportions as well as sandstone with grains of clay (mainly in the lower parts). The thickness of the layer is 0.2 to 0.5 meters in boreholes 1 and 8 while it varies between 1.0 to 1.6 meters in boreholes 2-7.
Sandstone Layer 3 (SL3) mainly consists of fairly light to light fine-grained sandstone with few sporadic layers of shale clay. The layer also contain a seg-

ment of gray striped sandstone in its bottom part, which form the boundary to the mineable sandstone underneath in all eight boreholes.

Sandstone Layer 4 (SL4) mainly consists of light fine-grained sandstone with very minor additions of clay. The thickness of the layer varies between 1.6 and 2.7 meters. This layer is the first layer after the gray striped sandstone segment.

Sandstone Layer 5 (SL5) consists of clay-layered light fine-grained sandstone with varying density between the clay layers. The clay-layering is particularly prominent in the lower parts of the layer and even more so in borehole 7 and 8.

The thickness of the profitable sublayers of sandstone varies, as can be seen in Figure 2.7. Table 2.8 presents the total thickness of the profitable sublayers for each borehole. The average thickness of the boreholes is calculated to 4.9 meters.

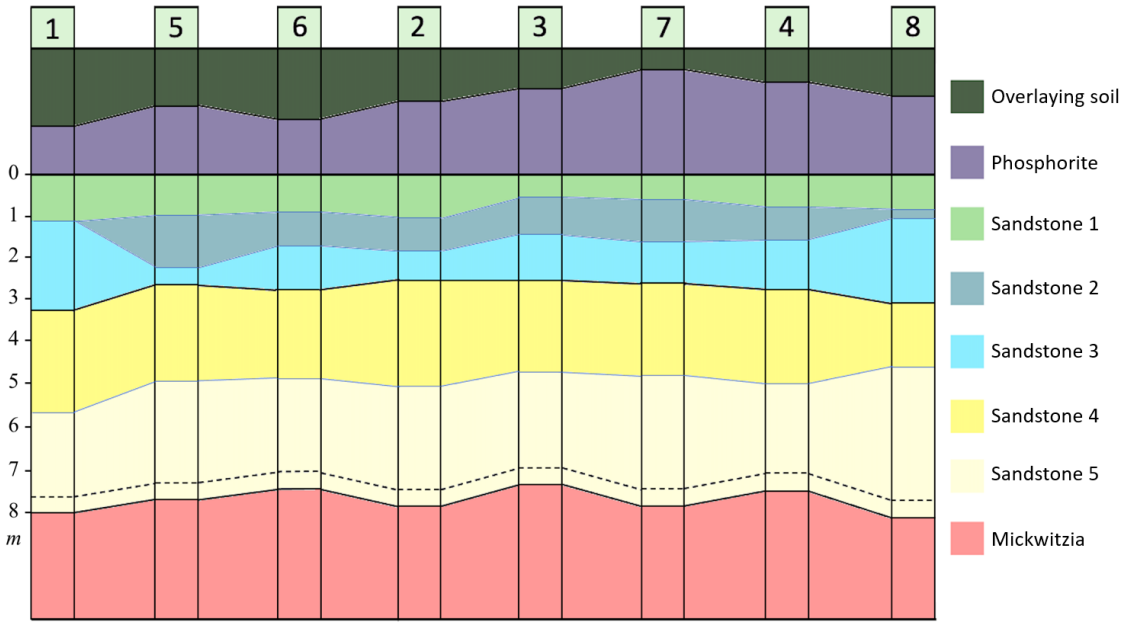

Figure 2.7: The soil and rock layers in Kvarntorp from boreholes created in 1980 [29]

2.5.2 Mine geometry

The mine in Kvarntorp has been shaped after the existing geological foundation described in Section 2.5.1. The principle of the excavation process is characterized as room and pillar mining, where the mined sandstone is extracted across a horizontal plane forming horizontal rooms with pillars of untouched rock between them [31]. In the Kvarntorp mine the pillars are not split up but instead shaped as a long rectangular wall along the rooms, as illustrated in Figure 2.8 [29]. This mining process is most suitable for deposits that are located in flat horizontal stratum as is the case with the sandstone in Kvarntorp [32]. Furthermore, it is specified that the bearing capacity is designed for the full operational period. This time period has passed and

Table 2.8: Thickness of the profitable sandstone for each borehole

Borehole	Thickness [m]
1	4.75
2	5.28
3	4.76
4	4.65
5	5.06
6	4.61
7	5.15
8	4.90

new reinforcement through renewed bolts has therefore been implemented [29].

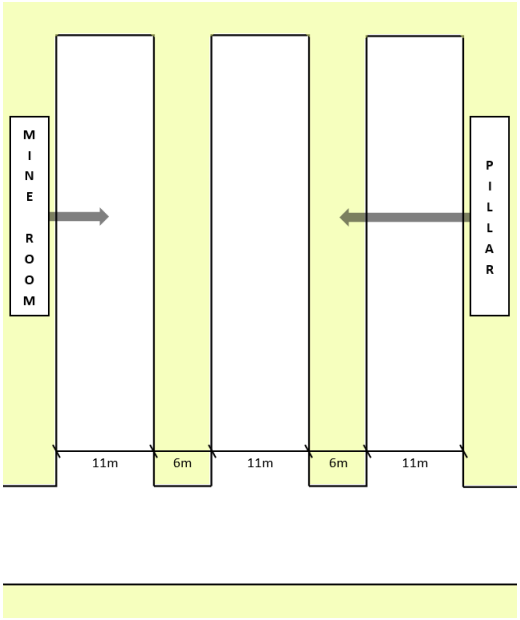

Figure 2.8: Illustration of the excavation rooms and pillars in the Kvarntorp mine

In the archived investigation material it is reported that the mickwitzia sandstone is very sensible to moisture as it can reduce it's strength significantly. Therefore it was determined that a 0.3m thick layer of the profitable sandstone was to be left above the boundary to the mickwitzia sandstone. As a result, the height of the mine tunnels would consequently be 4.6 meters as the average thickness of the profitable sandstone is 4.9 meters. However, in a later investigation carried out in 1990 of the mine, the height is referred to as 5 meters. It is unclear if this is a simplification for the calculations or if the height actually ended up as 5 meters in the mine. However, in this study, a height of 5 meters will be used as this is the latest available data [29]. The thickness of the pillars was determined to 6 meters, which coupled together with their long rectangular formation establish a large pressure area. This reduces the specific load on the mickwitzia sandstone and consequently deformations in it.

Furthermore, the roof span in the mine is reported as 11 meters with a flat roof shape. The full geometry of the mine tunnels is illustrated in Figure 2.9.

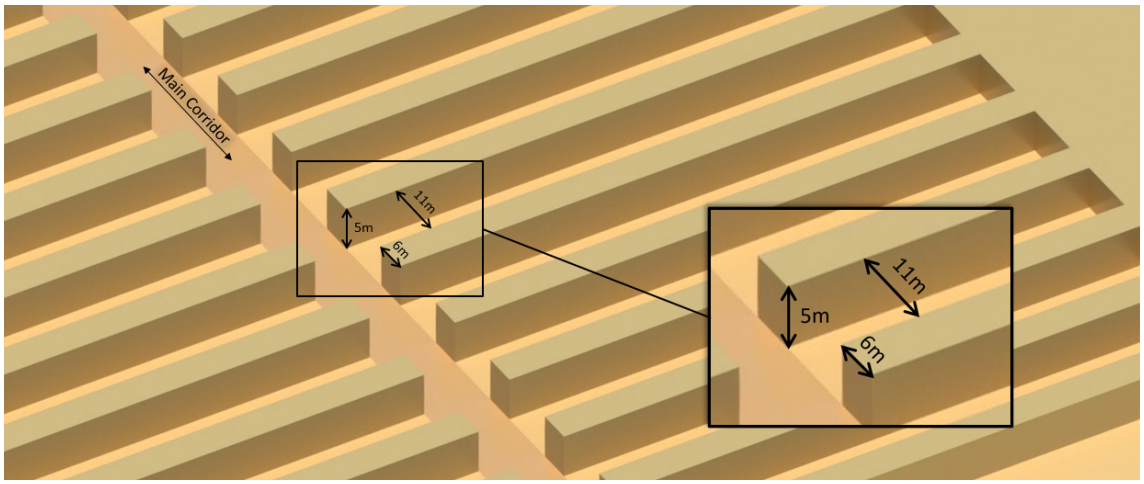

Figure 2.9: 3D sketch of a typical mine section

2.6 Laboratory Tests

Two tests were performed in the materials laboratory at Chalmers University of Technology to gather input data for the study. These two tests were a slake durability test and an immersion test. Furthermore, a point-load test was performed at the Sweco office in Gothenburg. The theoretical context of these tests will be presented in this section.

2.6.1 Point load test

Point load tests are used to determine the uniaxial compressive strength of rock. It is widely used due to the simplicity to perform it as it is an index test that requires little equipment. It is also capable to be used on specimens of various sizes, usually between 1.5 to 10 centimeters, and requires little to no specimen preparation. Due to the simplicity of the test it can easily be performed on-site and it is also simple to perform multiple tests. The shape of the specimen decides what type of point load test is to be performed. There are four commonly used types which are diametral, axial, block lump and irregular. The deciding factor for which type of test is the most suitable is the geometry of the available specimens. In the case of Kvarntorp, the available specimens are cylindrical, which is suitable for the diametral tests. Hence, only the diametral test type is further discussed in this report.

During a point load test a rock sample is subjected to compression between two conical steel units until it fails. The test apparatus is equipped with a loading measurement system and a system to measure the distance between the two steel units. It is deemed that the load measurements are accurate to at least 5%.

In a diametral point load test the dimensions of the specimen are crucial. The total length of the specimen must be twice as long as the diameter, as illustrated in Figure 2.10. The specimen is placed in the apparatus perpendicularly in order for the steel points to touch the specimen along its diameter. The distance between the steel points is measured, which should be equal to the diameter, before the sample is uniformly loaded until it breaks. Furthermore, anisotropic materials should be tested both parallel and perpendicularly to the anisotropy planes in order to determine maximum and minimum strength. As the sedimentary bedrock in Kvarntorp is anisotropic, this applies to this study [33][34].

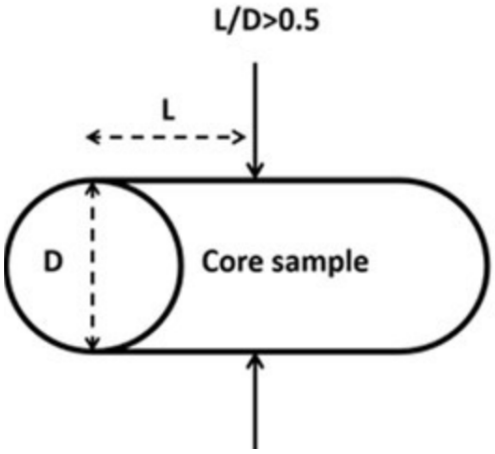

Figure 2.10: The required shape of specimen for a diametral point load test [35]

2.6.2 Immersion test

Immersion tests are used to determine the specimen's sensitivity to moisture or water [5]. It is performed on either one or multiple specimens and each part of the test is observed and given a score as in the data sheet shown in Figure A.3. The specimen(s) is first tested for hand-breakability. It is then rinsed to remove any dirt or dust on it, before being placed into water for 1 hour. The water and specimen(s) is observed as the specimen(s) has been raised from the water. The appearance of the water, the talus formation and the cracking of the sample is determined and rated according to Figure A.3. These ratings summed up determine the total immersion index. In order to observe changes in the breakability of the specimen(s), it has to be retested for hand-breakability. The change in breakability determine the breakability index. The final test index to be used is the greater of the total immersion index or the breakability index [5].

2.6.3 Slake durability test

Slake durability tests are used to determine how sensitive rock is towards water and erosion. It is performed on ten samples that each weight approximately half a kilogram (0.4kg - 0.6kg). The test is based on repeated wetting, drying and abrasion. The samples are dried in an oven and weighted before being rotated in a cylindrical metallic drum partially submerged in a waterbath for 10 minutes. This process of

repeated wetting and drying causes moisture or water sensitive rock to fracture or break down. The test can be used to determine the natural moisture content as well as a slake durability index. The natural moisture content is calculated through Equation 2.20 and the slake durability index through Equation 2.21, with the latter being the ratio between the initial dry weight and the final dry weight expressed in procent which is utilised as an input parameter in CMRR [5].

$$\mathrm{w} = \frac{\mathrm{A\ -\ B}}{\mathrm{B\ -\ C}} \cdot 100 \tag{2.20}$$

where :

w = percentage of water content
A = mass of drum and samples at natural moisture content
B = mass of drum plus oven-dried samples before first slake durability cycle
C = mass of drum

$$\mathrm{SDI} = \frac{\mathrm{W_f\ -\ B}}{\mathrm{B\ -\ C}} \cdot 100 \tag{2.21}$$

where :

SDI = slake durability index
W_f = mass of drum and oven-dried samples retained after the second slake durability cycle
B = mass of drum plus oven-dried samples before first slake durability cycle
C = mass of drum

The full procedure of the test based on the established procedure by ASTM International is listed below [36].

1. Weigh the drum.
2. Place the samples in the drum and weigh the drum and samples together.
3. Dry the drum with the samples in an oven for 16 hours or to a constant mass. Take out the drum and let it cool for 20 minutes.
4. Weight the drum and the samples together again.
5. Calculate the natural water content using Equation 2.20.
6. Fill the water basin with distilled water at a temperature of 20°C. Mount the drum in the water basin and to the rotation motor so that 60mm of the drum is below the water surface.
7. Perform the first slake durability cycle by rotating the drum for 10 minutes at a speed of 20 rpm.
8. Remove the drum immediately as the slake durability cycle is completed and dry it in the oven for 16 hours or to a constant mass again. Weigh the drum and samples after drying.

9. Repeat steps 6-8 again to obtain a final mass.
10. Calculate the slake durability index using Equation 2.21.

3
Methods

The method of this study evolved from the purpose to evaluate the applicability of CMRR in sedimentary bedrock. To achieve this, it was considered necessary to make a comparison between CMRR and the existing reinforcement system in Kvarntorp. To further broaden the scope of the comparisons, it was deemed appropriate to also include another classification system into the study. To fully comprehend the available classification systems as well as the existing reinforcement system in Kvarntorp a thorough investigative literature review as well as an observational site visit was carried out, which is presented in Chapter 2.

RMR is deemed to be the classification system that is most suitable to compare to CMRR, as described in Section 2.3.6. Consequently, both CMRR and RMR were evaluated for the Kvarntorp mine in order to retrieve the support recommendation appurtenant to each system, which is described in Section 3.2.2 and 3.2.1. The existing support system in Kvarntorp as well as the support recommendations obtained from the classification systems were then analysed through finite element simulations, described further in Section 3.3 and 3.4. Furthermore, GSI and Generalized Hoek-Brown were used to model the characteristics of the existing bedrock. The purpose of the finite element analysis was to observe deviations between the methods and from that establish which method is the most representative and suitable for rock construction in sedimentary bedrock.

3.1 Laboratory tests

Three laboratory tests were performed for this study, a slake durability test as well as an immersion test that was performed in Chalmers laboratory as well as point load tests at Sweco office in Gothenburg. The execution of these tests is outlined below.

3.1.1 Point load tests

Four point load tests were performed in Sweco's laboratory, as it is the recommended test to determine the compressive strength when using CMRR [5]. The tests were performed on drill cores and tested both normal and parallel to the horizontal joint set in order to better understand how the strength of the rock will behave in different directions. The procedure used for the point load tests is described in Section 2.6.1.

3.1.2 Immersion test

The immersion test was performed according to the standard described in Section 2.6.2. As the test is very simple in it's execution, no deviations from the standard had to be made. The test was carried out using five different specimen of slightly varying sizes.

3.1.3 Slake durability test

The slake durability test was performed according to the standard set out by ASTM International, described in detail in Section 2.6.3. However, as no equipment specifically manufactured for a slake durability test was available in the laboratory, equipment had to be crafted from scratch and certain minor deviations therefore had to be made. The dimensions described for the drum by ASTM International could not be fulfilled, and instead a larger drum had to be used [36]. The specified diameter was 14cm but the drum used for this study instead had a diameter of 15.5cm. ASTM International specifies that the drum should be submerged 2cm below the drum axis and as a result the water level was adjusted to reach the same submersion with the larger drum. The drum crafted for this test can be seen in Figure 3.1. Furthermore, the motor used for the test could not be set to a constant speed and instead had to be manually maneuvered. As a result, the speed varied slightly during the test. Though, the correct amount of rotations were still done in a 10 minute period as specified by ASTM International.

Figure 3.1: The drum constructed for the slake durability test filled with the 10 selected samples

3.2 Rating of Classification Systems

In order to acquire support recommendations from the classification systems a thorough rating process must be performed for each system. The process of acquiring these ratings is outlined in this section. Furthermore, as described in Section 2.3.6, the RMR system is better suited for the specific case of the Kvarntorp mine than the Q-system, as Kvarntorp is a sedimentary mine and the input data for this study contain uncertainties. Consequently, the RMR system will be used in this study and not the Q-system.

3.2.1 RMR

The theoretical foundation, charts and tables used for the RMR assessment is described in Section 2.3.1. More specifically, Figure A.1 was used when determining the classifications and acquiring ratings for the RMR assessment. All parameters were judged based on visual determination on-site and the Sweco archived material [29]. Certain parameters were hard to determine with certainty and therefore a con-

servative approach was taken when making the assessment. As a result, an interval was established with a minimum and maximum value. For the minimum value the lower rating was always chosen if there was any uncertainty regarding the rating output of a parameter and vice-versa for the maximum value.

The **strength of the intact rock material** was determined through the uniaxial compressive strength of 100 MPa available in the Sweco archived material [29].
The **rock quality designation, RQD,** was calculated using Equations 2.6, 2.7 and 2.8. However, no exact value for $\overline{x}$, the average distance between discontinuities, was available. Therefore intervals of $\overline{x}$ were established for each possible rating output available for the RQD parameter, as can be seen in Table A.1. Table 3.1 shows the possible values calculated for each rating. This approach allowed an estimation to be made based on the available intervals, which was carried out based on the descriptions of the overlaying sandstone layers described in Section 2.5.1 as well as observations of Sandstone layer 4 and 5 on-site.

Table 3.1: RQD rating for different average distances between discontinuities

RMR Rating for RQD Parameter	20	17	13	8	3
Average discontinuity spacing $[cm]$	18.8	10.4-18.8	6.1-10.4	4.31-6.1	0-4.31

Similarly, the **spacing of joints** was estimated based on the descriptions of the overlaying sandstone layers described in Section 2.5.1 as well as observations of sandstone layers 4 and 5 on-site, as no exact value could be acquired. As described in Section 2.3.1, it is advised to add 30% to the rating of this parameter if there is less than three joint sets in the rockbed. As only one joint set is to be found in the Kvarntorp mine this was done in this study.
The **condition of discontinuities** was also assessed based on the descriptions of the sandstone layers in Section 2.5.1 together with observations on-site.
The **groundwater** was assessed using the 'general conditions' section of Table A.1. It was based on on-site observations and the information available about the geological layers and groundwater from the archived material.
Furthermore, the **effect of discontinuities' strike and dip orientation** was taken into account using part F of Table A.1. In the case of Kvarntorp, a horizontal banking plane with a dip of 0.7° was the only present discontinuity.

The support recommendation acquired through RMR was retrieved from Table 2.2 using the calculated rock mass rating. As RMR is designed for tunnel excavations and not mines, the recommendation for shotcrete and steel sets is deemed to have a very minimal impact on the structural integrity necessary for the excavation in this specific case. Consequently, only the rock bolts are included in the finite element analysis described in Section 3.3. This simplification is further discussed in Section 5.2.

3.2.2 CMRR

The theoretical foundation, charts and tables used for the CMRR assessment is described in Section 2.3.3.

The **strength parameter** used in CMRR can be determined in a number of ways. In the CMRR-chart it is suggested to use a ball-peen hammer and to analyze the impact and indentation it creates in the rock. The indentation in the rock will correspond to different compressive strengths of the material, as can be seen in Figure A.1. This method makes it easy to quickly and visually assess the features of the rock on site. Alternatively, laboratory tests such as uniaxial compressive strength tests and/or point load tests can be performed. These tests are more advanced and their execution demands more resources but they do make it more reliable for inexperienced engineers to assess the strength of the rock, rather than determining rock strength on the spot. For this study, old results of uniaxial tests available in the archived material from Sweco were used as it was deemed more reliable than ball-peen tests and cheaper than performing new uniaxial tests [29].

There are several ways to determine the resilience to weathering of rock. The parameter called "*Moisture Sensitivity*" in the CMRR-chart shown in Figure A.1 can be assessed by either visually inspecting it or using an immersion and/or slake durability test as described in Section 2.3.3. For the purposes of this thesis, both an immersion test and a slake durability test has been performed. The method of these tests is presented in Section 3.1.

A visual assessment of the joints were made on-site in the mine. The distance between the joints were measured with a ruler.
Assessing the **joint spacing** in the three overlaying layers (SL1, SL2 and SL3), it was determined that the spacings were in the span of 0.2-0.6, this is representative but probably in the conservative end of the spectrum but a good point for assessing the worst case scenario. Since the discontinuities in the mine all come from horizontal joints that span most or often the entirety of the mine, the persistence was determined to 3m or above which results in an UR-rating from Table 2.7 of 20.

The **joint roughness** was observed on site and determined to be 'Wavy'. The **joint cohesion** was harder to determine as one would need to be very experienced to reliably determine it through the chisel method outlined in Section 2.3.3. However, it was noted that it was not possible to split the intact rock by hand but it was possible in certain joints. This indicates that the joints are significantly weaker than the intact rock. Similarly, the **joint cohesion** was determined on site and was established to be 'Weak'. Choosing 'Weak' and 'Wavy' results in an UR-rating of 20, as shown in Table 2.5.

The results of the observations on site as well as the calculated UR values are presented in Figure A.2. These values were then used in Equation 2.13 to get the RRW value as seen in Table 4.8. The adjustment rating was subtracted in and the final adjusted CMRR-value is also shown in Table 4.8.
Rearranging Equation 2.15 to solve for N_b gives the number of necessary bolts per row. The values used for this are seen in Table 4.8 and are acquired from the existing support in the mine as described in Section 2.2.3.

3.2.3 GSI

As described in Section 2.3.4, GSI utilises observations of existing rock mass in order to determine its overall quality. Using Table A.2 and matching the observations from the mine with the descriptive axis of the chart a final GSI-value can be obtained. This value can later be utilised for the Hoek-Brown failure criteria.

The rock in the mine is not very fractured based on what can be observed from the open surfaces in the mine, as can be seen in Appendix C. Almost all joints originate from the sedimentation stages during the formation of the sandstone itself. Among the alternatives on the left axis in Table A.2 the most fitting description was deemed to be blocky. Though, in some places it is almost intact while it is severally fractured in others. Generally, the sandstone looked and felt quite unweathered in most places. Based on the site visit and the pictures from it the sandstone was deemed to fit within the 'Good' column, being described as slightly weathered with some stains of iron, other metals and minerals along the length of the mine.

These observations and descriptions bring the final GSI range between 70 and 80, with slight variation between the different sandstone layers.

It is however hard to be able to assess how the fractures look in the layers above the roof with certainty but a range of 70-80 is considered reasonable for most of the general mine. Furthermore, based on the descriptions of the 5 main sandstone layers in Section 2.5.1, different values will be used for the different layers within the range of 70<GSI<80 in the RS2 model for the Hoek-Brown failure criterion. A sensitivity analysis of this parameter is presented in Section 4.3.9 investigating the effect of these assumptions.
The final GSI values used for the simulation are presented in Table 3.2.

Table 3.2: Summary of GSI-values for the different sandstone layers

Sandstone Layer	**GSI**
SL1	77
SL2	72
SL3	75
SL4	80
SL5	70

3.3 Finite Element

In RS2, the existing support as well as the recommended support from RMR and CMRR will be modelled, as well as a model with bolts mounted with an angle of 45°. In addition to those, a model with an increased height of the middle room will be made, both with existing bolt patters as well as a concrete liner. To compare these a final model without any support will also be analysed. The finite element analysis was carried out as a 2D analysis using the condition of plain strain.

As the mine consists of parallel tunnels, a cross-section of three representative tunnels will be drawn. This is to be able to analyze how the load will affect the long wall pillars that are a vital part of the supporting structure, as can be seen in Figure 2.8 and 2.9.
The bolt lengths used in Kvarntorp is almost exclusively 2.4m [17]. This will be used as the basis for the modeling of the existing support.

3.3.1 RS2 models and anisotropy

In order to establish a finite element analysis that represent the reality as well as possible two separate model types were created with the same geometry. The two model types were called *Anisotropic material model* and *Jointed material model*. Both model types were used for the the scenarios assessing the classification systems while five extra scenarios were created explicitly using the anisotropic material model. All the different models created for the scenarios are listed below. Additionally, images of bolting patterns and liner placement for each scenario can be found in Appendix B.

List of created models:

- Existing support - Anisotropic material model
- Existing support - Jointed material model
- RMR maximum value - Anisotropic material model
- RMR maximum value - Jointed material model
- RMR minimum value - Anisotropic material model
- RMR minimum value - Jointed material model
- CMRR - Anisotropic material model
- CMRR - Jointed material model
- Bolts installed at an angle of 45°- Anisotropic material model
- Increased height of the middle room without support - Anisotropic material model
- Increased height of the middle room with bolts - Anisotropic material model
- Increased height of the middle room with concrete liner - Anisotropic material model
- Unsupported initial conditions - Anisotropic material model

The difference in the model types concerned the anisotropy of the rock mass and thus how the joints were incorporated within the model. As this did not concern the geometry of the model it could be kept identical for both models. The geometry of the model in the region around the excavations is specified in Figure 3.2. However, the model size was increased significantly in order to assure that the side and bottom boundaries were not affected by the excavations. As a result, the model was increased by 800 meters from the excavations on each side and 100 meters from the bottom of the excavation. This resulted in a very stable stress state around the boundaries.

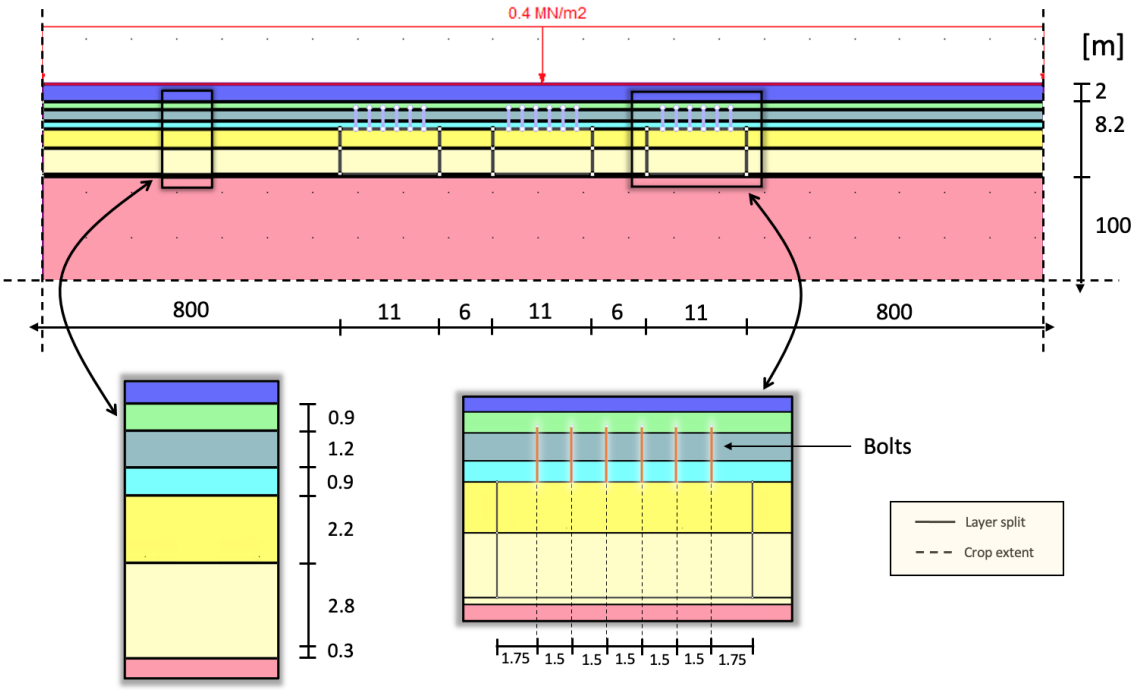

Figure 3.2: The geometry of the models zoomed in around the excavations, presented in meters with each color representing a unique rock layer

3.3.2 Overburden and pore water

In order to minimize the calculation times within RS2, the overlaying soil was reorganised into a load distributed evenly over the top of the model. The structure of the overburden in terms of soil layers and their thickness was retrieved from the Sweco archive and is illustrated in Figure 3.3 [29]. Representative values for the unit weight were then retrieved for each soil type which was used to calculate the distributed load through Equation 3.1 [29][37][38]. These unit weights can be seen in Figure 3.3. Furthermore, the load was increased to take the pore water of the overburden into account. As no information was available regarding the porosity of the overburden, an estimation had to be made. This resulted in the load being rounded up from 0.37905 MN/m to 0.4 MN/m as this increase was deemed to be on the conservative side. The distribution of the load is shown in Figure 3.2.

$$\text{Distributed load} = \gamma_{\text{ob}} \cdot 5.1 + \gamma_{\text{s}} \cdot 2.5 + \gamma_{\text{cs}} \cdot 9 \tag{3.1}$$

where :

γ_{ob} = unit weight of overburden

γ_{s} = unit weight of shale

γ_{cs} = unit weight of clay shale

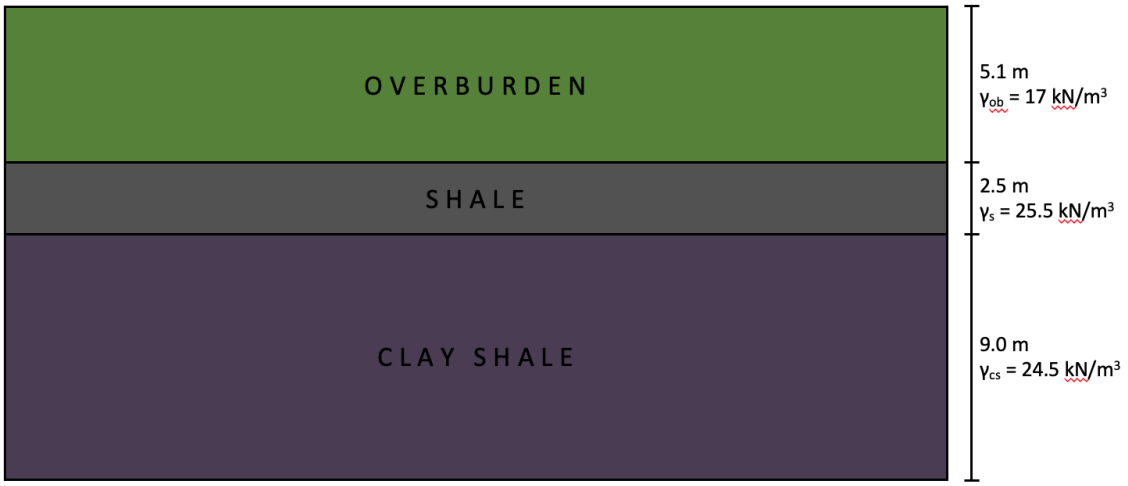

Figure 3.3: The overlaying soil reorganised into an evenly distributed load

As previously mentioned, two different models were created in order to handle the anisotropy of the model in two different ways within RS2. These two models are described below.

Anisotropic Material Model
The Anisotropic material model was created using an anisotropic failure criterion for the materials within RS2. This failure criterion is called the 'Jointed Generalized Hoek Brown' and it functions in the same was as the 'Generalized Hoek Brown' criterion described in Section 2.3.5 but also takes joints into account. This jointed failure criterion use multi-yield plasticity formulation to take one failure criterion for the jointed rock mass matrix and a virtually unlimited number of joints. The material model is further described in the 'Anisotropic Material Models' section of the manual for RS2 [27].

Jointed Material Model
The Jointed material model was created using the 'Generalized Hoek Brown' failure criterion described in Section 2.3.5. Unlike in the anisotropic model though, the joints were not taken into account in the material model and were instead added manually to the model. It is highly likely that the weakest joints are found in the border of the different sandstone layers described in Section 2.5.1. In order to simplify the model these joints were the only ones to be created as these are the most probable locations of failure.

3.3.3 Boundries of the FEM Model

As described in Section 3.3.1 above, two different types of models were made. However, both models have the same boundaries and mesh type. Low coverage and modeling most of the overburden as a distributed uniform load led to the model having a unrestrained top surface. The sides were instead restrained in the horizontal direction, but not vertical. Vice-versa the bottom boundary was restrained

in the vertical direction, but not the horizontal. Furthermore, the connecting nodes between the sides and bottom boundaries were restrained in both directions.
In order for the boundaries to not affect the results close to the excavations, the model was made very wide and deep, as described in Section 3.3.1. This was done through an iterative process until the stress state at the boundaries had no significant changes through the excavation process. Figure 3.4 and 3.5 shows the vertical and horizontal stress state at the vertical boundaries and bottom horizontal boundary respectively for the initial stage and the excavation stages. As can be seen, the variation of the stress is very minor and as a result deemed to be neglible.

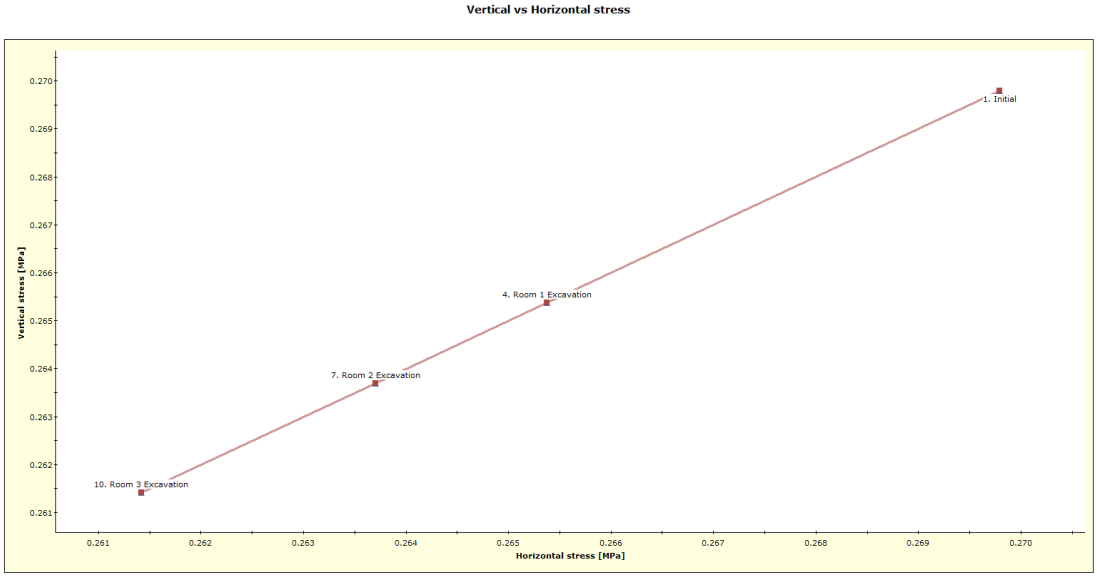

Figure 3.4: Vertical and horizontal stress state at the node with the most significant stress fluctuations at the vertical boundary

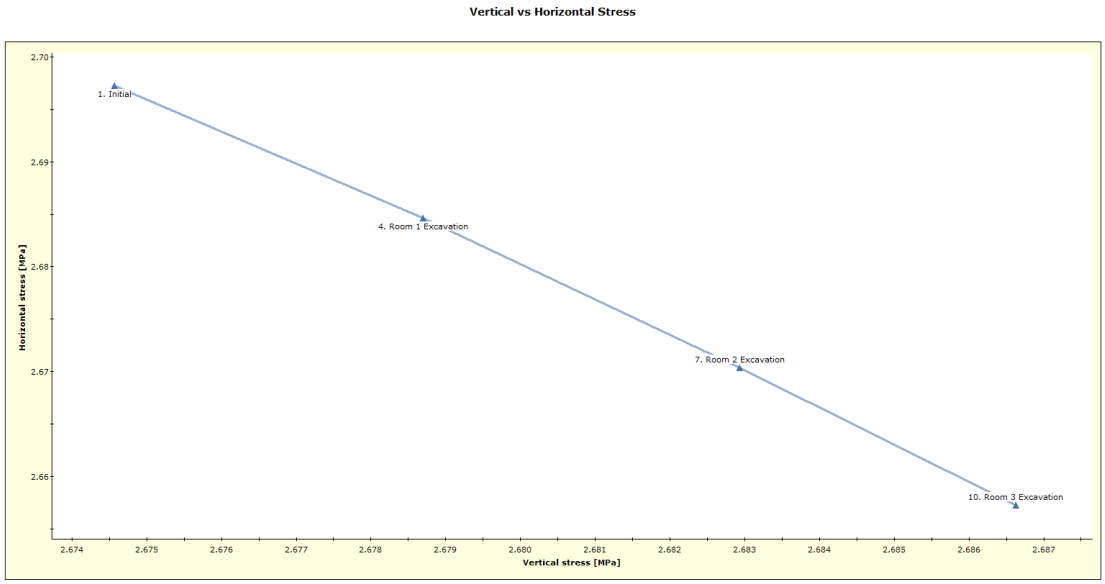

Figure 3.5: Vertical and horizontal stress state at the node with the most significant stress fluctuations at the bottom horizontal boundary

3.3.4 Excavation stages

Besides the initial stage, the stages in all models and for each separate mining room are: "Material", "Bolt" and "Excavation". In the material stage, Young's modulus is reduced with one third in order to simulate the initial deformation caused by the progressing excavation. This was done as in reality, the rock is first excavated and left unsupported whilst the support is installed. The bolts are then installed for each stage after the "Material" stage, right before the actual excavation is carried out in RS2. This was done in order to simulate that the bolting process occur as quickly as possible after any excavation progression.

3.3.5 Mesh discretization

A thorough mesh study was performed in order to generate a mesh that find an accurate solution but simultaneously keeps the computational times reasonable. Firstly, a large array of input settings was tested for the mesh of the full model. The main objective of this part was to create a mesh that has the same quality over the full model without any clearly noticeable discrepancies. This was done to assure the mesh will create similar results for all three different excavations within the model. Furthermore, the model size was increased significantly in order to assure that the side and bottom boundaries were not affected by the excavations, as described in Section 3.3.1. As a result, the model was increased by 800 meters from the excavations on each side and 100 meters from the bottom of the excavation. This part of the mesh study resulted in the general mesh setup settings shown in Table 3.3.
Secondly, an *Advanced Mesh Region* was created with the intention to further improve the mesh quality in the region around the excavations, where most of the displacement occur. The mesh region was setup to include all three excavations and

Table 3.3: General mesh settings

Parameter	**Input**
Mesh type	Graded
Element type	6 noded triangles
Gradation factor	0.02
Default number of nodes on all excavations	110

at least one excavation width extra on each side. The geometry for the advanced mesh region was set to x_1 = 15, x_2 = 95, y_1 = -14, y_2 = 2. This resulted in the advanced mesh region shown in Figure 3.6.

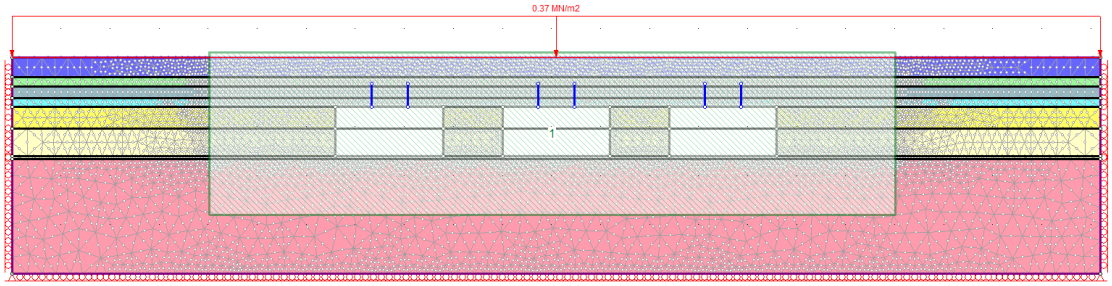

Figure 3.6: Advanced mesh region of the model in RS2

The element length of the advanced mesh region was then further tested through an iterative process. This process was performed to assure that the mesh produced accurate results around the excavations, as this area is the most interesting area for the study. The iterative process was performed by testing different element lengths and observing the maximum displacement occurring within the model, as shown in Table 3.4. The final element length was determined as the change of maximum displacement within the model became negligibly small between tests even as the element length was improved, which is illustrated in Figure 3.7.

Table 3.4: Iterative process to determine element length of advanced mesh region

Element length	**Maximum Displacement** *[m]*
3	$2.03 \cdot 10^{-3}$
2.5	$2.02 \cdot 10^{-3}$
2	$2.04 \cdot 10^{-3}$
1.75	$2.04 \cdot 10^{-3}$
1.5	$2.04 \cdot 10^{-3}$
1.4	$2.05 \cdot 10^{-3}$
1.3	$2.05 \cdot 10^{-3}$
1.2	$2.05 \cdot 10^{-3}$
1.1	$2.05 \cdot 10^{-4}$
1	$2.05 \cdot 10^{-4}$
0.9	$2.05 \cdot 10^{-4}$
0.8	$2.06 \cdot 10^{-4}$
0.7	$2.06 \cdot 10^{-4}$
0.6	$2.06 \cdot 10^{-4}$
0.5	$2.06 \cdot 10^{-4}$
0.4	$2.06 \cdot 10^{-4}$
0.3	$2.07 \cdot 10^{-4}$
0.2	$2.07 \cdot 10^{-4}$
0.1	$2.07 \cdot 10^{-4}$

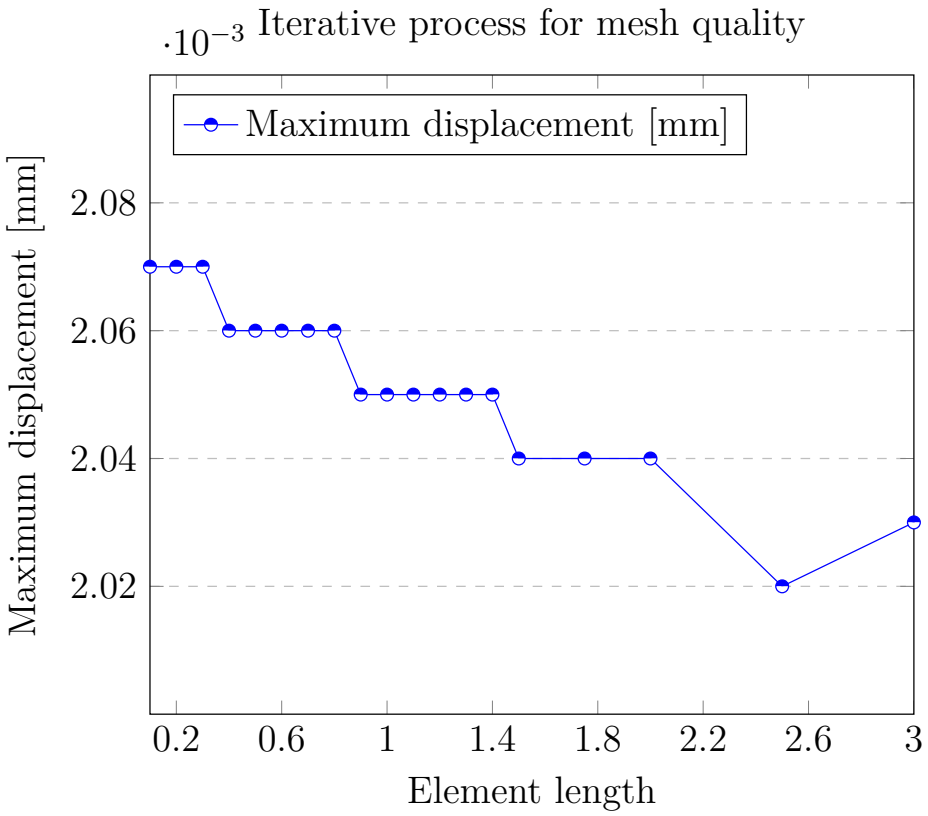

Figure 3.7: Plot of the iterative process to determine the element length of the advanced mesh region

Lastly, the mesh quality was investigated through the tool *Show Mesh Quality* within RS2. This highlights any problematic low quality sliver elements within the mesh. The criteria that define a low quality element was set according to Table 3.5. The mesh quality control was run with element lengths of 0.8 and below. It showed a total of zero problematic elements when being reduced to 0.5. As a result, an element length of 0.5 was determined as the final element length as the change in maximum displacement had halted at this point with no further significant changes if the element length was further reduced and no low quality elements were found. Simultaneously, the calculation time for the model was still deemed reasonable for the scope of the study.

Table 3.5: Criteria defining a low quality element

Parameter	**Input**
Ratio of (maximum side length / minimum side length)	30
Minimum interior angle	2°
Maximum interior angle	175°

3.4 Material Parameters and Assumptions

This section presents the material properties used in the finite element analysis. It also describes assumptions that had to be made and uncertainties are highlighted.

3.4.1 Sandstone parameters

The input parameters for the rock in the mine were gathered from a few different sources. In all cases possible, the archived material available from the investigations carried out in 1980 and 1990, previously mentioned as the archived material from Sweco in Section 2.5, was utilised. The available parameters that were utilised from this archive are listed in Table 3.6 and were assessed to have a low uncertainty as they are from on-site investigations carried out by professionals.

Table 3.6: Input data from the sweco archive

Parameter	Abbreviation	Value	Unit
Compressive Strength	UCS	100	MPa
Tensile Strength	UTS	4	MPa
Density	ρ	2.65	g/cm^3
Unit Weight	γ_{ss}	2650	kg/m^3

As the elastic modulus and Poisson's ratio were not available from the initial investigations, both had to be estimated. Unfortunately, sandstone has a massive variation in both parameters and as a result the determination of it was difficult and uncertain.
The elastic modulus is deemed to have a large variation. Several empirical equations between the elastic modulus and the compressive strength of sandstone are compared

in Figure 3.8 [39]. A potential range of values for the elastic modulus can be assessed through these empirical relationships and the UCS from Table 3.6 resulting in a range between 3 and 50 GPa.

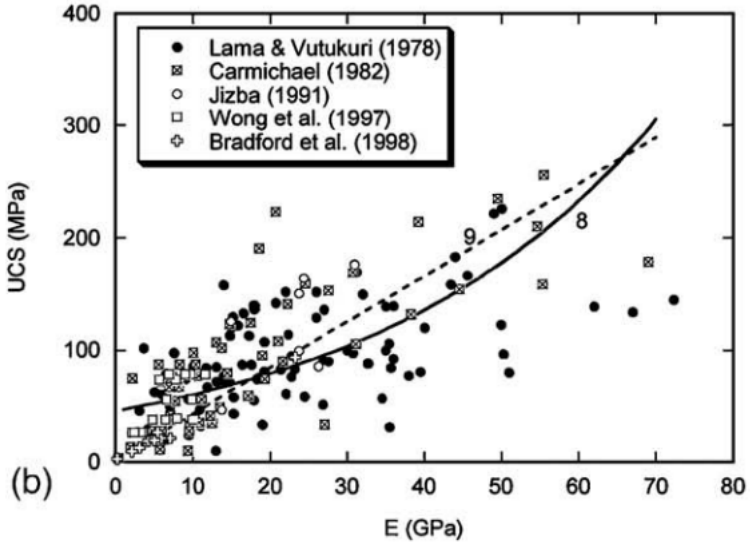

Figure 3.8: Correlation of the compressive strength and elastic modulus from different empirical equations on 260 sandstones [39]

A multitude of sandstone properties were analysed in order to find reasonable values for the elastic modulus and Poisson's ratio to be used in this study. Among all of the analysed sandstones, the ones with the closest correlation to the known values of the Kvarntorp sandstone were summarised in Table A.3. The variation of the parameters remain very large and no clear correlations between them were found. As a result, the values had to be assessed through a qualified estimation using the values available. The elastic modulus was estimated to 25 GPa and Poisson's ratio was estimated to 0.2. The uncertainty of this is further discussed in Section 5.1.

3.4.2 Joint parameters

The parameters for the joints were acquired separately for the two different models described in Section 3.3.1. Table 3.7 and Table 3.8 shows the input parameters used in the models.

Table 3.7: Joint input parameters for the anisotropic model

Parameter	**Value**	**Unit**
Dilation angle	0	°
Tensile Strength	0.4225	MPa
Peak cohesion	2	MPa
Friction angle	35	°
Incliation	0	°

In order to determine the tensile strength of the rock mass for the RS2 model, the

Table 3.8: Joint input parameters for the jointed model

Parameter	Value	Unit
Normal stiffness	25000	GPa/m
Shear stiffness	2.540	GPa/m
Tensile Strength	0.4225	MPa
Peak cohesion	2	MPa
Friction angle	35	°

Hoek-Brown failure criterion was used with Equation 2.16. The tensile strength of the rock mass can be acquired using this equation together with the input values listed in Table 3.6 while letting σ_1 be equal to zero and solving for σ_3.

3.4.3 Shear strength of joints in isotropic model

The normal- and shear strength of the joints are unknown. It can however be estimated based on the shear stiffness and the normal stiffness of the intact rock. The stiffness of the intact rock is 25 000 MPa and since the joints are very thin, their thickness is assumed to be 1mm. Assuming a strain of 0.1 in the peak strength scenario makes the total displacement in the joint 0.0001m.

$$\sigma = \epsilon \cdot E \tag{3.2}$$

Normal stiffness
Solving for σ in Equation 3.2 with E_{joint}=25 000 MPa and ϵ=0.1 gives σ=2500 MPa. The unit used in RS2 is MPa/m, and to achieve this σ is divided by the total displacement of $\delta_l = 0.0001$m, which results in Equation 3.3.

$$E_{Normal} = \frac{\sigma_{joint}}{\Delta_l} = \frac{2500}{0.0001} = 25000 \text{ GPa/m} \tag{3.3}$$

Shear stiffness
The shear stiffness is estimated similarly but is taking Poisson's ratio into account. Following the same procedure as for the normal stiffness, the normal strength σ=2500 MPa and the Poisson ration ν=0.2 results in Equation 3.4.

$$E_{Shear} = \frac{\sigma}{2 \cdot (1+\nu) \cdot \Delta_l} = \frac{2500}{2 \cdot (1+0.2) \cdot 0.0001} = 10.4 \text{ GPa/m} \tag{3.4}$$

3.4.4 Bolts

The bolts in the mine are as described in Section 2.2.3. They are all 2.4 meters in length and have a spacing of 1.5m and 2m as shown in Figure 2.3. Furthermore, the bolts have a diameter of 25mm and a steel class equal to B500-BT. This class means that the steel achieves an elastic peak tensile strength of 500 MPa at a strain

of 5%. Using this diameter and the peak tensile strength, the peak tensile force F_{mt} can be calculated through:

$$F_{mt} = \sigma \cdot A_s = 500 \cdot 0.00049 = 245 \text{ kN} \tag{3.5}$$

Where F_{mt} is the maximum tensile capcity of the bolt and A_s is the area of the cross-section of the bolt. With σ being 500 MPa in B500-BT and A_s=0.00049m^2 with a cross-section diameter of 25mm the tensile capacity result in 245 kN.

3.4.5 Calculating largest block

The largest block possible will be assessed in the yielded elements analysis from the RS2 output. Since the fractures in the mine are all horizontal, the block size will depend on local weakness zones and fractures due to displacement originating from the excavation. The maximum length of the block in the out of plane direction that any one row have to carry will be two times the out of plane spacing of the bolt rows, as illustrated in Figure 3.9. This is deemed to be the worst case scenario.

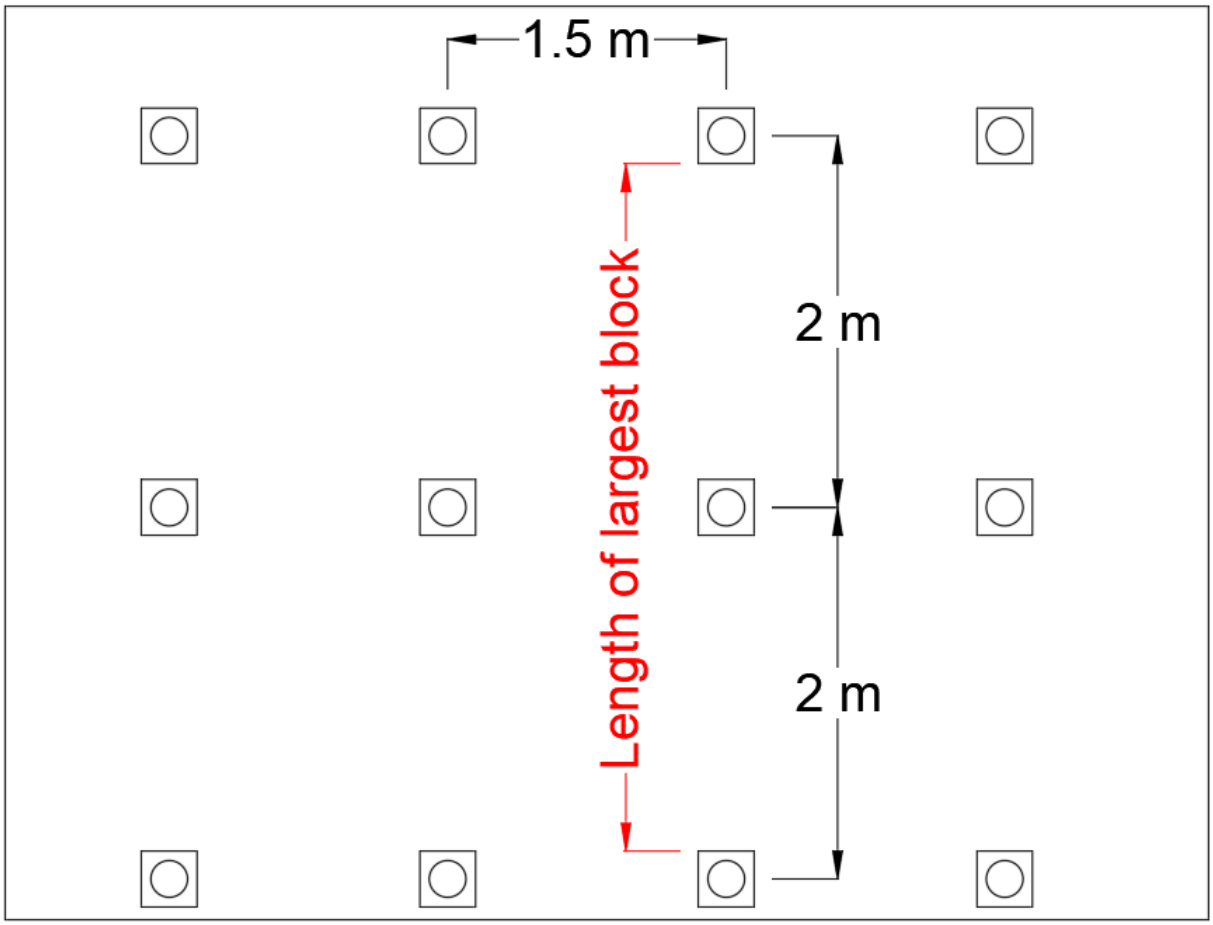

Figure 3.9: Theoretical maximum length of the largest block that any one row of bolts has to carry, with an example with 2m out of plane spacing

From the yield analysis in the unsupported anisotropic model, the size of the block

face will be measured using the software Bluebeam which allows the total volume of the largest block to be calculated.

$$F_{block} = V_{block} \cdot \gamma_{ss} \tag{3.6}$$

where :

F_{block} = Force of the block *[kN]*

V_{block} = Volume of the block *[m^3]*

γ_{ss} = Unit weight of sandstone *[kg/m^3]*

F_{block} is then compared to F_{mt} from Equation 3.5 to assess if the bolt capacity is sufficient.

3.4.6 Sensitivity analysis

Since many input parameters are unknown and some are estimated based on limited background data it is deemed necessary to perform a sensitivity analysis. In the analysis it, different values on a few key and uncertain parameter will be tested to see of they affect the model overall. Specifically how this variation will affect the yielded elements and maximum vertical displacement.
The parameters that are deemed to be the most critical as well as the most uncertain and thus subject to sensitivity analysis are:

- GSI
- m_i
- Young's modulus

3.4.7 Groundwater

The mine is located underneath an aquifer but is shielded from it by the quite impermeable sandstone and other soil layers, which makes the mine almost completely dry. For the FEM modeling, groundwater and pore pressures will hence be ignored, except for the increase in the overburden load described in Section 3.3.2, as it is not thought to be a major contributing factor for the overall stability. Also, since the sandstone isn't calcitic, it is not very sensitive to moisture. The slake durability test along with the chemical structure indicates that the rock is not very sensitive even if water condition would be damp or somewhat wet.

4

Results

The following section will present the results of the laboratory tests carried out, the evaluation of CMRR and RMR as well as the FEM models.

4.1 Laboratory tests

The following section will present the results of the laboratory tests conducted for the study.

4.1.1 Point load tests

The results shown in Table 4.1 show the point load test required to break the samples in different directions. Due to the limited sample size and values not quite corresponding to the expected absolute values and anisotropy, a decision was made to not include these results further in the investigations.

Table 4.1: Results from point load tests conducted at Sweco

Point Load Tests [MPa]	
Normal to discontinuities	**Parallel to discontinuities**
9	4.5
7.5	9
8.5	9
9	11

4.1.2 Immersion test

The results for the immersion test were acquired through the methodology described in Section 3.1.2.

Table 4.2 presents the results of the immersion test.

Table 4.2: Results acquired from immersion test

Immersion		**Breakability**	
Observation	Rating	Observation	Rating
Appearance of water Clear = 0 Misty = -1 Cloudy = -3	0	No change = 0 Small change = -2 Large change = -6	-2
Talus formation None = 0 Minor = -1 Major = -3	-1		
Cracking of samples None = 0 Minor/Random = -1 Major/Preferred Orientation = -3 Specimen breakdown = -9	-1		
Immersion Index	-2	Breakability Index	-2
Total immersion test index = -2			

4.1.3 Slake durability test

The results for the slake durability test were acquired through the methodology described in Section 3.1.3.

Table 4.3 presents the data gathered from the test as well as the natural moisture content and slake durability index calculated through Equation 2.20 and 2.21 respectively.

Table 4.3: Data acquired from slake durability test and calculated indexes

Unit	**Weight** *[g]*	**Label**
Drum	579.4	C
Drum and samples at natural moisture content	1082	A
Drum and oven-dried samples before first slake cycle	1081.4	B
Drum and samples after first water rotation cycle	1091.8	-
Drum and samples after second oven-drying	1068.7	-
Drum and samples after second water rotation cycle	1083.5	-
Drum and oven-dried samples after the second slake cycle	1060.85	Wf
Final mass of drum and samples	1083.5	-
Calculated indexes	[%]	**Label**
Natural water content	12	w
Slake durability index	95.91	SDI

4.2 Classification Systems and Recommended Support

The following section describes the recommended support acquired through the classification systems CMRR and RMR.

4.2.1 RMR

The support recommended by RMR was acquired from the methodology described in Section 3.2.1.

The rating determined for each parameter of RMR is presented in Table 4.4. Due to uncertainty when determining some of the parameters several ratings had to be acquired for certain parameters. This was done in order to present an interval of possible values based on the available material and observations made. The minimum column represent the smallest possible value while the maximum column represent the largest possible value. The columns SL1, SL2 and SL3 represent the rating deemed most probable for sandstone layer 1, sandstone layer 2 and sandstone layer 3 respectively. The rating of these three columns were acquired using a conservative approach as described in Section 3.2.1.

Table 4.4: Minimum, maximum and each sandstone layers rating for each parameter in RMR

Parameter	**Min**	**Max**	**SL1**	**SL2**	**SL3**	**Uncertainty**
Strength of intact rock	7	12	7	7	7	Very certain
RQD	17	20	17	17	17	Relatively certain
Spacing of joints*	10.4	13	10.4	10.4	10.4	Relatively uncertain
Condition of joints	12	15	15	15	15	Relatively certain
Groundwater	10	15	10	10	10	Certain
Strike/dip reduction	5	5	5	5	5	Certain
RMR	51.4	70	54.4	54.4	54.4	

**Increased 30% as only one joint set. See Section 3.2.1.*

Two different support variations are recommended depending on which RMR value is to be used, as can be seen in Table 2.2. The minimum rating as well as the rating for the sandstone layers were all in the same rock mass class "Fair rock". However, if the maximum value were to be used the rock mass class would instead be "Good rock". These classes result in the following support recommendations:

Fair rock - *Systematic bolts 4m long, spaced 1.5-2m in crown and walls with wire mesh in crown.*

Good rock - *Locally bolts in crown, 3m long, spaced 2.5m with occasional wire mesh*

4.2.2 CMRR

The support recommended by CMRR was acquired from the methodology described in Section 2.3.3.

The final assessments and the chosen values for the respective category are presented in Appendix A.2, as well as in decontructed form in Tables: 4.5, 4.6 and 4.7. The results for the base value RRW along with the final adjusted CMRR-value as well as the preliminary support PRSUP are presented in Table 4.8.

Table 4.5: Results from CMRR classification table 1 of 3

Bolt lenght 2.4					
UNIT BY LAYER					
Layer	Name	Thickness	UCS [Mpa]	Strenght rating	Moisture sensitivity
1	SL1	0.9	100	22	0
2	SL2	1.2	100	22	0
3	SL3	0.9	100	22	-3

Table 4.6: Results from CMRR classification table 2 of 3

UNIT DISCONTINUITIES					
Joint set number	Description	Cohesion	Roughness	Spacing	Persistance
Joint.1.1 Joint.1.2 Joint.1.3	Banking Plane	Weak	Wavy	200-600mm	3m
Joint.2.1 Joint.2.2 Joint.2.3	Banking Plane	Weak	Wavy	200-600mm	3m
Joint.3.1 Joint.3.2 Joint.3.3	Banking Plane	Weak	Wavy	200-600mm	3m

Table 4.7: Results from CMRR classification table 3 of 3

	Cohesion rating	Bedding rating	UR
Joint 1.1	20	13	55
Joint 2.1	20	13	55
Joint 3.1	20	13	52

Table 4.8: Table showing results from the CMRR process

RRW	54.6
Groundwater	-2
Number of unit	0
Surcharge	0
Strong bed	0
Adjusted CMRR	52.6
L_{bolt} [m]	2.4
N_b [-]	
C [kN]	245
S_b [m]	2
W_c [m]	11
PRSUP	3.4
solve for N_b	1.8

4.3 Finite Element Analysis

The following section will present the results acquired through the finite element analysis of the different scenarios investigated. The geometry used in the models is specified in Figure 3.2 and the support for each model is shown in Appendix B.

4.3.1 Anisotropic model - CMRR, RMR Maximum, RMR Minimum, Existing Support and Unsupported

The results acquired from the anisotropic models listed below was identical in terms of vertical displacement and yielded elements. These results are presented in Figure 4.1 - 4.3 and apply to all the models listed below. The bolt axial force varied slightly between the same models and is presented in Figure 4.5 - 4.8 for each model separately.

The forces in the bolts are shown to vary between the support cases depending on their length and numbers. However, the forces are very minor and the bolts aren't loaded all that much in any of the scenarios.

Model results presented in this subsection:

- Existing support - Anisotropic material model
- RMR Maximum value - Anisotropic material model
- RMR Minimum value - Anisotropic material model
- CMRR - Anisotropic material model
- Unsupported initial conditions - Anisotropic material model

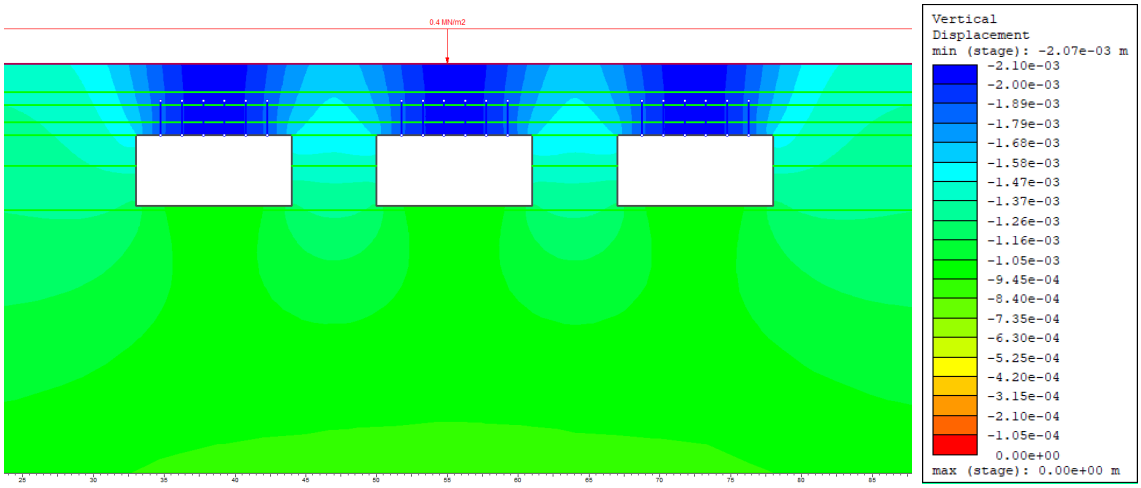

Figure 4.1: Illustration of the vertical displacement after all 3 excavations in the anisotropic model for the different scenarios listed in Section 4.3.1

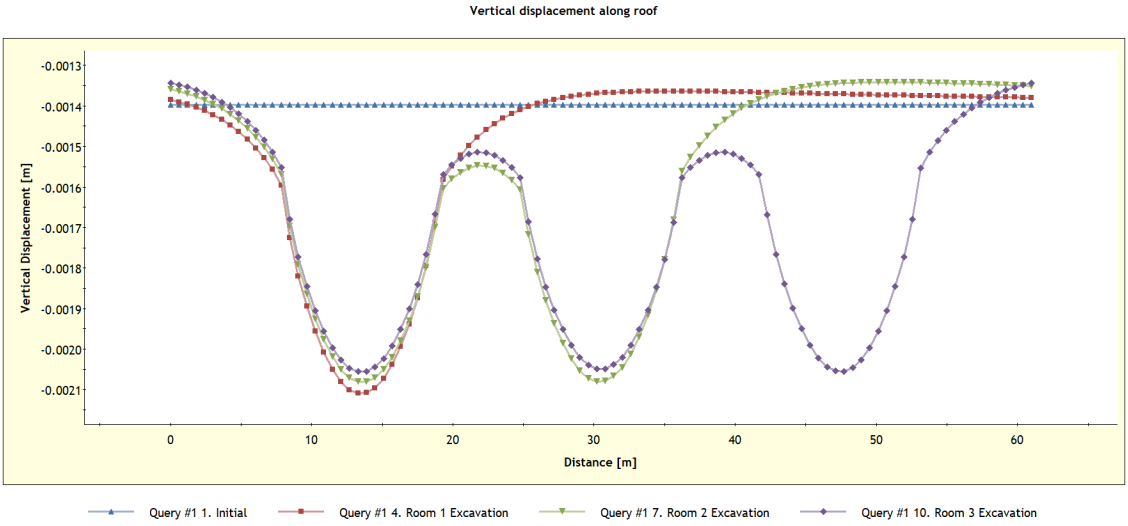

Figure 4.2: Plot over the vertical displacement along the roof for the initial stage and each excavation stage in the anisotropic model for the different scenarios listed in Section 4.3.1

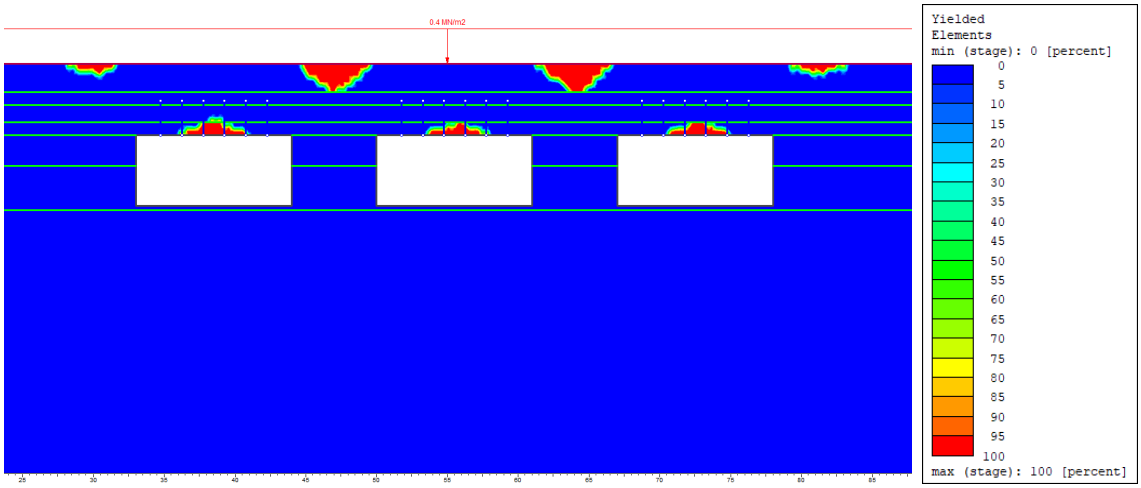

Figure 4.3: Depiction of the yielded elements in the anisotropic model for the different scenarios listed in Section 4.3.1

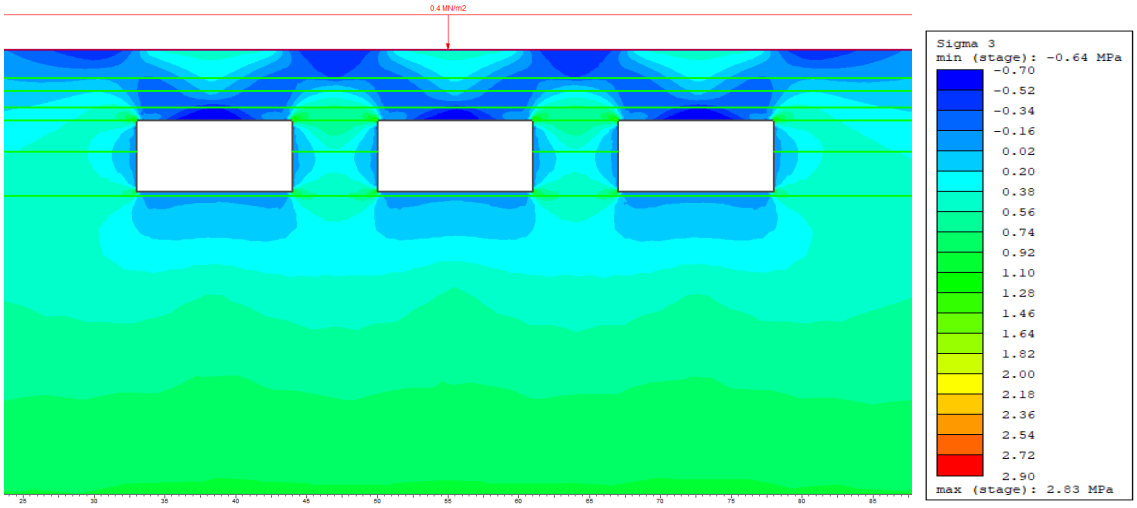

Figure 4.4: Principal stress σ_3 acting on the mine in the anisotropic unsupported case

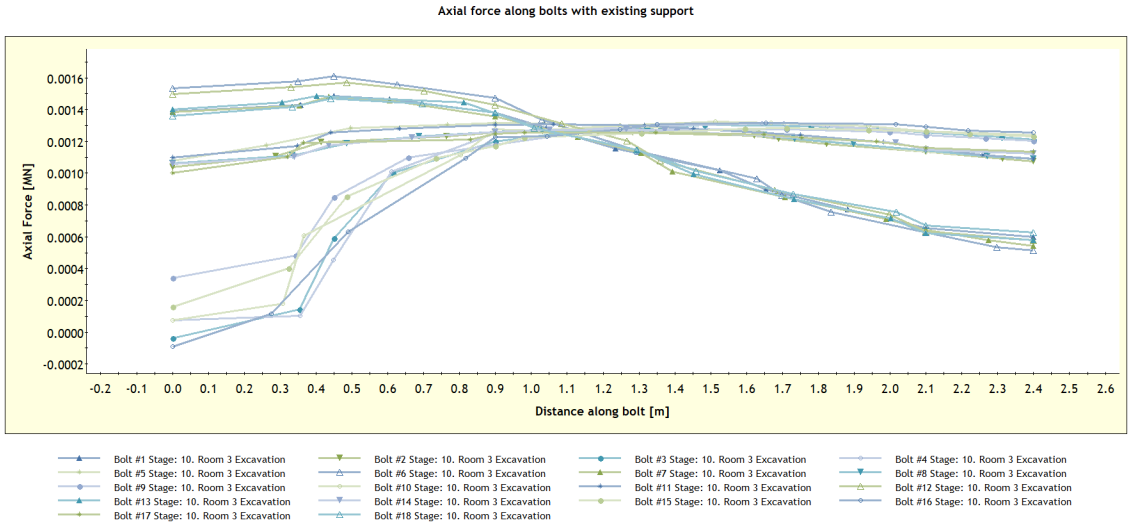

Figure 4.5: Plot of the bolts axial force against the bolt distance in the anisotropic model with existing support

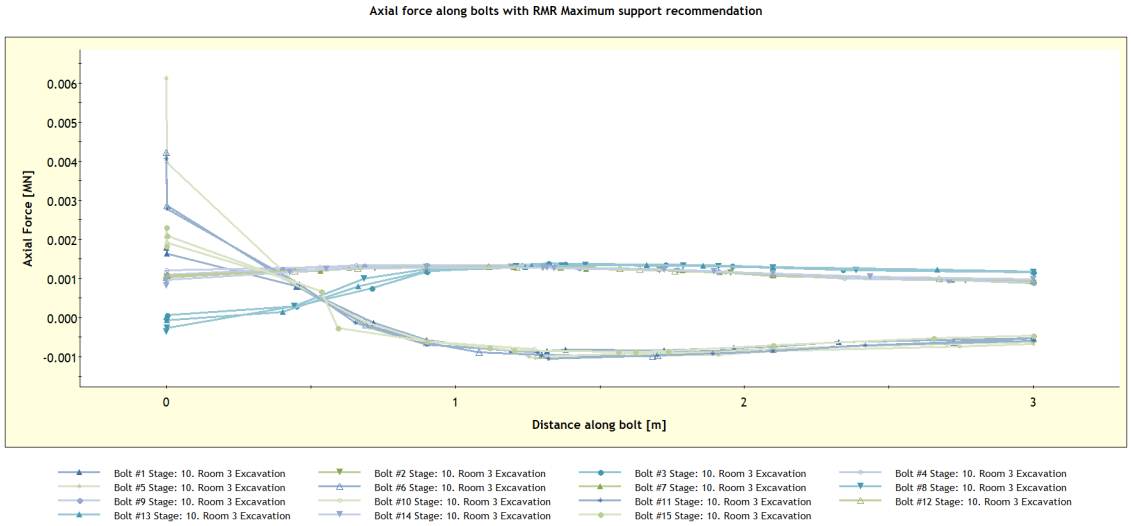

Figure 4.6: Plot of the bolts axial force against the bolt distance in the anisotropic model with RMR Maximum support recommendation

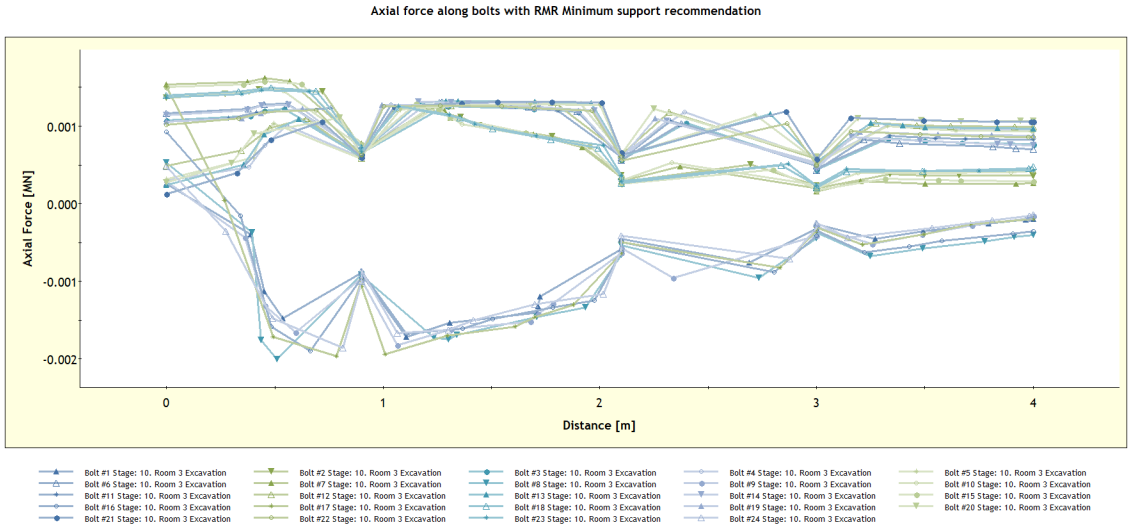

Figure 4.7: Plot of the bolts axial force against the bolt distance in the anisotropic model with RMR Minimum support recommendation

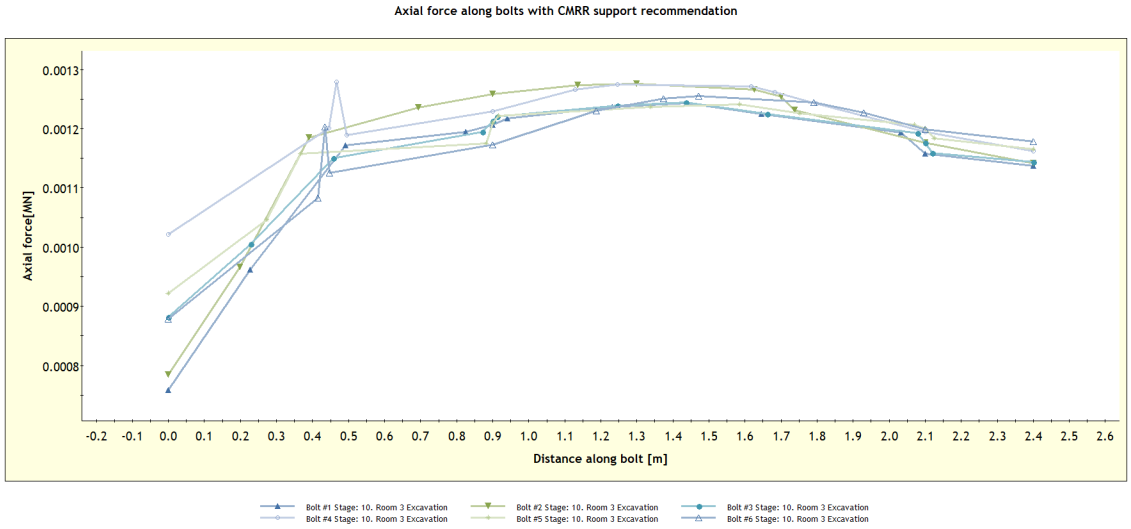

Figure 4.8: Plot of the bolts axial force against the bolt distance in the anisotropic model with CMRR support recommendation

4.3.2 Jointed model - CMRR, RMR Maximum, RMR Minimum, Existing Support and Unsupported

The results acquired from the jointed models listed below were identical in terms of vertical displacement and yielded elements. These results are presented in Figure 4.9 - 4.11 and apply to all the models listed below. The bolt axial force varied slightly between the models and is presented in Figure 4.13 - 4.16 for each model separately.

Much like in the anisotropic model, the bolt forces are shown to vary between the support cases and the maximum forces are very small overall in the same way as well.
Model results presented in this subsection:

- Existing support - Jointed material model
- RMR Maximum value - Jointed material model
- RMR Minimum value - Jointed material model
- CMRR - Jointed material model
- Unsupported initial conditions - Jointed material model

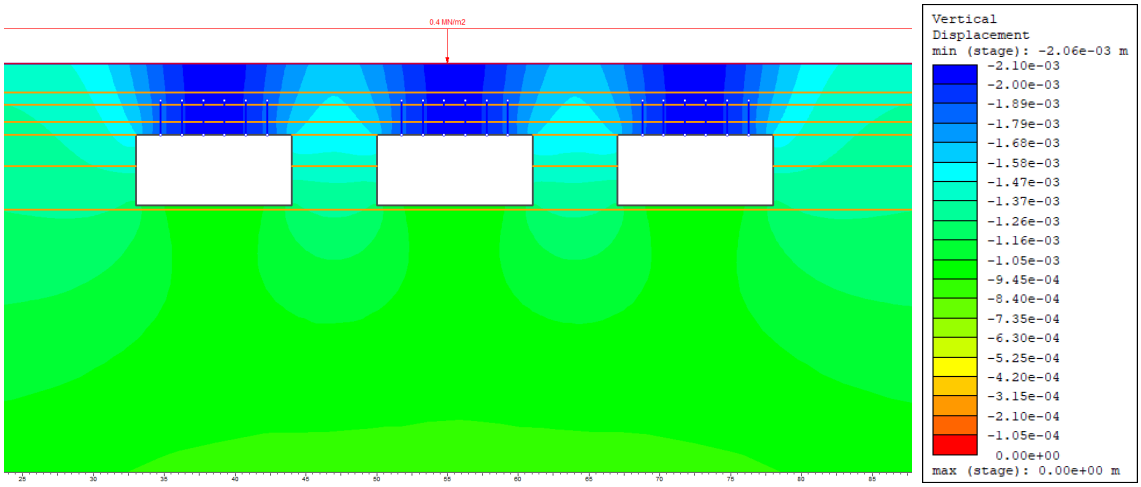

Figure 4.9: Illustration of the vertical displacement after all 3 excavations in the jointed model for the different scenarios listed in Section 4.3.2

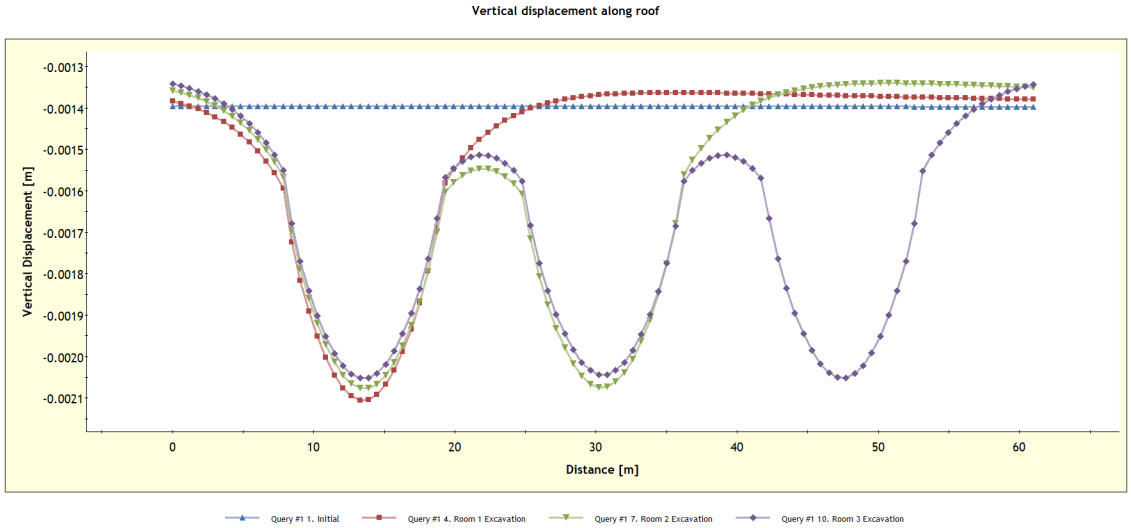

Figure 4.10: Illustration of the vertical displacement after all 3 excavations in the jointed model for the different scenarios listed in Section 4.3.2

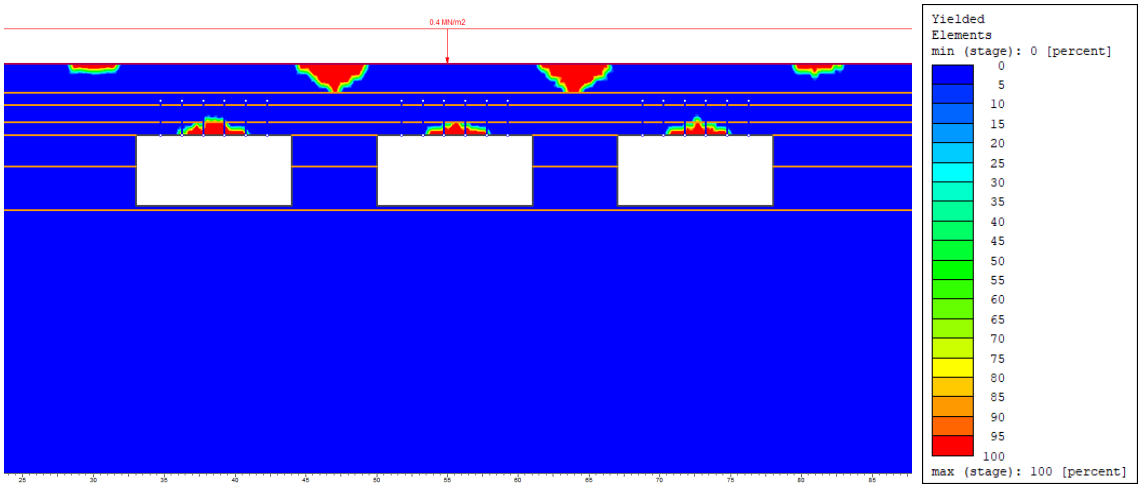

Figure 4.11: Depiction of the yielded elements in the jointed model for the different scenarios listed in Section 4.3.2

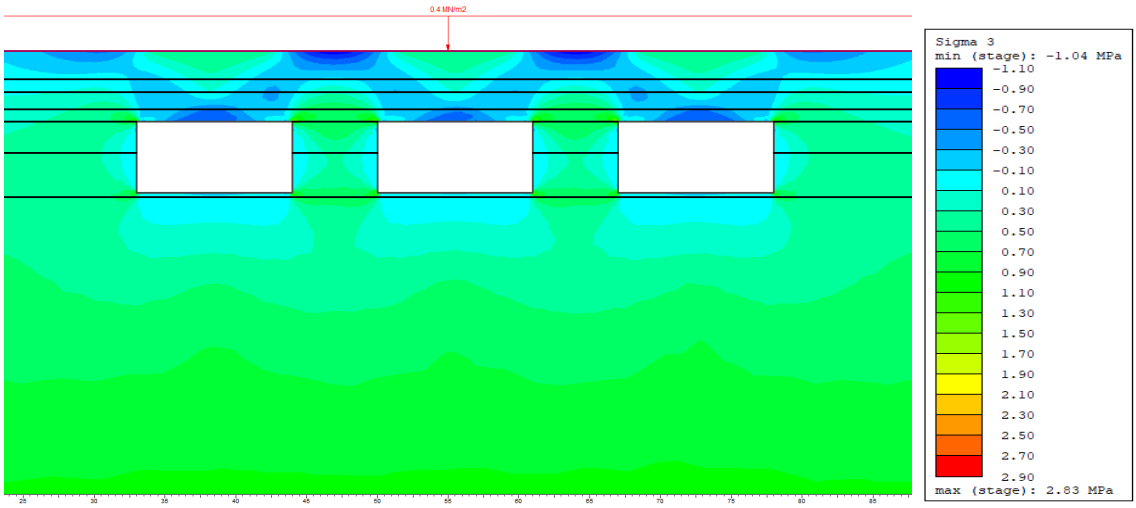

Figure 4.12: Principal stress σ_3 acting on the mine in the jointed model in the unsupported case

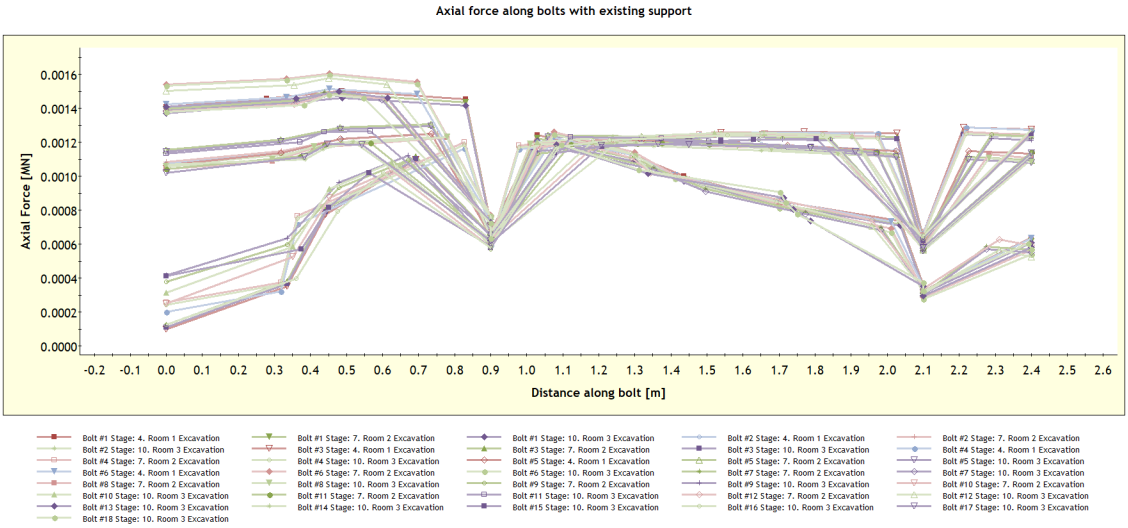

Figure 4.13: Plot of the bolts axial force against the bolt distance in the jointed model with existing support

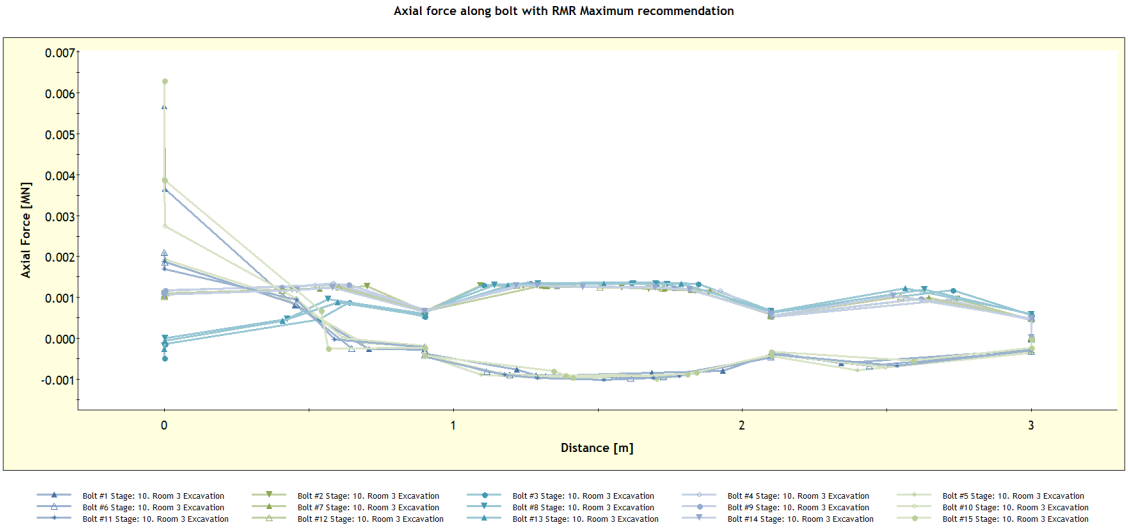

Figure 4.14: Plot of the bolts axial force against the bolt distance in the jointed model with RMR Maximum support recommendation

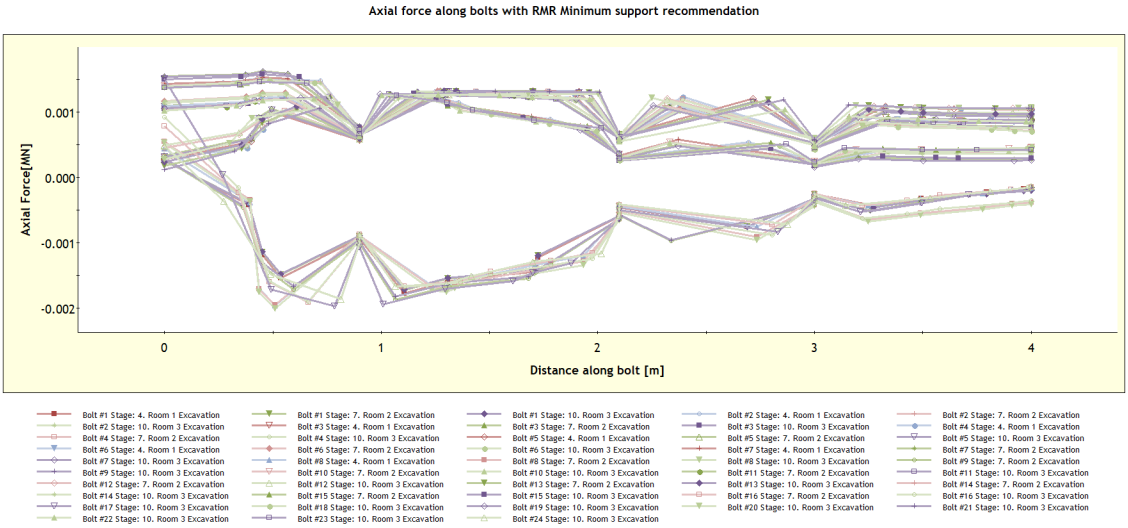

Figure 4.15: Plot of the bolts axial force against the bolt distance in the jointed model with RMR Minimum support recommendation

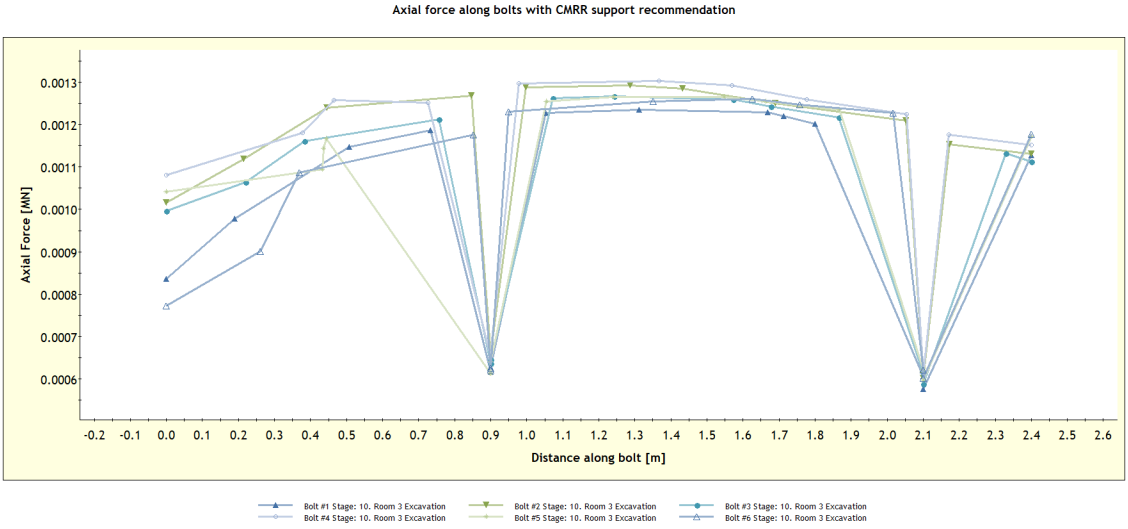

Figure 4.16: Plot of the bolts axial force against the bolt distance in the jointed model with the CMRR support recommendation

4.3.3 Bolts installed at an angle of 45°- Anisotropic model

The results acquired from the anisotropic model with bolts installed at an angle are presented in Figure 4.17 - 4.20.

The bolts in this scenario are shown to experience a higher maximum force. This is due to the angled bolts are anchored in different layers that displace differently. In turn, this also leads to a greater displacement in the bolts themselves. However, the maximum force is still very low in comparison to the tensile capacity of the bolts.

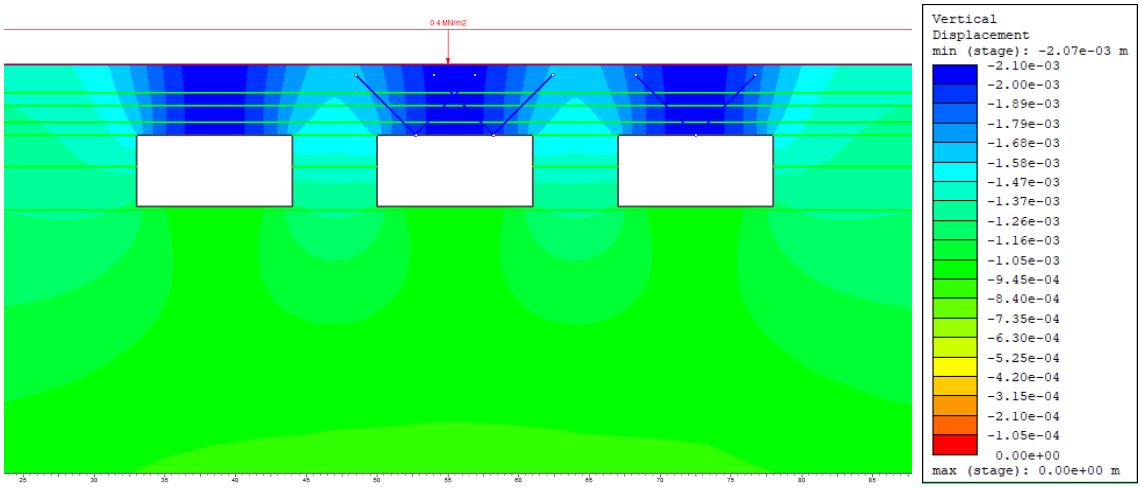

Figure 4.17: Illustration of the vertical displacement after all 3 excavations in the anisotropic model with bolts installed at an angle of 45°

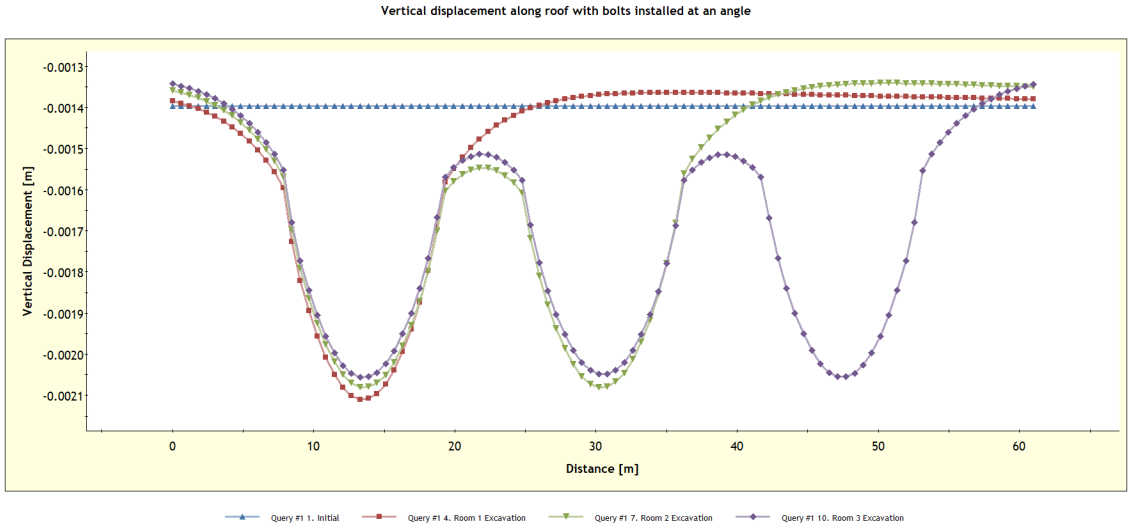

Figure 4.18: Plot over the vertical displacement along the roof for the initial stage and each excavation stage in the anisotropic model with bolts installed at an angle of 45°

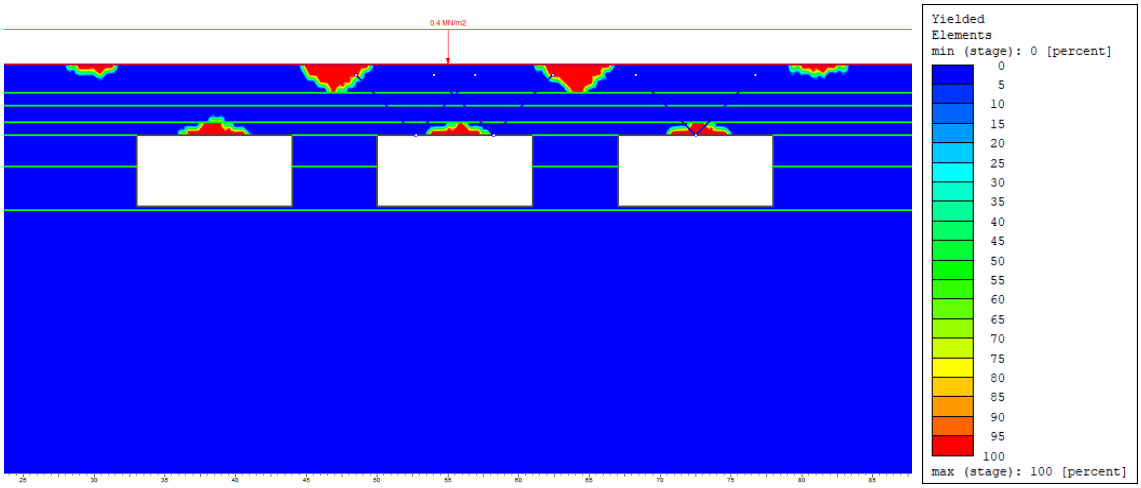

Figure 4.19: Depiction of the yielded elements in the anisotropic model with bolts installed at an angle of 45°

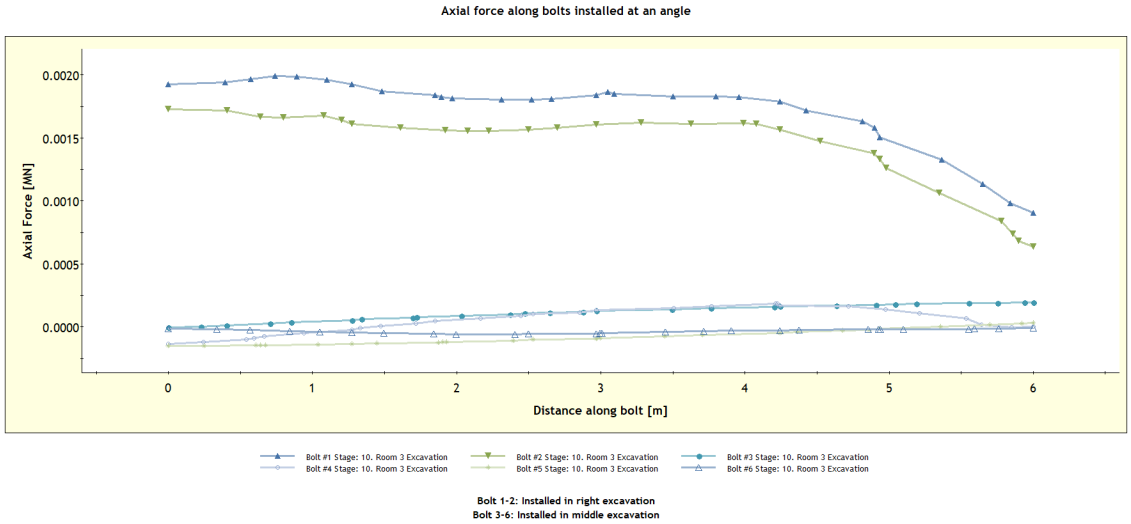

Figure 4.20: Plot of the bolts axial force against the bolt distance in the anisotropic model with bolts installed at an angle

4.3.4 Increased height of the middle room without support - Anisotropic model

The results acquired from the anisotropic model with the height increased in the middle without any support is presented in Figure 4.21 - 4.23.
The displacement in the different rooms changes when the roof is elevated in the middle room. More displacement is focused on the elevated roof. Some bolts in this scenario do also experience negative forces which could indicate that some parts of the bolts are experiencing compression forces. This is unusual as bolts are not manufactured to work in compression, but the values are very low.

The liner is shown to carry some load and works as intended. A great reduction in vertical displacement is not seen however and the liner would likely mostly work to keep blocks in place as will be discussed further in section 5

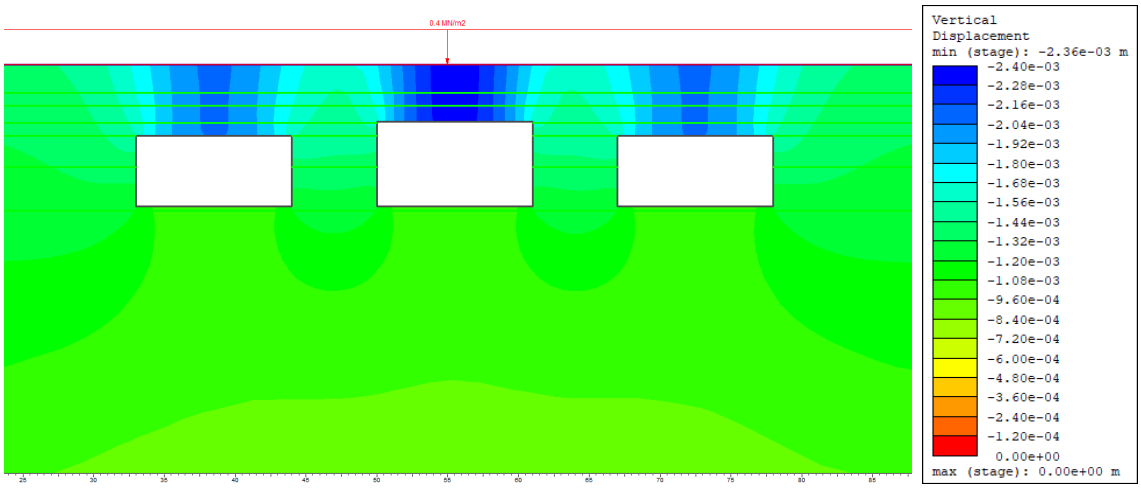

Figure 4.21: Illustration of the vertical displacement after all 3 excavations in the anisotropic model with increased roof height and no support

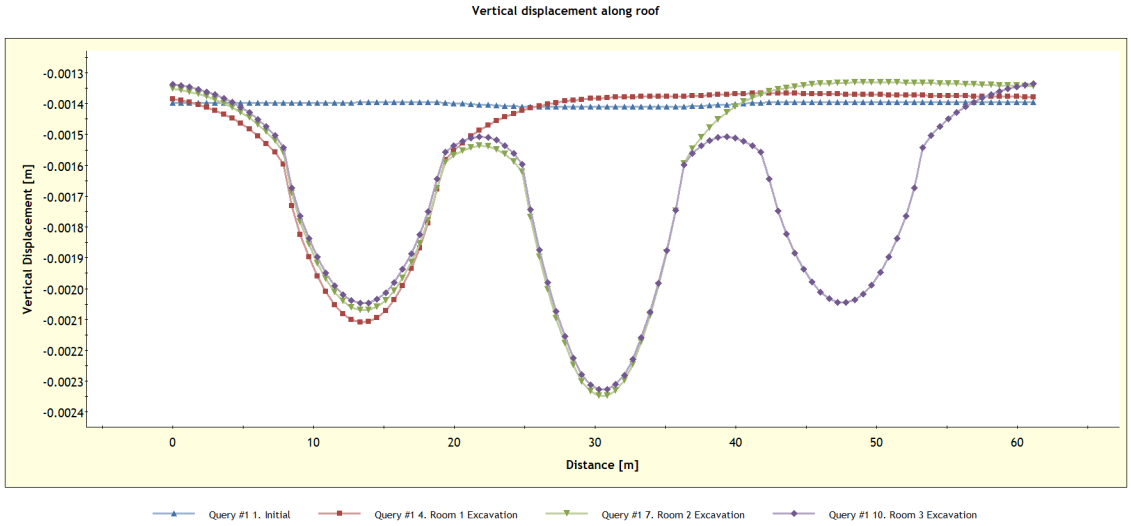

Figure 4.22: Plot over the vertical displacement along the roof for the initial stage and each excavation stage in the anisotropic model with increased roof height and no support

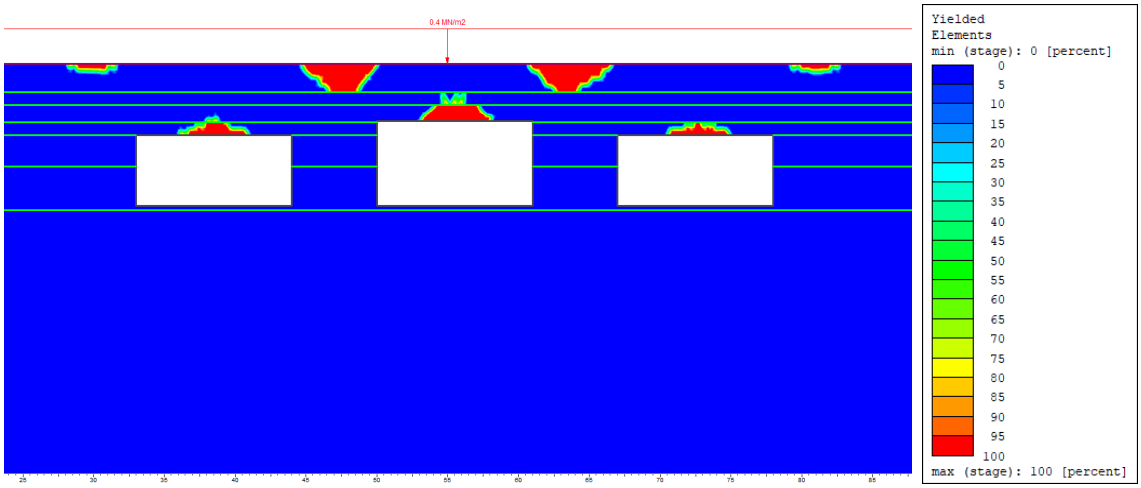

Figure 4.23: Depiction of the yielded elements in the anisotropic model with increased roof height and no support

4.3.5 Increased height of the middle room with bolts - Anisotropic model

The results acquired from the anisotropic model with the height increased in the middle with bolts as support is presented in Figure 4.24 - 4.27.

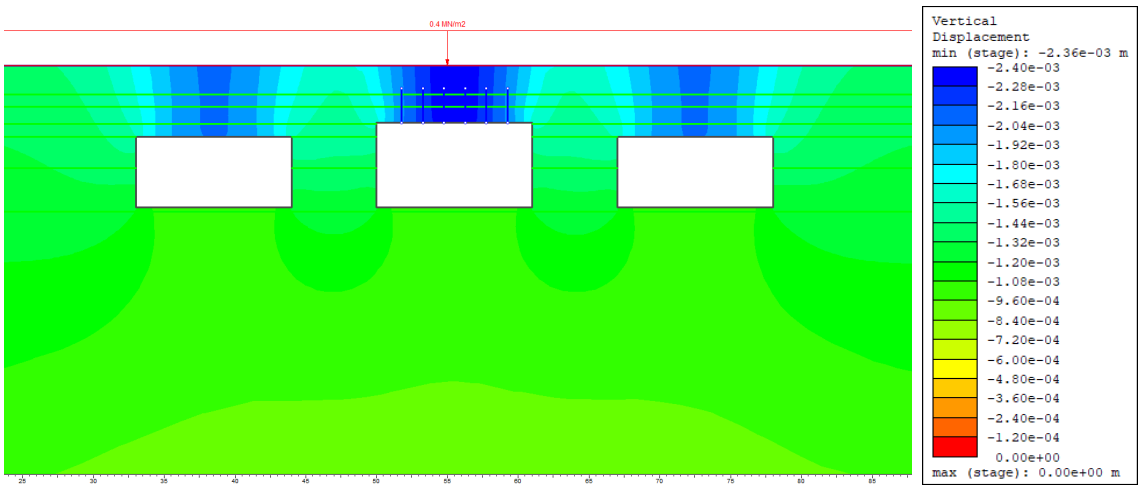

Figure 4.24: Illustration of the vertical displacement after all 3 excavations in the anisotropic model with increased roof height and bolts

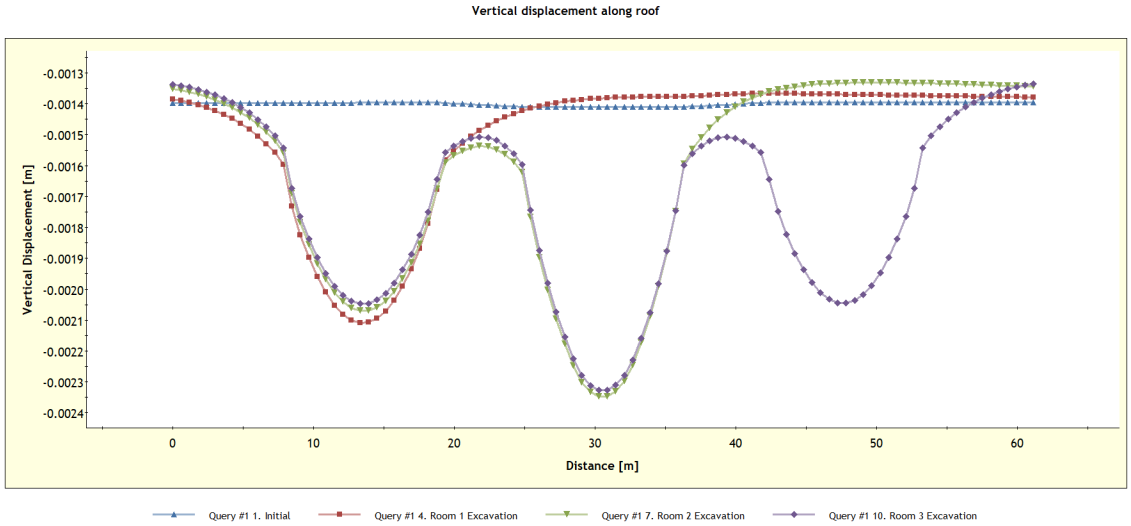

Figure 4.25: Plot over the vertical displacement along the roof for the initial stage and each excavation stage in the anisotropic model with increased roof height and bolts in the middle room

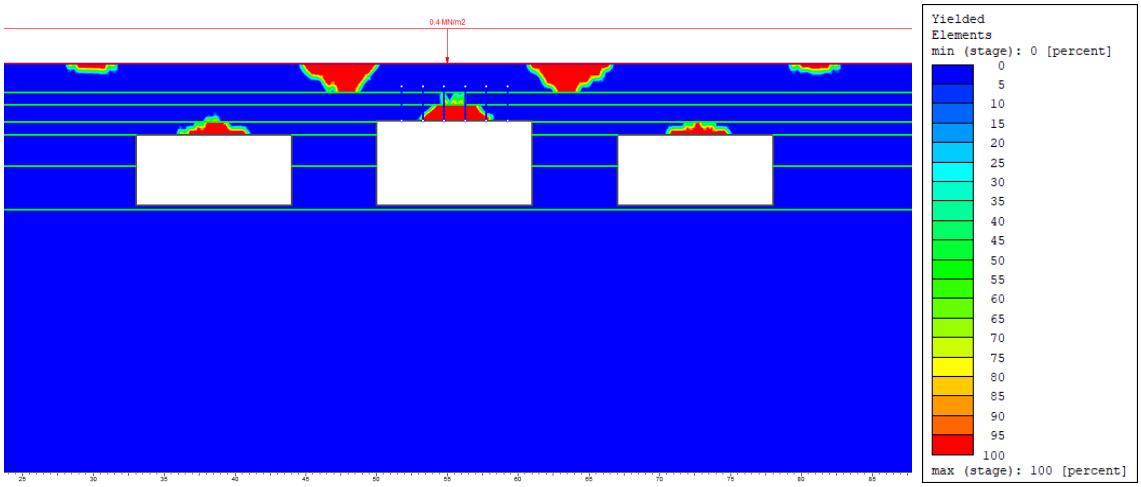

Figure 4.26: Depiction of the yielded elements in the anisotropic model with increased roof height and bolts in the middle room

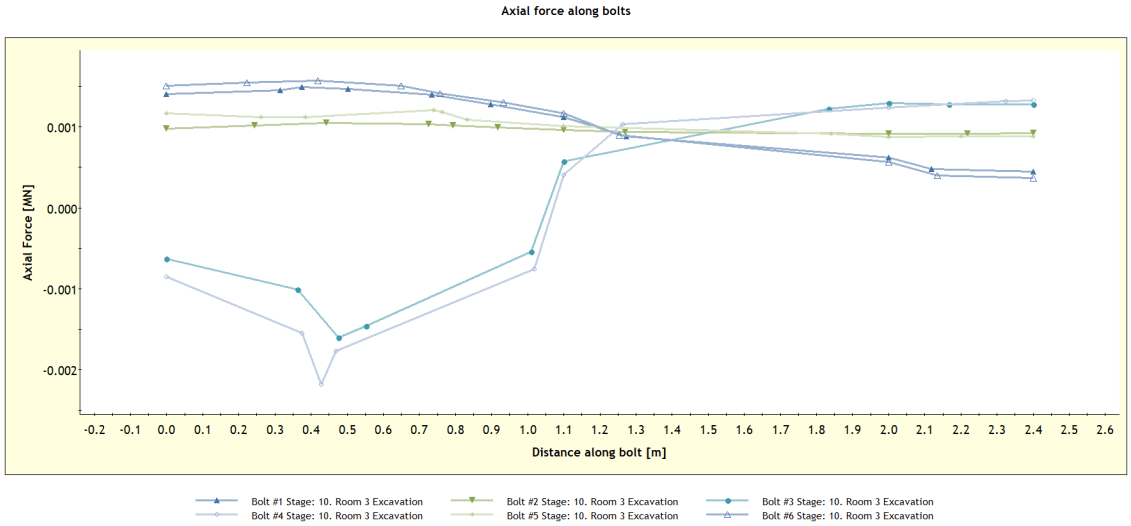

Figure 4.27: Plot of the bolts axial force against the bolt distance in the middle room in the anisotropic model with increased roof height

4.3.6 Increased height of the middle room with concrete liner - Anisotropic model

The results acquired from the anisotropic model with the height increased and concrete liner as support in the middle room is presented in Figure 4.28 - 4.32.

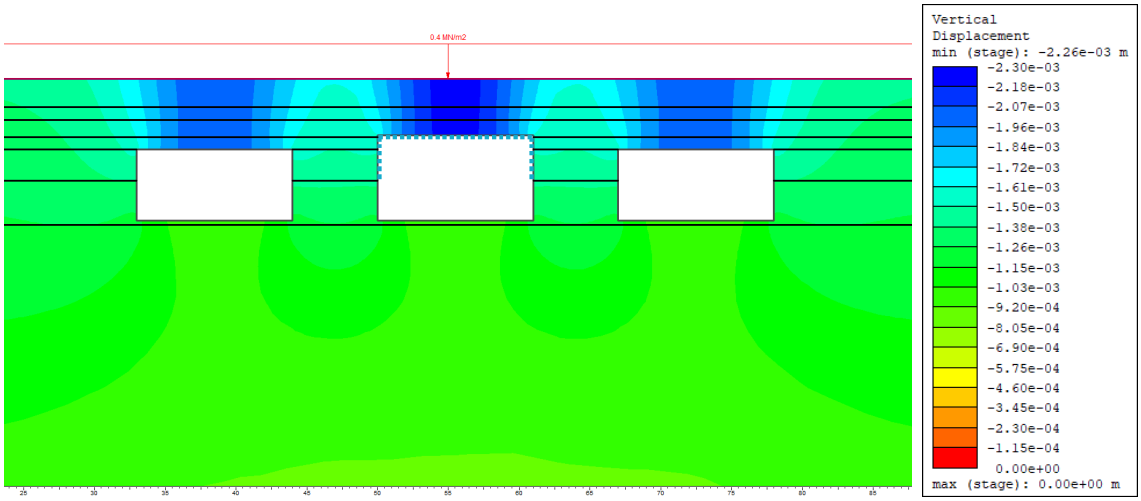

Figure 4.28: Illustration of the vertical displacement after all 3 excavations in the anisotropic model with increased roof height and concrete liner in the middle room

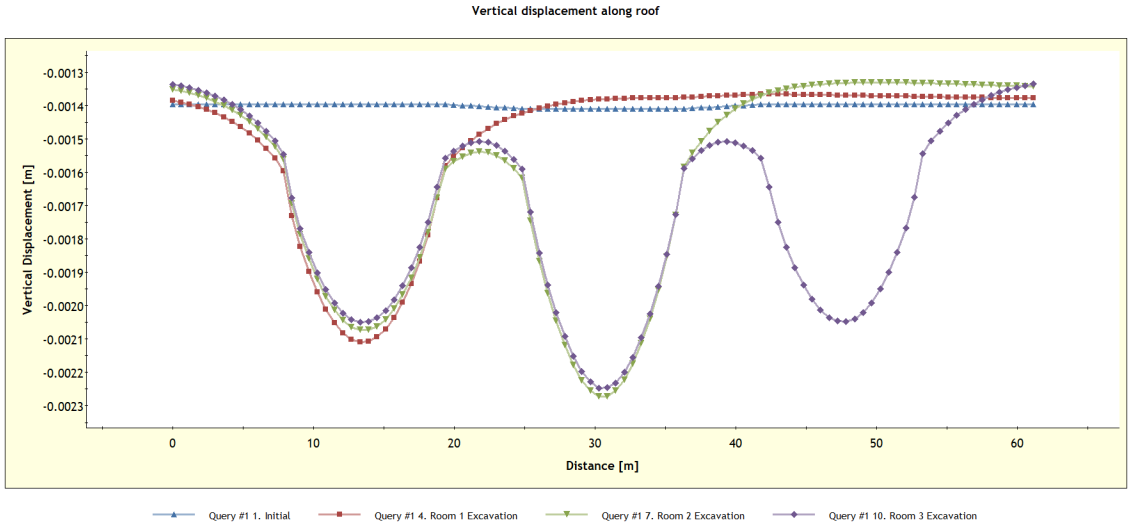

Figure 4.29: Plot over the vertical displacement along the roof for the initial stage and each excavation stage in the anisotropic model with increased roof height and concrete liner in the middle room

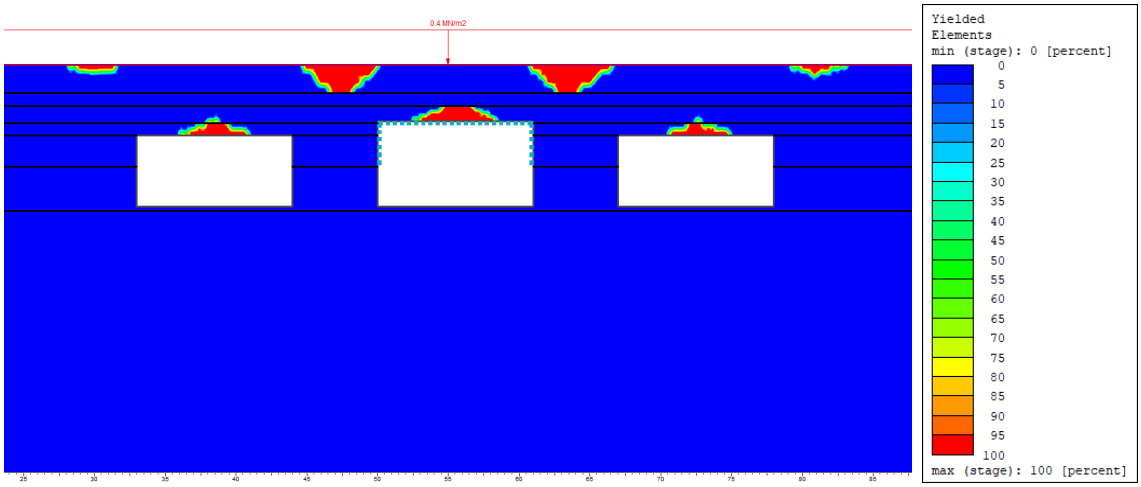

Figure 4.30: Depiction of the yielded elements in the anisotropic model with increased roof height and concrete liner in the middle room

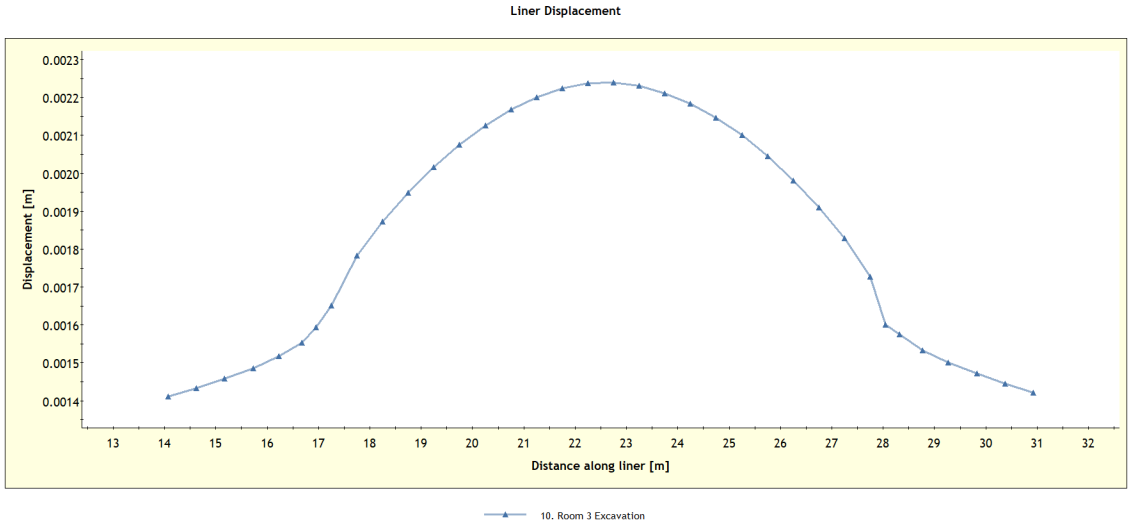

Figure 4.31: Plot over the vertical displacement along the liner after all 3 excavations in the anisotropic model with increased roof height and concrete liner in the middle room

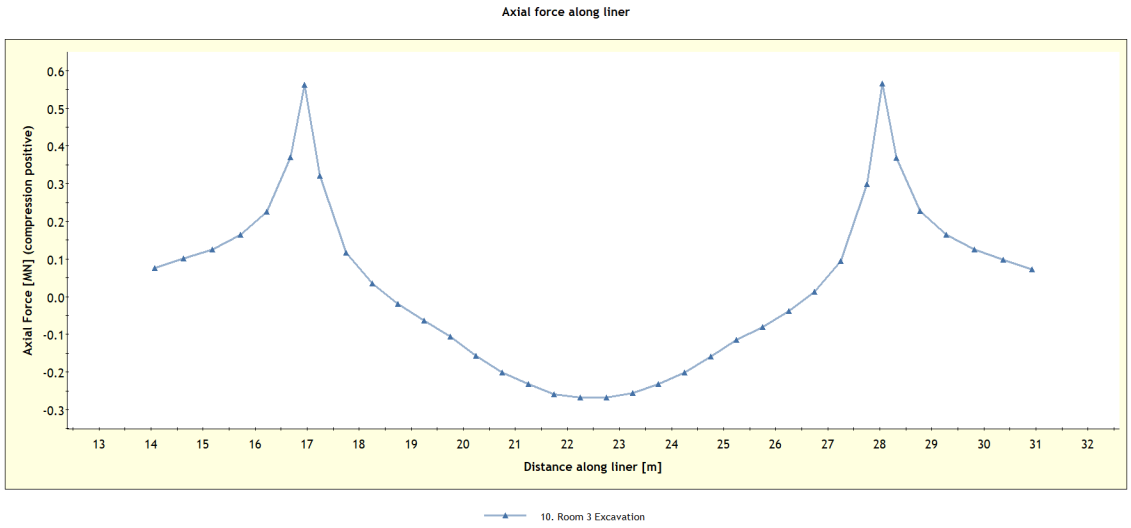

Figure 4.32: Plot over the axial force along the liner after all 3 excavations in the anisotropic model with increased roof height and concrete liner in the middle room

4.3.7 Vertical stress in initial unsupported conditions

The vertical stress acquired from both the anisotropic model and the jointed model for the initial unsupported scenario is presented in Figure 4.33 and 4.34.

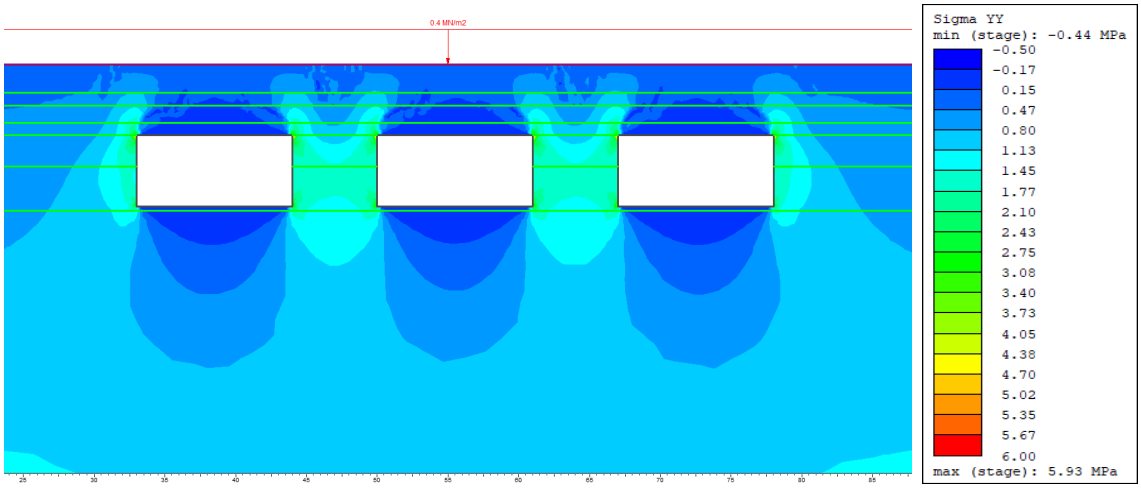

Figure 4.33: Illustration of the vertical stress after all 3 excavations in the anisotropic model for the different scenarios listed in Section 4.3.1

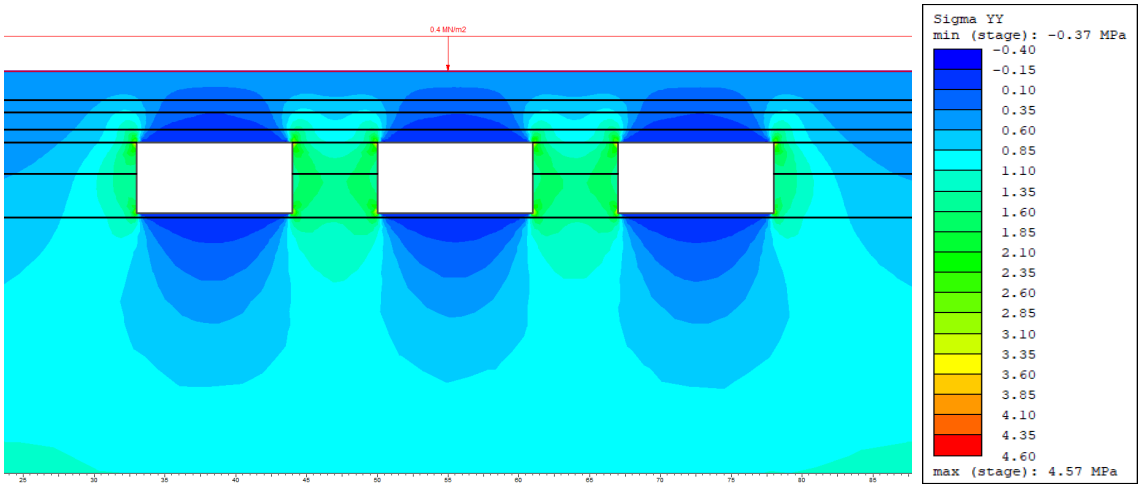

Figure 4.34: Illustration of the vertical stress after all 3 excavations in the anisotropic model for the different scenarios listed in Section 4.3.2

4.3.8 Weight and support of largest block

The face of the largest block measured based on the yielded elements acquired from initial unsupported scenario in the anisotropic model is illustrated in Figure 4.35. The area of the face of the block was measured in Bluebeam Revu 20 (a blueprint and PDF reviewer) and resulted in 3.85 square meters.

As described in Section 3.4.5, the theoretical lenght of the largest block would be two times the distance between the bolt rows which for the existing support system and the CMRR suggestion is two times two meters. Hence the lenght of the largest block would be four meters.
Table 4.9 shows the results of the largest block calculations. Where F_{Block} is the maximum force, the block could exercise on the bolts.

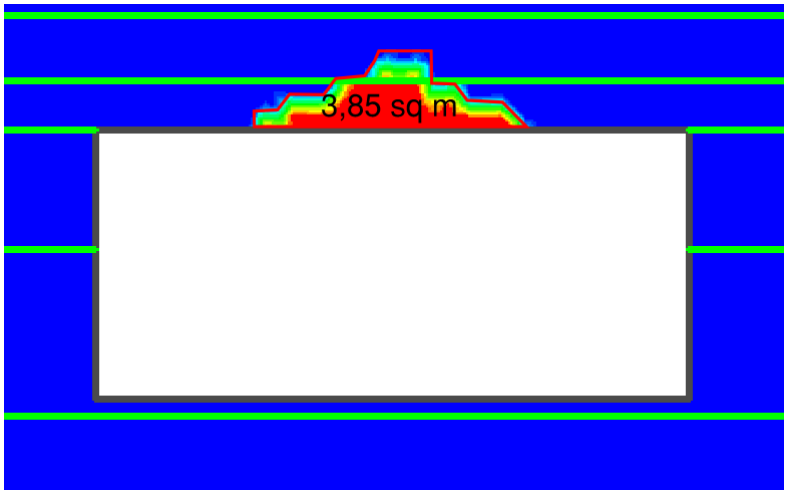

Figure 4.35: Face of the largest block based of yielded elements

Table 4.9: Ultimate block force from largest block according to yielded elements

$A_{Largestblock}$	3.85	m^2
$L_{Largestblock}$	4	m
$V_{Largestblock}$	15.4	m^3
γ_{ss}	0.0265	MN/m^3
F_{Block}	0.4081	MN
F_{mt}	0.245	MN

4.3.9 Sensitivity analysis

The results of the sensitivity analysis are presented by the graphs in this sub-chapter. The results shown will focus on how the changes in one individual parameter will affect the yielded elements as well as the maximum vertical displacement in the mine. Charts showing all the effects on displacement from all changes in parameters are included and images of how this affects the yielded elements in those cases were a significant change has occurred in the result.

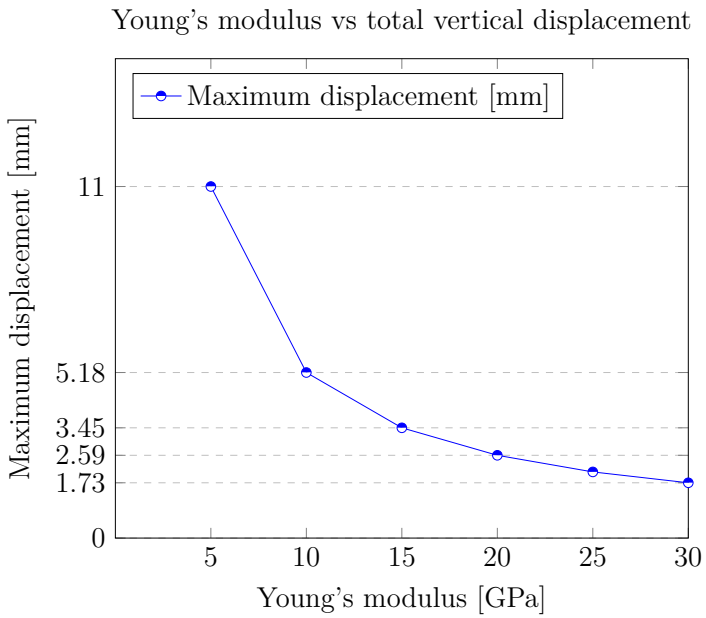

Figure 4.36: Plot of the effect Young's modulus has on the maximum vertical displacement

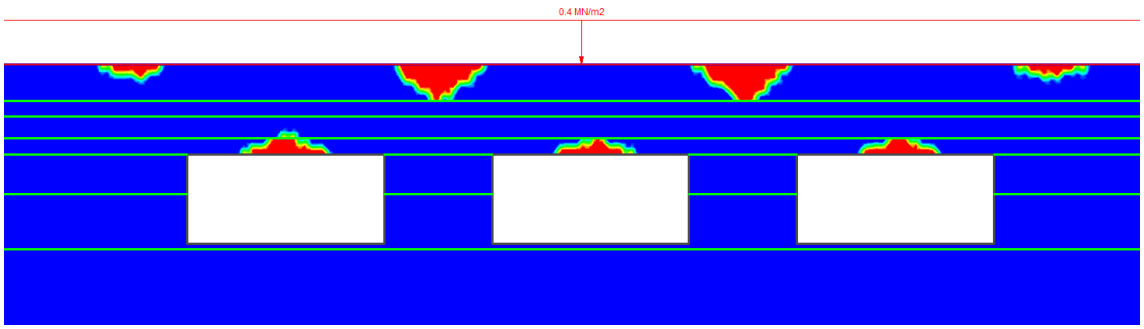

Figure 4.37: Yielded elements with Young's modulus reduced to 5000 MPa

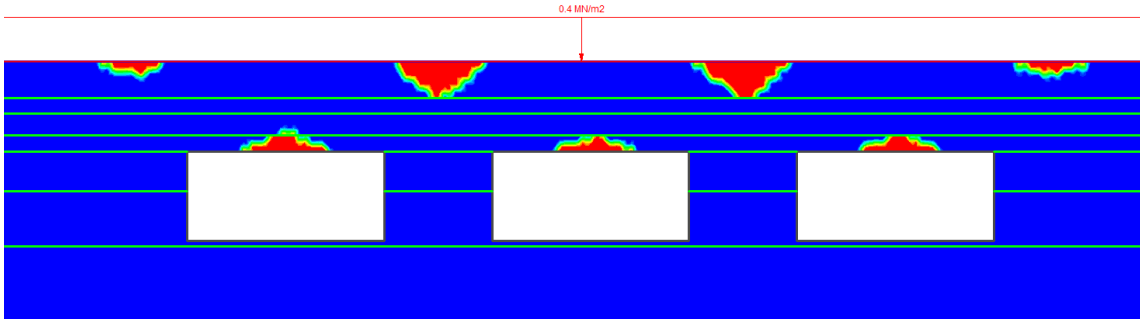

Figure 4.38: Yielded elements with Young's a modulus of 25000 MPa

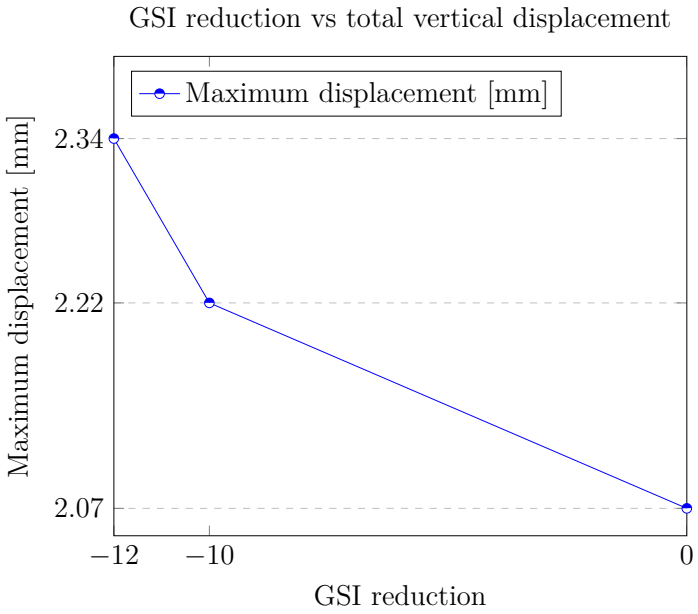

Figure 4.39: Plot of the effect GSI has on the maximum vertical displacement. x-axis represents the amount reduced from the 'original' GSI values found in table 3.2. The model collapsed when the GSI-values from table 3.2 was reduced by 14 points.

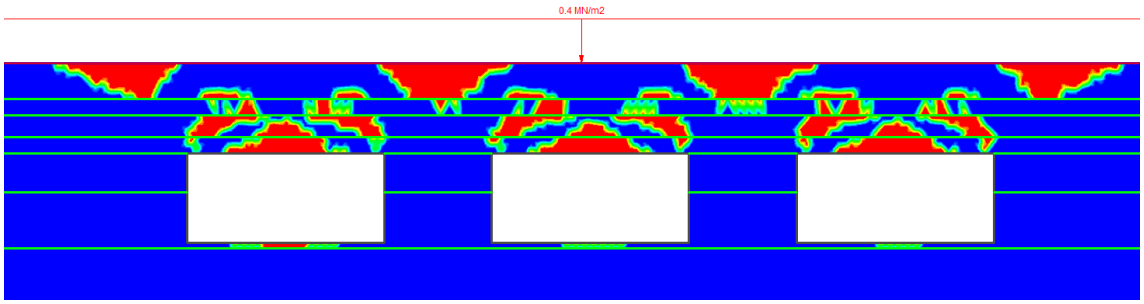

Figure 4.40: Yielded elements with GSI reduced by 12 points

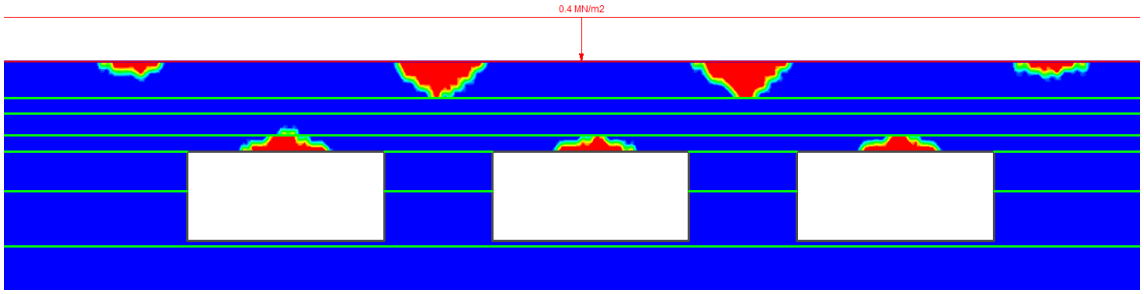

Figure 4.41: Yielded elements with the original GSI

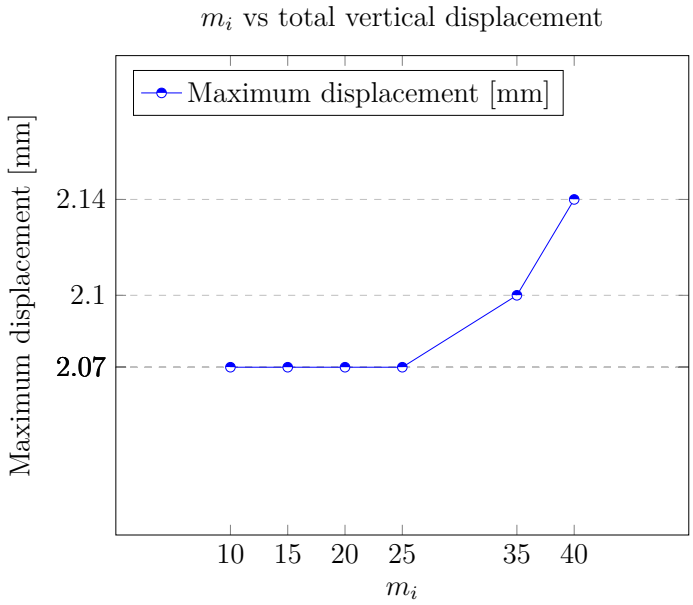

Figure 4.42: Plot of the effect m_i has on the maximum vertical displacement

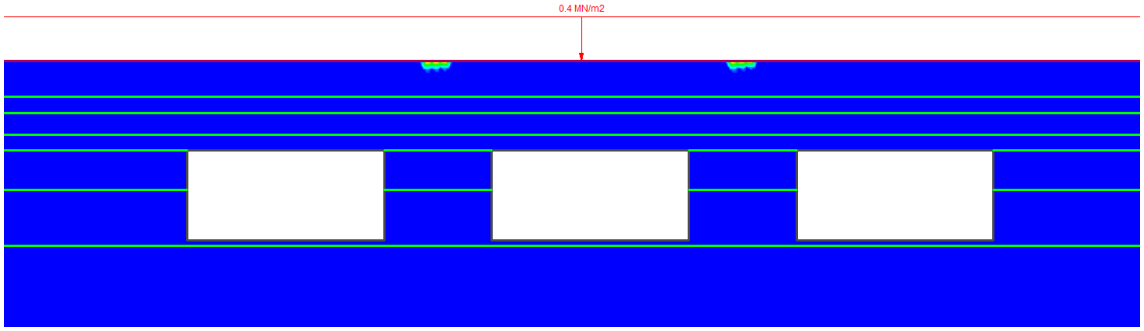

Figure 4.43: Yielded elements with m_i reduced to 10

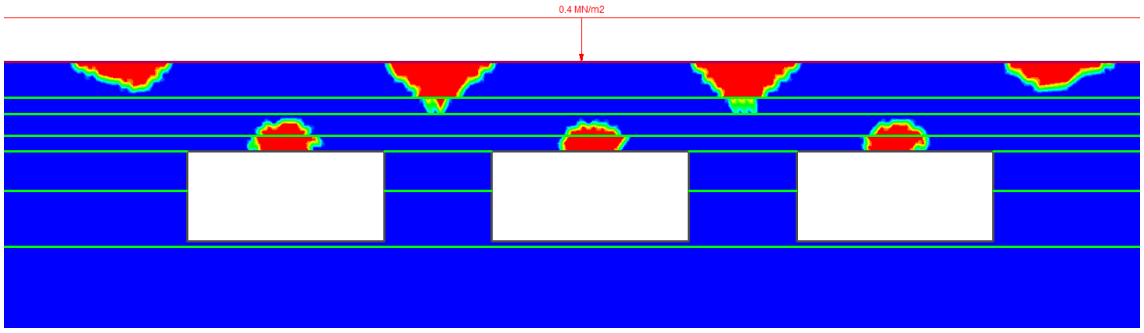

Figure 4.44: Yielded elements with m_i increased to 40

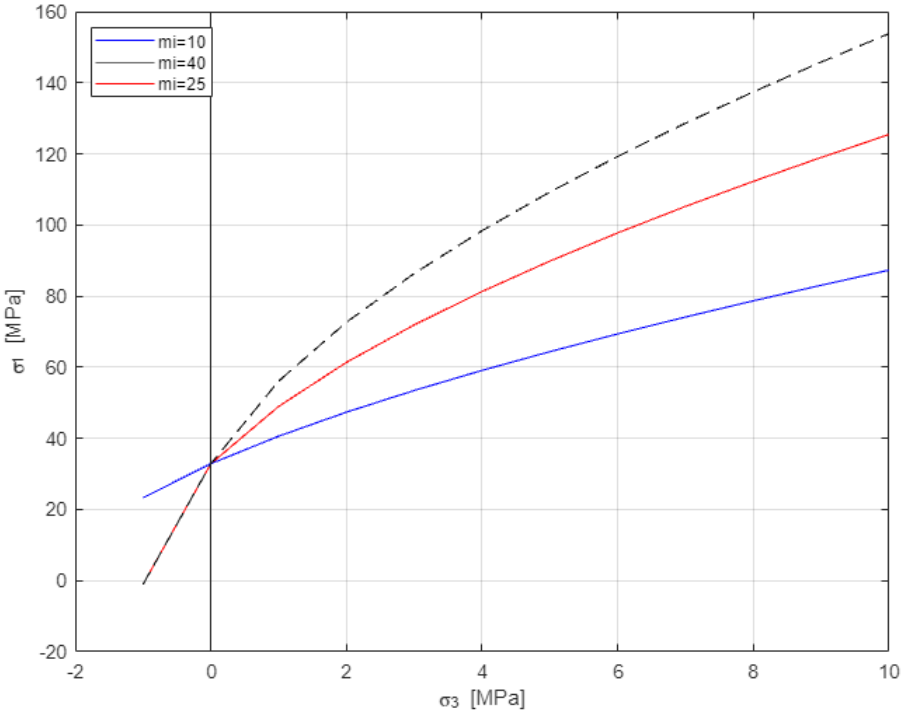

Figure 4.45: Plot showing how m_i affects the Hoek-Brown failure criterion

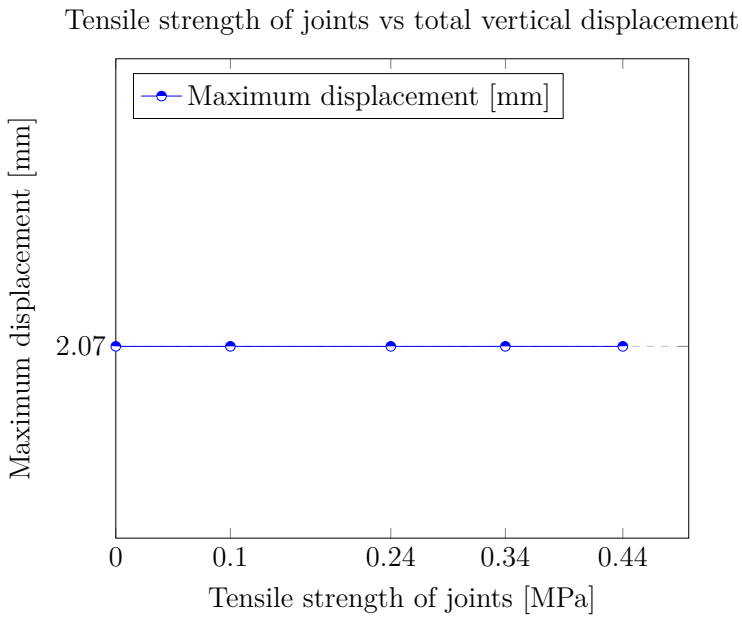

Figure 4.46: Plot of the effect tensile strength has on the maximum vertical displacement

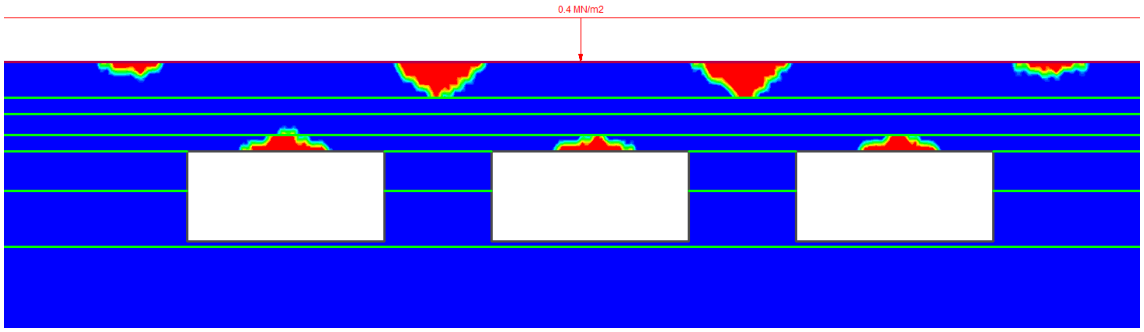

Figure 4.47: Yielded elements with joint tensile strength reduced to 0.1

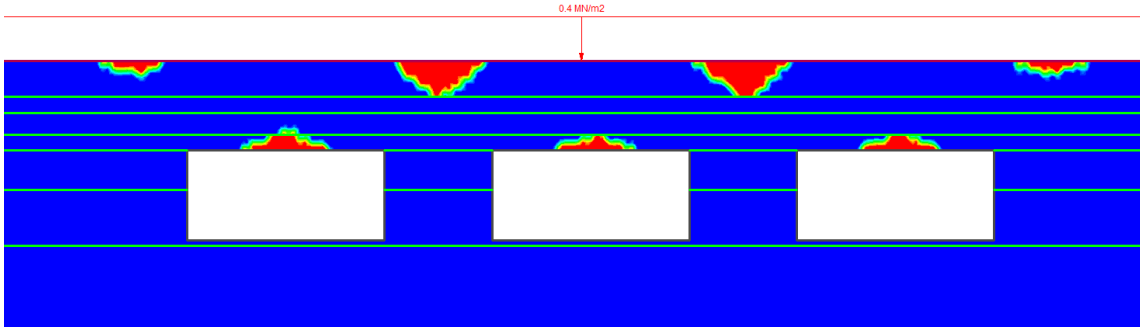

Figure 4.48: Yielded elements with joint tensile strength of 0.4425

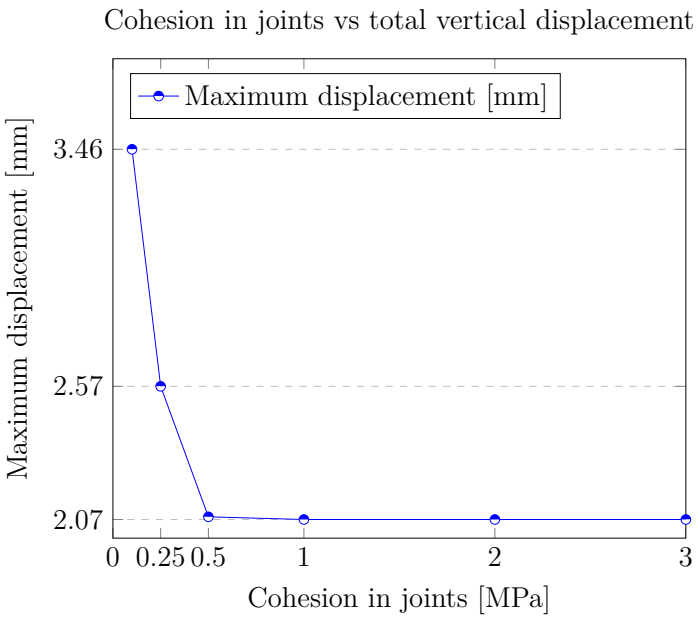

Figure 4.49: Plot of the effect cohesion has on the maximum vertical displacement

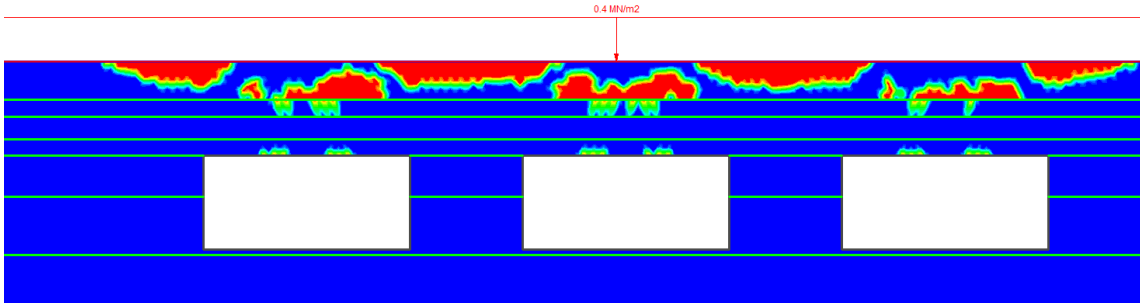

Figure 4.50: Yielded elements with c = 0.1 [MPa]

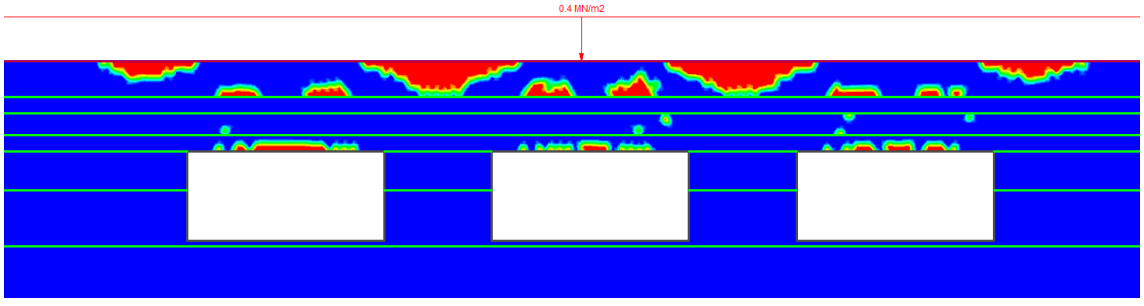

Figure 4.51: Yielded elements with c = 0.25 [MPa]

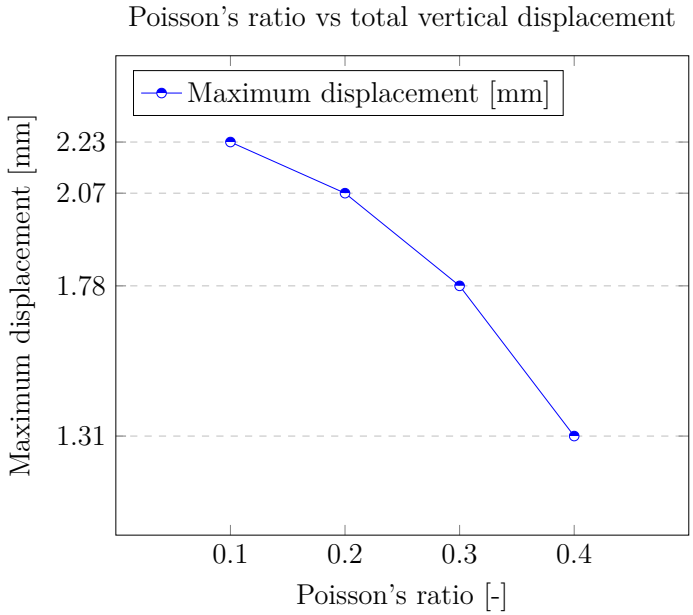

Figure 4.52: Plot of the effect Poission's ratio has on the maximum vertical displacement

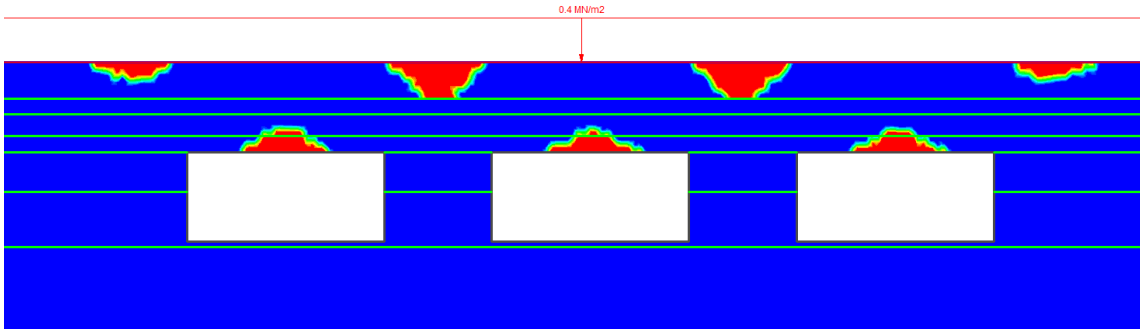

Figure 4.53: Yielded elements with Poisson's ratio being $\nu = 0.1$

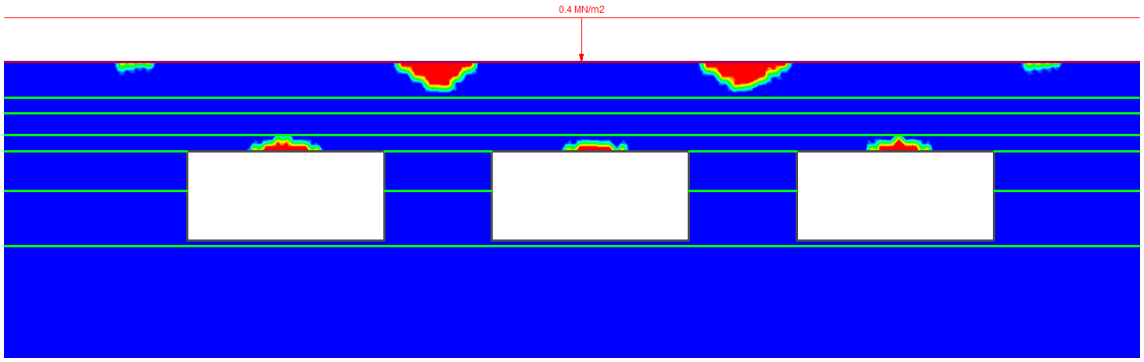

Figure 4.54: Yielded elements with Poisson's ratio being $\nu = 0.3$

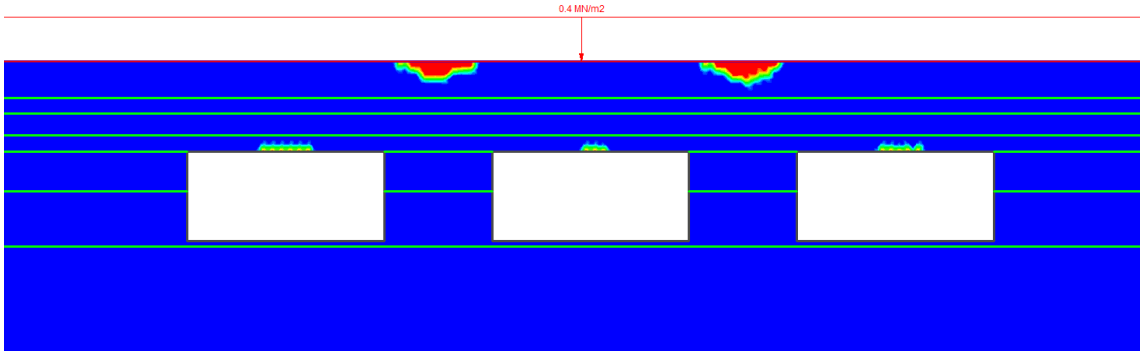

Figure 4.55: Yielded elements with Poisson's ratio being $\nu = 0.4$

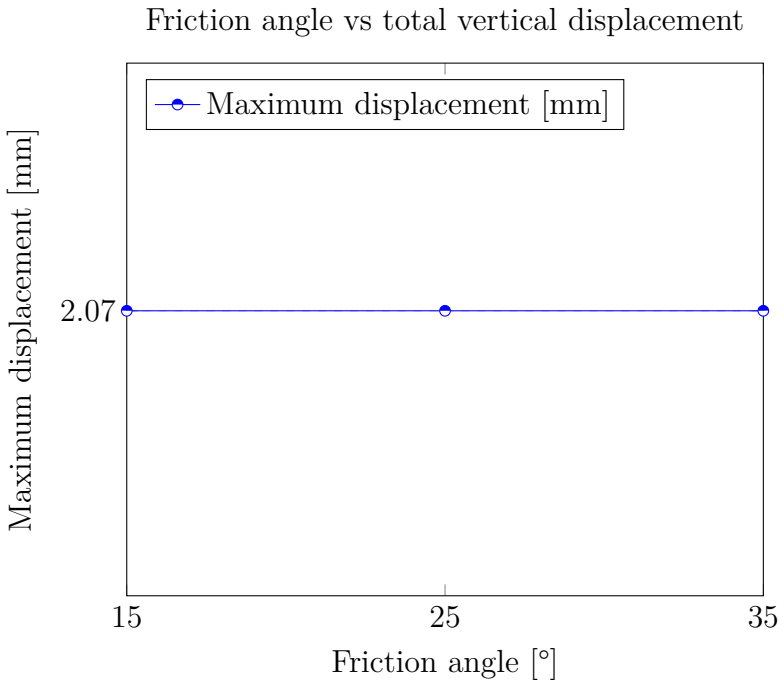

Figure 4.56: Plot of the effect friction angle has on the maximum vertical displacement

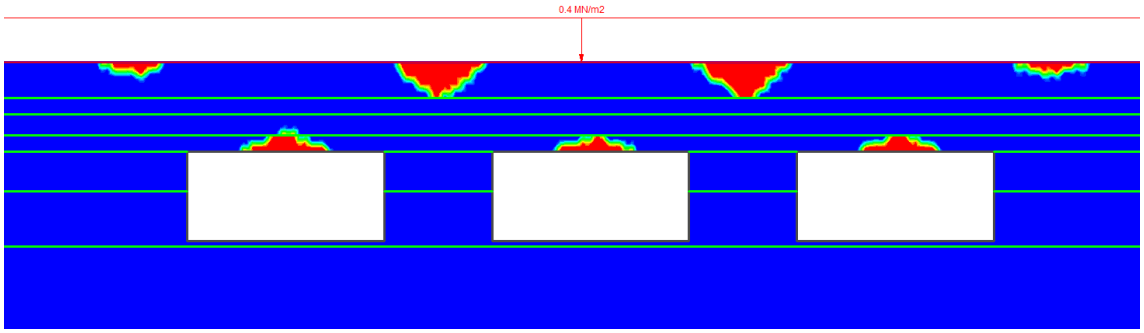

Figure 4.57: Yielded elements with the friction angle reduced to 15°

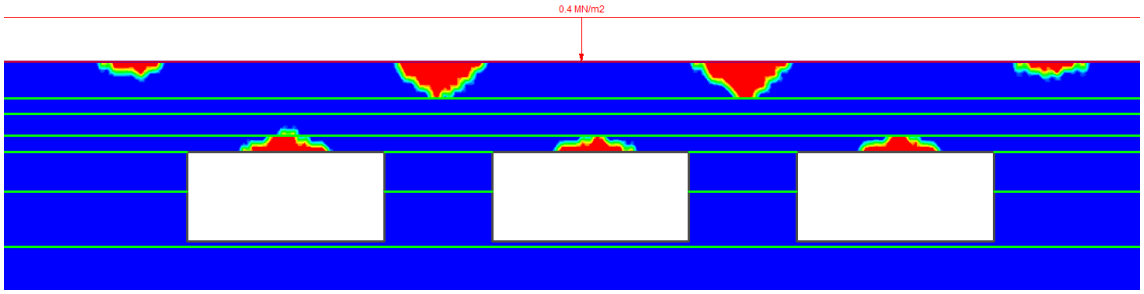

Figure 4.58: Yielded elements with the original friction angle of 35°

5
Discussion

The following section will discuss the results of the study as well as uncertainties of the method.

5.1 Uncertainty of input properties

There are many uncertainties linked to this study. A computer model is only as strong as the certainty of the parameters available or worse. Many of the parameters used in this study, such as the compressive strength, friction angle and tensile strength are based on investigations made in the 1980's and 1990's. To make the analysis as reliable as possible it would have been a good idea to redo these tests in order to confirm the results. However, no reason was found to distrust the investigations. They were all performed by skilled engineers and miners and their results are reasonable in magnitude and thus deemed reliable for this study.

The information that was not available from the archived material has either been extrapolated or compared to those of rock in similar conditions to find a representative value. This method is viable and should in theory generate somewhat representative values for the respective parameters. However, it is hard determine how representative it really is to reality and unfortunately, it is impossible to know without an extensive testing procedure. However, extensive testing was not possible for this study and the extrapolated or estimated values were deemed to be representative enough.

The GSI input is arguably one of the most crucial input parameters in geological estimation in general and specifically when used in computer modeling. The GSI value is the basis for the Hoek-Brown failure criterion used in the models and also used for many of the strength parameters used in the software. It really is a good tool to use, the fact that visual observations can be used numerically and it makes investigations standardized and neatly packaged. However, since its descriptors can be subjectively interpreted it can and most often will be subject to discrepancies.

Figure 4.39 shows the variation of the vertical displacement with differing GSI ranges. When reduced by 12 points in all layers the vertical displacement increases by about 13% and if GSI is reduced by 14 points the model ceases to converge and the mine seems likely to collapse. The estimations done for GSI in this study are uncertain as it is impossible to see the condition of the rock in the layers above and

below the mine rooms. They have been assessed by looking at the rock that is visible within the mine and compared to text descriptions from the borehole investigations in the archived material from Sweco. To make this assessment safer it would be necessary to make new drill-cores and observe them thoroughly.

The bottom line is that it is crucial to estimate GSI correctly. The risk of misusing the classification system has been subject for debate previously, as mentioned in Section 2.3.4, and the only way to be able to use it with certainty is to gather experience of it as well as having a vast experience of rock behavior in general.

Rock mass classification systems such as CMRR and RMR all come with similar challenges. Much like GSI, some parameters are descriptive and subject to subjective decisions which can make it hard for inexperienced engineers to use them properly. The anchoring suggestions made from the systems are often used as a guidelines in preliminary stages in the design phase to get an idea and an overview before active construction takes place. For the applications of RMR, CMRR and GSI in this thesis, both supervisor from Chalmers and Sweco have been consulted in order to make the most use and and with the most certainty possible.
Young's modulus and Poisson's ratio were particularly hard to estimate, as the possible ranges of both parameters are very large in different types of sandstone. In a case with a large discrepancy in Young's modulus the results may vary largely, as illustrated in Figure 4.36. However, the disparity in the results is relatively small for the adjacent intervals to the value used in the study. In other words, as long as the estimation is not off by a significant margin, the variation in the results will be minor. The scenario is similar for the case of Poisson's ratio as illustrated in Figure 4.52 - 4.55. However, the variation in maximum vertical displacement is lower for Poisson's ratio compared to the variation with Young's modulus. The yielded elements are affected more by Poisson's ratio though, and become slightly larger with a lower value. As can be seen in Table A.3 it is not unlikely that the Poisson's ratio is lower than 0.2, which could be problematic. However, the location of the yielded elements is relatively unchanged and as a result any supporting structure would be installed similarly anyways. The only alteration would be the weight the support would need to hold up and the distance potential bolts would need to penetrate in order to reach a layer with stable rock. Though, with a greater risk of yielded elements as in the case with a lower Poisson's ratio, any weakness zones could potentially become even more problematic.

Furthermore, the cohesion was also estimated. However, as is shown in Figure 4.49, the cohesion has a negligible effect unless it's below 0.5, and the effects at that point is relatively small. However, as it approaches zero the model starts to see large variations in vertical displacement and yielded elements. However, it is safe to assume that it is above zero and most likely higher than 0.5 as well.

Regarding m_i, a higher value results in a lower displacement and a decrease in yielded elements. This is due to σ_3 being negative in the places where the yielded elements and vertical displacements occur. See Figures 4.4 and 4.12. Figure 4.45

shows that in the Hoek-Brown failure criterion, the strength is lower when σ_3 is negative for the cases with a lower m_i. This likely means that the rock fails in tension as the horizontal principal stress is negative.

5.2 Simplification of RMR support recommendation

Technically, the RMR output suggestions seen in Table 2.2 also call for a concrete liner in the *Fair rock* class, which is the rock class attained for the RMR Minimum scenario. However, a decision was made not to include this liner. The reasoning for this is that concrete liners will cover the materials that are desired to extract and as a result it is not very suitable for mining applications in general. In many cases with room-pillar mining it is desired to even extract the pillars at the end of the mines lifespan, in order to maximize the economical returns. This would be a lot harder with a liner installed, and it's also more expensive and arduous to install compared to bolts. Furthermore, the existing mine does not have a liner and it is clear that the mine is stable without support at all based on the other scenarios. A liner could however prove beneficial for catching smaller blocks and rocks falling from ceiling. However, in the Kvarntorp mine, a rock net has been fitted where this is deemed to be a problem instead.

However, one could argue that since this particular mine is no longer used for sandstone extraction but instead mainly used for storage and testing, concrete liners could be a good alternative. It would both hold blocks in place as well as create a more refined look to surfaces that may better serve the new purpose. Though, this is not a typical situation for a mine and as a result it was not taken into account in the finite element analysis to any large extent.

5.3 Disparity between model types

The anisotropic model and jointed model behaved very similarly in most aspects. This is not unexpected as the models share the same input parameters for the intact rock, such as GSI, UCS, Young's Modulus and Poisson's ratio. However, the joints are handled quite differently in the models. The jointed model only have a total of six horizontal joints placed in the material transitions while the anisotropic model assumes there may be planes of weakness anywhere. As a result, the anisotropic model was deemed to be more nuanced and its result to be on the more conservative side. Furthermore, the input parameters of the joints in the jointed model also take the normal and shear stiffness into account while the anisotropic model doesn't. Both of these parameters were estimated based on shear and normal stiffness of the intact rock and are therefore deemed relatively uncertain. Consequently, the same uncertainty is carried over to the jointed model as a whole.
Due to this uncertainty and the knowledge of a much larger amount of joints being present in the mine than what was incorporated into the jointed model it was deemed

that the anisotropic model better represents reality. Therefore the anisotropic model was used for the analysis of the additional scenarios beyond the CMRR and RMR scenarios and the sensitivity analysis was carried out using the anisotropic model.

5.4 Impact of bolts

The tensile load experienced on the bolts is not anywhere close to their capacity in any scenario. This is due to the roof displacing as a single unit downwards resulting in the bolts being displaced in the same rate as the roof. In this aspect the bolts seem to be unnecessary for the overall stability and displacement and the existing bolt pattern can be considered excessive. However, from the results showing the yielded elements it is clear that failure and loose blocks are present. In this case the bolts percolating the yielded elements would definitely help to keep them in place. For example, when looking at Figure 4.19, the results show failure in the form of yield in the middle while not much occurs at the edges. Judging by that, it would be a good idea to focus the bolting to the middle of the rooms and thus reducing the overall amount of bolts.

5.5 Three-dimensional problem in a two-dimensional model

This thesis has focused on a two dimensional analysis but in reality the mining rooms and their intersection to the main corridor is very much a three dimensional problem. Each mine room perpendicularly intersects the main corridor in reality, illustrated in Figure 2.9. The 2D-model does not accurately represent the situation in the vicinity of the main corridor as the supporting capacity of the pillars will diminish closer to their ending. This could lead to larger amounts of yielded elements in the pillars and the roof in these areas and additional support may be needed as a result, such as clearing up small loose blocks and/or spot bolting. As a result, further stability assessment is required in these areas.

Also worth noting is that the model was limited to only include three adjacent mine rooms, whilst in reality the mine is much more extensive. The reasoning was that for the scopes and purposes for this study it was sufficient to model a representative sample of the mine. Three adjacent rooms still gives an indication of how one room affects the other and the simulations in the end seems to confirm this.

5.6 Reinforcement suggestion based on the findings in this thesis

It is clear from the finite element analysis that the bolts have a negligible effect on the vertical displacement and the general behaviour of the models. However, it is also clear that the roof easily suffers from yielded elements that needs to be controlled. If blocks are allowed to fall, the stress distribution could eventually change in the overlaying segments of the roof leading to further stability issues. As a result, it is crucial to handle these loose blocks properly. Using a rock net would control blocks from falling down, but would not necessarily maintain the stress in the overlaying roof. Using a liner would cope with both issues, but is an expensive and impractical alternative for a large mine as in the case of Kvarntorp. Using bolts, as is the current method utilised, would both maintain the stress distribution and keep blocks from falling down, while simultaneously being relatively inexpensive and easy to install. However, the difficulty with bolting yielded elements is to safely assess where it is necessary to bolt. The quality of the roof undoubtedly has variations and consequently the assessment is arduous. This is currently solved by bolting densely and therefore minimizing the risk of any blocks having the possibility to fall. However, as can be seen in the results of the models of the CMRR scenario and the unsupported scenario this method clearly exaggerate the necessary amount of bolts for a regular part of the mine. In a sense, the recommendation from CMRR is very feasible if the yielded elements always are centered in the middle of the tunnel roof as is the case in the models. This would allow the usage of two bolts which would most likely be enough to sustain the weight of those blocks. This method would be cheaper, more environmentally friendly as less steel has to be used and easier to install and maintain than the existing support and the RMR recommendation. Still, the reality of the precise location of the yielded elements is hard to assess through a finite element analysis, as the quality of the roof may vary throughout the mine. Consequently, the trouble with the recommendation is the need to clearly locate any weakness zones in the rock mass. If those are located, the specific location of the bolts can be altered in weaker areas to accommodate for the irregular rock behaviour. As the Kvarntorp mine mainly consist of sandstone with strictly horizontal joints, such an assessment is deemed to be possible. Deviating joints could possibly be located in such a homogeneous rock mass and as a result the weakness zones are also easier to locate. However, many other aspects also affect the roof quality such as the filling material of the joints and the proportion of other material bound within the sandstone.

If it is not possible to locate the weakness zones, it may be hard to simply follow the support recommendation established by CMRR as it would be a risk. In that case, the RMR recommendation or existing support would be a safer bet.

5.7 CMRR outside of the coal mining industry

As this study has focused on the Kvarntorp mine in particular, the conclusions that can be established are mainly applicable to this specific case only. They may be considered as indicators of the general functionality of the classification systems in horizontally layered sandstone, but as only one case has been studied no wider conclusions can safely be determined.
However, in the case of Kvarntorp this study provides a competent foundation for the implementation of CMRR. In general, the mine seems to be stable without any support aside from the yielded elements that need to be supported by bolts. The existing support has six bolts in a row which is similar to the recommendation provided by RMR Maximum. RMR minimum instead gives an even more extensive support suggestion while CMRR gives a preliminary support suggestion PRSUP of only two bolts in a row with an out of plane spacing of two meters. If the yielded elements are located as in the model results and the bolts are placed in the middle to support the falling block it might be sufficient to only use two or maybe three bolts instead of the current six.

The results of the study indicate that CMRR actually suggested the most efficient solution for this particular scenario and could potentially be more economical and easier to implement than the other alternatives. It is however hard to determine for certain if the entirety of the mine behaves the same. As there have been instances of roof collapses throughout the mine this is deemed unlikely. This has mainly occurred in older sections of the mine though where the old bolts already have served their lifespan. However, in some areas of the mine it is possible that six or even more bolts would be required, but if the rock mass could be assessed to locate weakness zones, the amount of overall bolts in the mine could be reduced significantly.

Additionally, CMRR was found to be the more flexible classification system to work with. As described in Section 3.2.2, several input parameters can be decided by the user such as the bolt length or spacing between bolt rows. For certain cases, especially in sedimentary bedrock, it can be very valuable to allow the bolts to pierce into a stronger layer above. Consequently, it is very valuable for the user to be able to assign the length of the bolts for such cases. In comparison, RMR determines the bolt length through the rock mass class. This can be problematic as the option to bolt into a stronger layer above is harder to take into account while using the system.

Altogether, this indicates that CMRR has the potential to be valuable outside of the coal mining industry. As is clearly seen in this case, CMRR provides a more efficient support recommendation than RMR. If the recommendation is explicitly considered to be a recommendation and not a clear cut support affirmation, it is deemed to be useful for cases similar to Kvarntorp. However, in conjunction with CMRR it is important to investigate the rock mass properly in order to locate possible disparities in the rock quality and assess these properly. As a result, the option of using CMRR concerns the possibility and ability to assess the quality of the roof in a safe and simple manner. If this is possible, CMRR is a feasible method to proceed with.

However, if the rock quality has large disparities or is difficult to assess, the safer choice may be to follow the recommendation of RMR.

5.8 Stress distribution around mine rooms

As can be seen in Figure 4.33 and 4.34, the stress distribution around the mine room is constrained by the top side of the model. In reality, the phosphorite sandstone layer has a superjacent layer of soil above, as visualised in Figure 2.7. As the overburden soil was restructured into a distributed load, the stress distribution is confined within the sandstone and cannot disperse into the overlaying soil as it is not part of the model. This does not fully represent reality, as the stress would be further distributed into the overlaying layers. However, this is not deemed to have a significant effect on the results in general.

5.9 Conclusions

The distinct conclusions of this study is summarised below.

- CMRR is deemed to be a useful classification system for the case of Kvarntorp and the study indicate that that it may be useful for other locations with sedimentary bedrock as well
- CMRR is to be used in conjunction with a thorough assessment of possible weakness zones in the area, as they may generate zones requiring additional support or an alteration of the precise bolt location.
- CMRR is a more flexible system for the user compared to RMR, as it allows more control of the desired output
- CMRR is easier to perform on-site by an experienced user compared to RMR
- In cases where a thorough assessment of weakness zones is arduous or impossible, RMR gives a more conservative support recommendation associated with less risk of falling blocks.
- In the case of Kvarntorp, the bolting does not affect the vertical displacement. However, it is necessary to control the yielded elements.
- The existing support in Kvarntorp is excessive, as further assessment of weakness zones in conjunction with CMRR would allow for a more efficient bolting structure.
- Both the anisotropic model and the jointed model used in this study show very similar behaviour and results.
- Among the input parameters used in this study, the GSI value is the largest contributor to the models behaviour. Simultaneously it is also the parameter that leaves most interpretation up to the user. Consequently, experience becomes the most important input factor as all other parameters can be safely determined through on-site or laboratory testing.

5.10 Further studies

As the findings of this study indicate that CMRR can be applicable in other settings than coal mining the potential for further studies is vast. The scope of this study was the qualitative analysis of a single case, the Kvarntorp mine. However, a larger sample size would allow for broader conclusions concerning the applicability of CMRR. As an example, a study investigating a multitude of sedimentary mines with slightly differing properties would be able to gather correlations between the cases and allow for a more thorough investigation of CMRR. This could determine the general usability of the system in different types of sedimentary bedrock. Additionally, it would allow for further evaluation of how CMRR may be utilised and if any adjustments to the system would be necessary to make it more versatile.

Furthermore, the effect of weakness zones is not investigated comprehensively in this study. Unfortunately, the assessment of weakness zones can be arduous and expensive, in turn neglecting the economical and practical benefits of utilising CMRR. Consequently, the system would benefit greatly from being able to incorporate the assessment of weakness zones into the system itself. This could be possible if strong correlations between different types of weakness zones could be found. A thorough study with a large sample size comparing the CMRR support recommendation to the necessary support with weakness zones taken into account could potentially achieve this.

In general, any further studies within the subject would also benefit from further comparison between FEM model types with mines that have already had their stability thoroughly assessed through traditional methods. Further investigation of correlations and possible issues with utilising finite element analysis would improve the credibility of studies in the subject area.

For the specific case of Kvarntorp the largest obstacle is considered to be the uncertainty of the input parameters. To be able to distinctly assess the applicability of CMRR or RMR in the mine extensive testing of the bedrock is necessary. All parameters that were linked to uncertainty in this study can be retrieved through further testing, except the GSI which is partly based on experience. However, further testing and investigation of the bedrock would also benefit the assessment of GSI.

In addition, the Kvarntorp case would benefit from a three-dimensional finite element analysis to evaluate the diminishing stability effect of the pillars closer to the intersection between the main corridor and mine rooms. The effect of this is assumed to be similar in most intersections, and thus a study investigating this effect would be valuable for the stability assessment of the full mine.

Bibliography

[1] Rob Tyson. *Innovative ways to repurpose old mines*. July 2020. URL: https://www.mining.com/web/innovative-ways-to-repurpose-old-mines/.

[2] Richard L Gordon. *Coal Industry, Energy Policy in*. Tech. rep.

[3] Mathew Hall. *Gathering dust: how can depleted mines be repurposed?* Apr. 2020. URL: https://www.mining-technology.com/features/how-can-depleted-mines-be-repurposed/.

[4] Göran Kempe. *Atlas Copco tar nya tag i Kvarntorp*. 2010. URL: https://www.na.se/2010-06-01/atlas-copco-tar-nya-tag-i-kvarntorp.

[5] C. Mark and G. M. Molinda. "The Coal Mine Roof Rating (CMRR) - A decade of experience". In: *International Journal of Coal Geology* 64.1-2 (Oct. 2005), pp. 85–103. ISSN: 01665162. DOI: 10.1016/j.coal.2005.03.007.

[6] Z.T. Bieniawski. *Engineering rock mass classifications : a complete manual for engineers and geologists in mining, civil, and petroleum engineering*. New York, 1989. ISBN: 0-471-60172-1.

[7] N. Barton, R. Lien, and J. Lunde. "Engineering classification of rock masses for the design of tunnel support". In: *Engineering Classification of Rock Masses for the Design of Tunnel Support* 6.4 (Dec. 1974), pp. 189–236. ISSN: 0035-7448. DOI: 10.1007/BF01239496.

[8] U.S. Energy Information Administration. *Coal Explained: Coal and the environment*. Dec. 2021. URL: https://www.eia.gov/energyexplained/coal/coal-and-the-environment.php.

[9] U.S. Energy Information Administration. *Coal explained - Mining and transportation of coal*. Dec. 2020. URL: https://www.eia.gov/energyexplained/coal/mining-and-transportation.php.

[10] LKAB. "Om LKAB - Teknik- och processutveckling". In: (June 2020). URL: https://www.lkab.com/sv/om-lkab/teknik-och-processutveckling/.

[11] B.H.G Brady and E.T. Brown. *Rock Mechanics: For underground mining*. 3rd. Springer, 2006, pp. 77–77.

[12] LKAB. *Våra underjordsgruvor*. Dec. 2017. URL: https://www.lkab.com/sv/om-lkab/fran-gruva-till-hamn/bryta/vara-underjordsgruvor/.

[13] Ali Somarin. *Mining and the Environment: What Happens When A Mine Closes?* Oct. 2014. URL: https://www.thermofisher.com/blog/mining/mining-and-the-environment-what-happens-when-a-mine-closes/.

[14] Trafikverket. *Projektering av bergkonstruktioner*. ISBN: 9789177254126.

[15] Sten Bjurström and Mats Heimersson. *BeFo: Bergbultning - Dimensionering, praxis och tillämpningar*. 2nd ed. Vol. 8. Stifltelsen bergteknisk forskning - BeFo, 1975, pp. 73–75.

[16] Trafikverket. *TRVK Tunnel 11 : Trafikverkets tekniska krav Tunnel*. Trafikverket, 2011. ISBN: 9789174671551.

[17] Nikola Ristov. *Personal communication with Kvarntorp mine investigator*. Kvarntorp, Apr. 2021.

[18] N.Y Barton and E Grimstad. *Updating the Q system for NMT*. Tech. rep. 1993. URL: https://www.researchgate.net/publication/284818046.

[19] N Barton. *Some new Q-value correlations to assist in site characterization and tunnel design Some new Q-value correlations to assist in site characterisation and tunnel design*. Tech. rep. 2002, pp. 185–216. URL: https://www.researchgate.net/publication/292056400.

[20] NGI. *Using the Q-System: Rock mass classification and support design*. URL: https://www.ngi.no/eng/Services/Technical-expertise/Engineering-geology-and-rock-mechanics/Q-system.

[21] W Gr et al. *314 MINING INDUSTRY ANNUAL REVIEW Using the coal mine roof rating (CMRR) to assess roof stability in U.S. coal mines*. Tech. rep.

[22] E. Hoek and E. T. Brown. "The Hoek–Brown failure criterion and GSI – 2018 edition". In: *Journal of Rock Mechanics and Geotechnical Engineering* 11.3 (June 2019), pp. 445–463. ISSN: 16747755. DOI: 10.1016/j.jrmge.2018.08.001.

[23] Kunui Hong, Eunchol Han, and Kwangsong Kang. "Determination of geological strength index of jointed rock mass based on image processing". In: *Journal of Rock Mechanics and Geotechnical Engineering* 9.4 (Aug. 2017), pp. 702–708. ISSN: 16747755. DOI: 10.1016/j.jrmge.2017.05.001.

[24] Ewert Hoek, T.G. Carter, and M.S. Diederichs. "2013-Quantification-of-the-GSI-Chart (1)". In: ().

[25] B Nilsen et al. "RMR VS Q VS RMI". In: *Tunnels & Tunnelling International* 35.5 (Apr. 2003), pp. 45–48.

[26] Navid Hosseini et al. *USING SEMI-FUZZY RMR TO DETERMINE THE REQUIRED SUPPORT SYSTEM FOR GHESHLAGH COAL MINE*. Tech. rep. 2014. URL: https://www.researchgate.net/publication/267512129.

[27] Roscience. *RS2 User Guide*. URL: https://www.rocscience.com/help/rs2/documentation.

[28] Sveriges Geologiska Undersökning. *Sveriges Geologiska Undersökning: Kartvisare*. URL: https://apps.sgu.se/kartvisare/.

[29] Sweco. *Archived material from Sweco*.

[30] Mikael Erlström. *Litologisk och geokemisk karaktärisering av berggrundsavsnitt på södra Öland*. Tech. rep. 2016. URL: www.sgu.se.

[31] Jong-Gwan Kim, Mahrous A. M. Ali, and Hyung-Sik Yang. "Robust Design of Pillar Arrangement for Safe Room-and-Pillar Mining Method". In: *Geotechnical and Geological Engineering* 37.3 (June 2019), pp. 1931–1942. ISSN: 0960-3182. DOI: 10.1007/s10706-018-0734-1.

[32] V. Hudeček et al. "Experience in the Adoption of Room & Pillar Mining Method in the Company OKD, a.s., Czech Republic". In: *Journal of Mining Science* 53.1 (Jan. 2017), pp. 99–108. ISSN: 1062-7391. DOI: 10.1134/S1062739117011908.

[33] E. Broch and J. A. Franklin. "The point-load strength test". In: *International Journal of Rock Mechanics and Mining Sciences and* 9.6 (1972), pp. 669–676. ISSN: 01489062. DOI: 10.1016/0148-9062(72)90030-7.

[34] J Franklin. "Suggested method for determining point load strength". In: *International Journal of Rock Mechanics and Mining Sciences & Geomechanics Abstracts* 22.2 (Apr. 1985), pp. 51–60. DOI: https://doi.org/10.1016/0148-9062(85)92327-7.

[35] Geoengineer. *Point Load Test*. URL: https://www.geoengineer.org/education/laboratory-testing/point-load-test.

[36] ASTM International. *Standard Test Method for Slake Durability of Shales and Other Similar Weak Rocks*. 1998. DOI: 10.1520/D4644-16.

[37] Rolf Larsson. *Jords egenskaper*. Tech. rep. Linköping: Swedish Geotechnical Institute, 2007.

[38] Ed Vitz et al. *Density of Rocks and Soils*. June 2021. URL: https://chem.libretexts.org/@go/page/49946.

[39] Chandong Chang, Mark D. Zoback, and Abbas Khaksar. "Empirical relations between rock strength and physical properties in sedimentary rocks". In: *Journal of Petroleum Science and Engineering* 51.3-4 (May 2006), pp. 223–237. ISSN: 09204105. DOI: 10.1016/j.petrol.2006.01.003.

[40] R Andy Erwin Wijaya, Dwikorita Karnawati, and Wahyu Wilopo. *Rock Mass Rating of Cavity Limestone Layer in Rembang, Central Java, Indonesia*. Tech. rep. 1, pp. 19–28.

[41] Paul Marinos and Evert Hoek. "GSI: A geologically friendly tool for rock mass strength estimation". In: *ISRM International Symposium 2000, IS 2000*. International Society for Rock Mechanics, 2018.

[42] V. S. Vutukuri, R.D. Lama, and S.S. Saluja. *Handbook on Mechanical Properties of Rocks*. Vol. 2. Clausthal: Trans Tech Publications, 1978.

A

Appendix 1 - Tables

Table A.1: Geomechanics classification of Rock Mass Rating system [40]

A. CLASSIFICATION PARAMETERS AND THEIR RATINGS									
Parameter			Range of values						
1	Strength of intact rock material	Point-load strength index	>10 MPa	4 - 10 MPa	2 - 4 MPa	1 - 2 MPa	For this low range - uniaxial compressive test is preferred		
		Uniaxial comp. strength	>250 MPa	100 - 250 MPa	50 - 100 MPa	25 - 50 MPa	5 - 25 MPa	1 - 5 MPa	< 1 MPa
	Rating		15	12	7	4	2	1	0
2	Drill core Quality *RQD*		90% - 100%	75% - 90%	50% - 75%	25% - 50%	< 25%		
	Rating		20	17	13	8	3		
3	Spacing of discontinuities		> 2 m	0.6 - 2 . m	200 - 600 mm	60 - 200 mm	< 60 mm		
	Rating		20	15	10	8	5		
4	Condition of discontinuities (See E)		Very rough surfaces Not continuous No separation Unweathered wall rock	Slightly rough surfaces Separation < 1 mm Slightly weathered walls	Slightly rough surfaces Separation < 1 mm Highly weathered walls	Slickensided surfaces or Gouge < 5 mm thick or Separation 1-5 mm Continuous	Soft gouge >5 mm thick or Separation > 5 mm Continuous		
	Rating		30	25	20	10	0		
5	Ground water	Inflow per 10 m tunnel length (l/m)	None	< 10	10 - 25	25 - 125	> 125		
		(Joint water press)/ (Major principal σ)	0	< 0.1	0.1, - 0.2	0.2 - 0.5	> 0.5		
		General conditions	Completely dry	Damp	Wet	Dripping	Flowing		
	Rating		15	10	7	4	0		

B. RATING ADJUSTMENT FOR DISCONTINUITY ORIENTATIONS (See F)						
Strike and dip orientations		Very favourable	Favourable	Fair	Unfavourable	Very Unfavourable
Ratings	Tunnels & mines	0	-2	-5	-10	-12
	Foundations	0	-2	-7	-15	-25
	Slopes	0	-5	-25	-50	

C. ROCK MASS CLASSES DETERMINED FROM TOTAL RATINGS					
Rating	100 ← 81	80 ← 61	60 ← 41	40 ← 21	< 21
Class number	I	II	III	IV	V
Description	Very good rock	Good rock	Fair rock	Poor rock	Very poor rock

D. MEANING OF ROCK CLASSES					
Class number	I	II	III	IV	V
Average stand-up time	20 yrs for 15 m span	1 year for 10 m span	1 week for 5 m span	10 hrs for 2.5 m span	30 min for 1 m span
Cohesion of rock mass (kPa)	> 400	300 - 400	200 - 300	100 - 200	< 100
Friction angle of rock mass (deg)	> 45	35 - 45	25 - 35	15 - 25	< 15

E. GUIDELINES FOR CLASSIFICATION OF DISCONTINUITY conditions					
Discontinuity length (persistence) Rating	< 1 m 6	1 - 3 m 4	3 - 10 m 2	10 - 20 m 1	> 20 m 0
Separation (aperture) Rating	None 6	< 0.1 mm 5	0.1 - 1.0 mm 4	1 - 5 mm 1	> 5 mm 0
Roughness Rating	Very rough 6	Rough 5	Slightly rough 3	Smooth 1	Slickensided 0
Infilling (gouge) Rating	None 6	Hard filling < 5 mm 4	Hard filling > 5 mm 2	Soft filling < 5 mm 2	Soft filling > 5 mm 0
Weathering Ratings	Unweathered 6	Slightly weathered 5	Moderately weathered 3	Highly weathered 1	Decomposed 0

F. EFFECT OF DISCONTINUITY STRIKE AND DIP ORIENTATION IN TUNNELLING**			
Strike perpendicular to tunnel axis		Strike parallel to tunnel axis	
Drive with dip - Dip 45 - 90°	Drive with dip - Dip 20 - 45°	Dip 45 - 90°	Dip 20 - 45°
Very favourable	Favourable	Very unfavourable	Fair
Drive against dip - Dip 45-90°	Drive against dip - Dip 20-45°	Dip 0-20 - Irrespective of strike°	
Fair	Unfavourable	Fair	

Table A.2: GSI Chart [41]

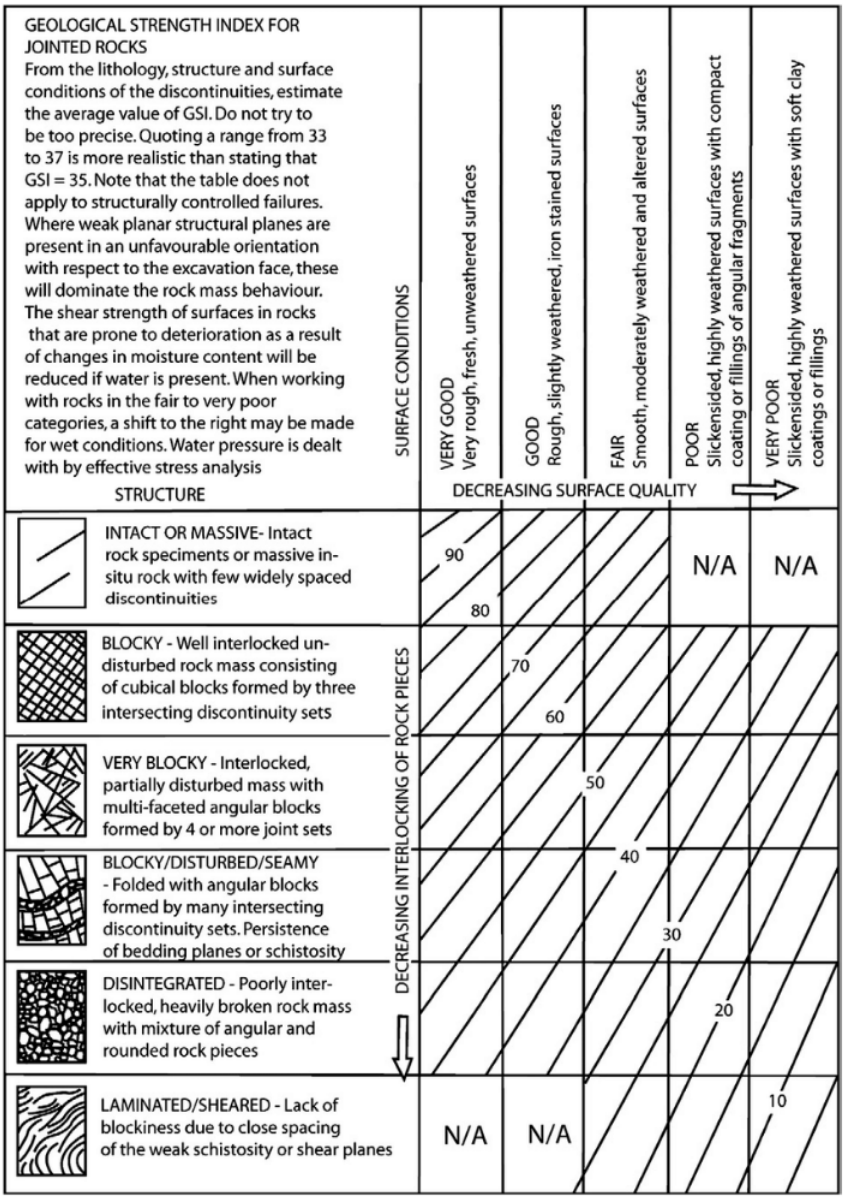

CMRR

DATE_____ MINE_____ LOCATION_____ PAGE____ OF_____ CMRR_____

TYPE OF EXPOSURE_____ NAME_____

UNIT						UNIT DISCONTINUITIES						
Unit No.	Unit Thickness	Strip Log	Description	Strength	Moisture Sensitivity	Disco. I.D.	Description	Cohesion	Roughness	Spacing	Persistence Lateral/Vert
3						A.					
						B.					
						C.					
	CONTACT										
2						A.					
						B.					
						C.					
	CONTACT										
1						A.					
						B.					
						C.					

	Rebounds	Not Sensitive	1	Strong (>7)**	Jagged	>1.8 m	0 - 0.9 m
2	Pits	Slightly Sensitive	2	Moderate (4-7)	Wavy	0.6 - 1.8 m	0.9 - 3 m
3	Dents	Moderately Sensitive	3	Weak (1-3)	Planar	20 - 60 cm	3 - 9 m
4	Craters	Severely Sensitive	4	Slicken-sided (0)		6 - 20 cm	>9 m
5	Molds		5			<6 cm	

Groundwater (inflow/10 m of entry length) L/min (Circle one)

Dry 0 1 Heavy Drip 2.7 - 12.2 4
Damp 0 - 1.3 2 Flowing >13.2 5
Light Drip 1.3 - 2.7 3

Describe condition in vicinity of fail (circle one)

1. Good 3. Heavy
2. Scaly 4. Failed

COMMENTS:

**Chisel blows necessary to split bedding.

Figure A.1: CMRR-CHART

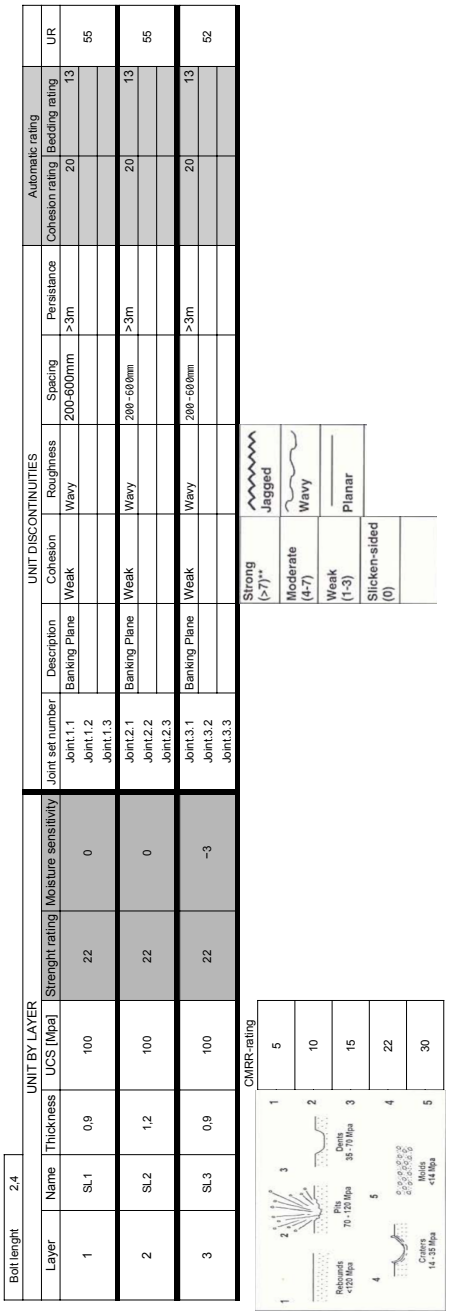

Figure A.2: CMRR-Chart with observed and calculated values

IMMERSION TEST

Mine: _____ Date: _____

Unit No.: _____ Tester: _____

Sample Description (Lithology, bedding, etc.):

_____

Immersion		**Breakability**	
Observation	Rating	Observation	Rating
Appearance of Water			
Clear = 0 Misty = -1 Cloudy = -3	_____	No Change 0 Small Change-2 Large Change -6	
Talus Formation		*Breakability Index* _____	
None = 0 Minor = -1 Major = -3	_____		
Cracking of Sample			
None = 0 Minor/Random = -1 Major/Preferred Orientation =-3 Specimen Breakdown = -9	_____		
Total Immersion Index _____			

Procedure for Immersion Test

1. Select sample(s) - ~ hand sized.
2. Test for hand breakability.
3. Rinse specimen (to remove surface dirt, dust, etc.).
4. Immerse in water for 1 hour.
5. Observe and rate water appearance, talus formation, and cracking of sample.
6. *Sum Rating for Immersion Index.*
7. Retest for hand breakability.
8. *Determine Breakability Index.*
9. The final Immersion Test Index is the greater of the Breakability Index or the Immersion Index.

Figure A.3: The data sheet used for determination of the breakability and immersion index in the immersion test [5]

Table A.3: Laboratory mechanical properties of different sandstones with similar quality to the Kvarntorp sandstone [42]

Sandstone Location	**Description**	**Density** *[g/cm^3]*	**Elastic Modulus** *[GPa]*	**Poisson's Ratio**	**Comp. Str.** *[MPa]*	**Tens. Str** *[MPa]*
USA, Pennsylvania	Sandstone	2.43	13.79	0.20	102.04	15.86
USA. W. Va. Kanawha Eagle	Argillaceous, mg-fg	2.80	31.50	0.05	105.49	4.14
USA. Bridge Canyon Dam, Arizona.	Ferruginous, mg, porous, massive	2.39	27.58	0.04	90.32	5.17
USA. Flaming Gorge Dam, Utah	Quartzitic, ferroginous, dense, mg	2.54	14.82	0.06	113.07	3.24
USSR, Prokopevsk, kieselevsk	Coal, mg, siliceous-argillicious	2.54	22.40	0.22	113.70	6.40
USSR, Prokopevsk, kieselevsk	Coal, fg, argillaceous, siliceous	2.66	32.0	0.28	149.50	9.90
USSR, Prokopevsk, kieselevsk	Coal, cg, aleurolites, argillaceous	2.80	30.0	0.34	99.80	9.0
USA, White Pine, S-W	Wet	2.80	49.99	0.11	122.73	13.1

B

Appendix 2 - Bolt patterns and liner placement in different models

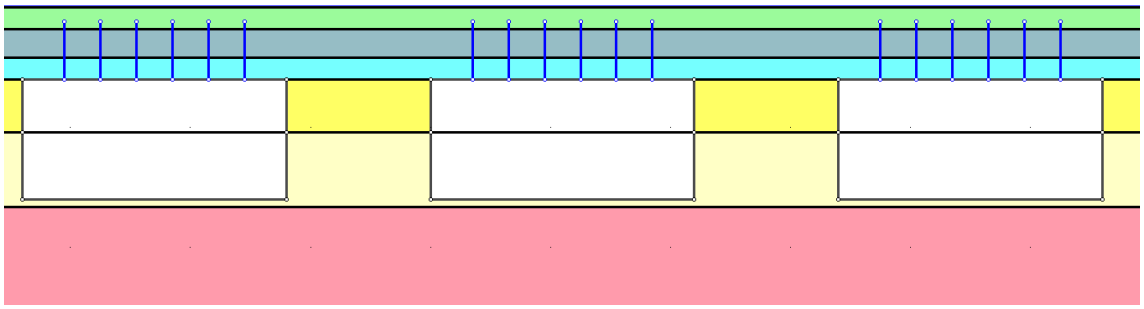

Figure B.1: Bolt pattern for scenario "Existing support"

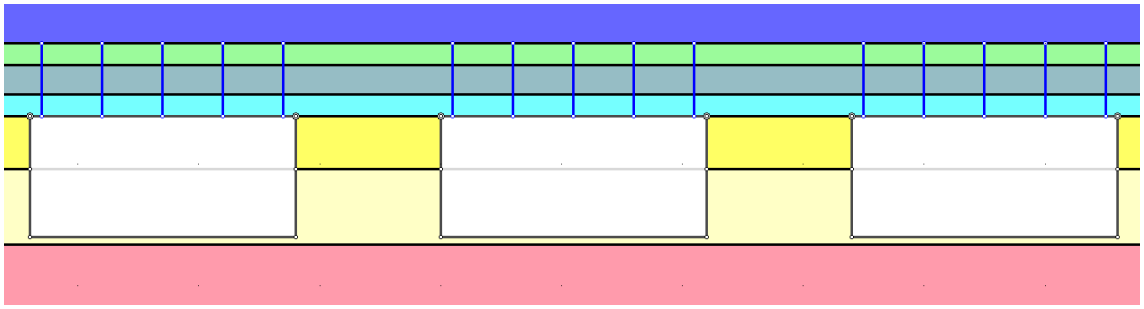

Figure B.2: Bolt pattern for scenario "RMR Maximum"

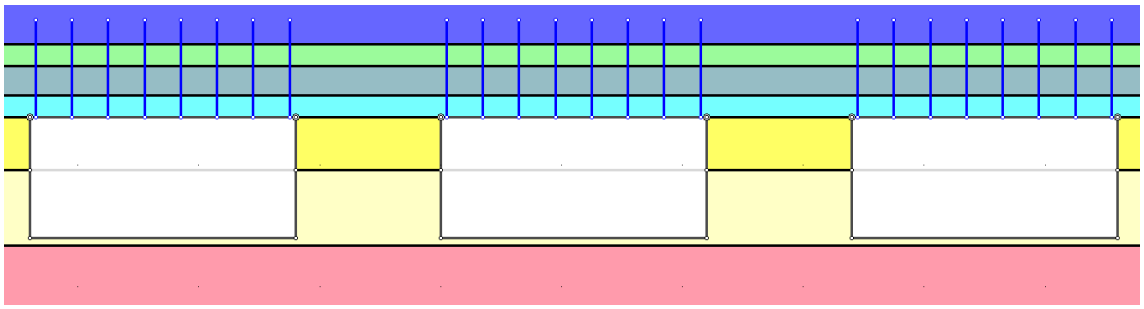

Figure B.3: Bolt pattern for scenario "RMR Minimum"

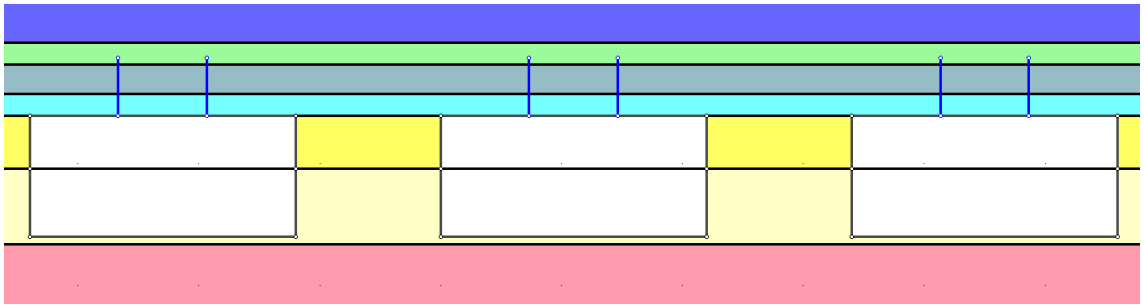

Figure B.4: Bolt pattern for scenario "CMRR"

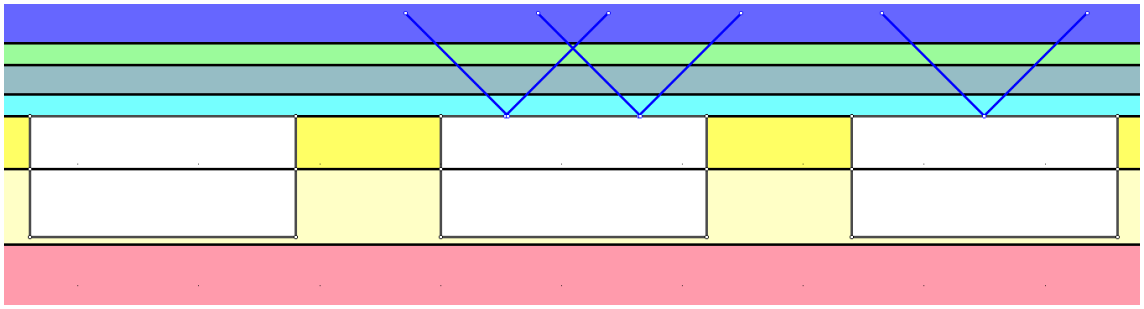

Figure B.5: Bolt pattern for scenario "Bolts installed at an angle of 45°"

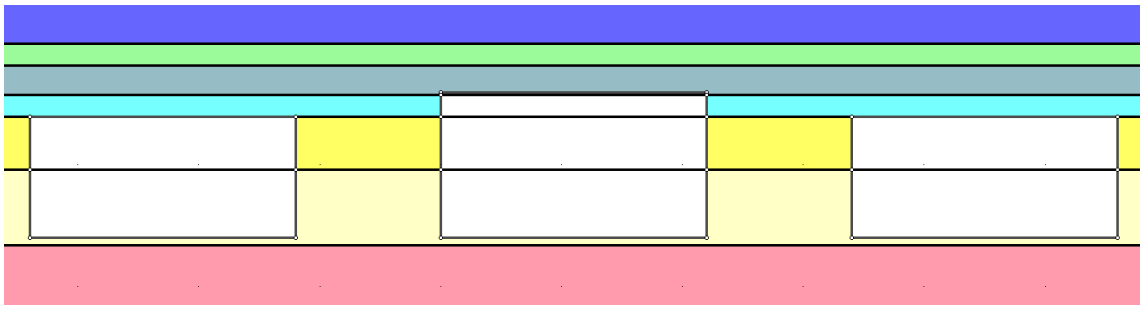

Figure B.6: Bolt pattern for scenario "Increased height of the middle room without support"

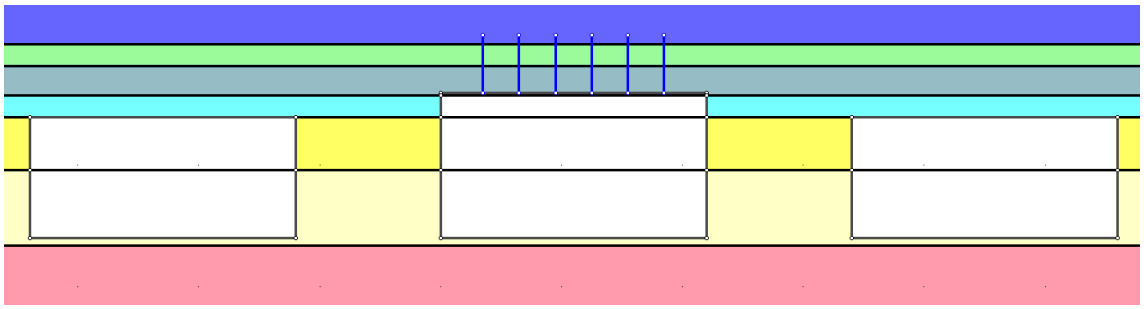

Figure B.7: Bolt pattern for scenario "Increased height of the middle room with bolts"

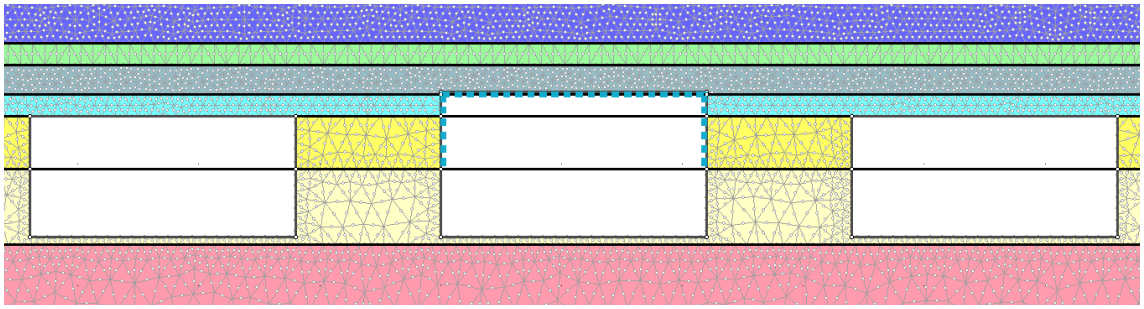

Figure B.8: Liner placement for scenario "Increased height of the middle room with concrete liner"

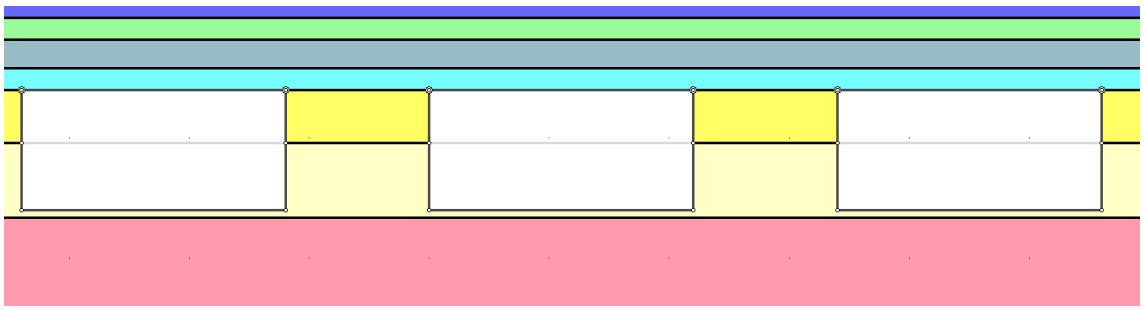

Figure B.9: Bolt pattern for scenario "Unsupported initial conditions"

C

Appendix 3 - Pictures from the Kvarntorp mine

Figure C.1: Inside one of the main corridors in the Kvarntorp mine. Sandstones layers SL4 and SL5 are visable

Figure C.2: Intersection between a main corridor and a mine room

Figure C.3: Wall of a main corridor. Ruler is 60 cm for scale.

Figure C.4: Intersection between a main corridor and a mine room

JSM AB
DIGGING FOR HOPE

DEPARTMENT OF Architecture and Civil Engineering
CHALMERS UNIVERSITY OF TECHNOLOGY
Gothenburg, Sweden
www.chalmers.se

CHALMERS
UNIVERSITY OF TECHNOLOGY